ABSTRACT

HERMAN, KIMBERLY NICOLE. Evaluation of the Role of Human DNA Polymerase η on Mutagenesis in a Cell-Based Model. (Under the direction of Scott D. McCulloch).

DNA damage occurs constantly throughout the cell cycle, and can occur intrinsically from DNA synthesis errors and as a side effect of oxidative respiration or extrinsically from DNA damaging agents such as chemical and dietary exposures or exposure to ultraviolet light (UV) from the sun. The main DNA damage caused by UV is cyclobutane pyrimidine dimers (CPDs). Additionally, DNA can be damaged by chemical exposure. An example is the use of mustard gas in military applications, which were later modified and utilized as chemotherapeutic agents. Two chemicals that we are studying include one of these modified mustard gases, *cis*-diamminedichloroplatinum (cisplatin), as well as another chemical called *N*-methyl-*N*'-nitro-*N*-nitrosoguanidine (MNNG). These treatments can cause lesions which block the replication fork and have to be bypassed by a special tolerance mechanism called translesion synthesis (TLS). TLS is performed by special polymerases which have wide open active sites to accommodate bulky lesions. These open active sites are great for accommodating lesions, but also do not have the tight fit of replicative polymerases which can lead to errors and mutagenesis.

We first an environmentally relevant UV-B treatment in a normal human fibroblast control line and a Xeroderma pigmentosum variant (XP-V) cell line, in which the POLH gene contains a truncating point mutation leading to a non-functional polymerase. We demonstrate that UV-B has similar but less striking effects compared to UV-C in both its cytotoxic and mutagenic effects. Analysis of the mutation spectra after a single dose of UV-B shows a majority of mutations can be attributed to mutagenic bypass of dipyrimidine

sequences. However, we do note additional types of mutations with UV-B that are not previously reported after UV-C exposure.

Reactive oxygen species (ROS) can also cause DNA damage. One of the main damaging oxidative lesions is 7,8-dihydro-8-oxoguanine (8-oxoG). This lesion can inhibit the replication fork and has been linked to mutagenesis, cancer and aging. *In vitro* studies have shown that the translesion synthesis polymerase, DNA polymerase η (pol η), is able to efficiently bypass 8-oxoG in DNA. In this study we wanted to investigate the mutagenic effects of oxidative stress, and in particular 8-oxoG, in the presence and absence of pol η. We quantified levels of oxidative stress, 8-oxoG levels in DNA, and nuclear mutation rates. We found that most of the 8-oxoG detected were localized to the mitochondrial DNA, opposed to the nuclear DNA. We also saw a corresponding lack of mutations in a nuclear encoded gene. This suggests that oxidative stress' primary mutagenic effects are not predominantly on genomic DNA.

Next we evaluated the response to DNA damage by evaluating the effects of DNA damaging agents on TLS polymerase mRNA levels over time. We used UV-B treatment, cisplatin, and MNNG on two cell lines with either, proficient, or deficient pol η. We measured mRNA levels by qPCR at 1, 4, 8 16 and 24 hours post treatment. We found an overall suppression of mRNA levels across most treatments and polymerases at 1 hour post treatment. A delayed increase in pol η expression was observed when a low dose of UV-B was used in the pol η proficient cells, and in the pol η deficient cells we saw a subsequent rise in likely back-up polymerases including pol ι. When using a high dose of UV-B we observed a prolonged suppression of mRNA levels of TLS polymerase genes. Our results for MNNG were similar to previously reported MNNG, and cisplatin results showed that the pol

η message increased in normal cells and that there was a rise in back-up polymerases message levels including pol ι in pol η deficient cells.

Evaluation of the Role of Human DNA polymerase η on Mutagenesis in a Cell-Based Model

by
Kimberly N. Herman

A dissertation submitted to the Graduate Faculty of
North Carolina State University
in partial fulfillment of the
requirements for the degree of
Doctor of Philosophy

Toxicology

Raleigh, North Carolina

2015

APPROVED BY:

_____	_____
Scott D. McCulloch	Yoshiaki Tsuji
Committee Chair	Committee Vice-Chair
_____	_____
John Cavanagh	Robert Smart
Minor Representative	Committee Member

DEDICATION

To my husband Matthew, whose love is never failing and belief in me ever strong. Thank you for helping me through this journey. And to my son, to whom I hope this will inspire and encourage you to reach for your dreams.

BIOGRAPHY

Kimberly N. Herman attended the University of Rochester, in Rochester, NY. After graduating she began working in cancer clinical research. It was here that she discovered she wanted to help increase the survival rate and lower the toxicity of the drugs and applied to Toxicology Ph.D. programs. After being accepted into NC State's Toxicology program, Kimberly and her husband moved to North Carolina in 2010 and there she joined Dr. Scott McCulloch's lab.

ACKNOWLEDGMENTS

I would like to thank my mentor, Dr. Scott D. McCulloch. I couldn't have asked for a better boss and advisor; without you this journey to a Ph.D. would have been much more difficult. You are a great teacher, and have imparted a vast amount of wisdom my way. Thank you for making such a rough road a little easier to travel.

I would like to thank my colleagues; Dr. Sam Suarez, Renee Beardslee and Shannon Toffton for all of their support, scientific advice and life advice.

I would also like to thank my committee members, Dr. Yoshiaki Tsuji, Dr. John Cavanagh and Dr. Robert Smart for their expertise, advice and for challenging me along the way.

Lastly, I would like to thank my family and friends for all of their encouragement and support.

TABLE OF CONTENTS

LIST OF TABLES

LIST OF FIGURES

GENERAL INTRODUCTION

CHAPTER 1

CHAPTER 3

Introduction

DNA is the essential genetic material that guides and controls the growth of organisms—it determines our individuality and defines our family history. It is why one sibling might be tall and have blue eyes while another is short with brown eyes; or why some individuals are more prone to certain diseases. DNA was discovered and described in the late nineteenth century, but that knowledge was limited to its chemical components (nucleotides).[1] By the early 1900's the idea was understood that nature or exposures caused clinical phenotypes including disease and cancer; however, the biological explanation for this phenomenon was not understood. It was not until 1953, that Watson and Crick formulated the idea that the structure of DNA was a double helix, leading to the proposal that DNA replication occurs in a semiconservative manner.[1-3] This was the catalyst for a shift in our understanding of DNA and biology.[1] The basic units of DNA are made up of nucleotides. The nucleotides are composed of a nitrogenous base, a sugar and a phosphate group. There are four different nitrogenous bases, adenine (A), thymine (T), cytosine (C) and guanine (G). These bases pair within the double stranded helix in specific combinations: A to T and C to G. This base paring lines up to make a DNA sequence, for example: 5'ATGCCCATGGCA 3', and its reverse complement, 5' TGCCATGGGCAT 3', which can be seen in Figure I.1. As cells divide, DNA must be replicated. DNA also is transcribed into RNA which is later translated into proteins. Changes in the linear sequence of DNA are termed mutations. Mutations alter the genetic material and can lead to downstream effects, such as changes in proteins (including non-functional proteins or over-expressed proteins) which can lead to

diseases, aging and cancer. The cellular response in the prevention and repair of these genetic changes is vitally important to cellular well-being.

DNA Replication

The human genome, or the entirety of genetic information in the form of DNA in each cell, is enormous. A normal human cell has approximately 2-3 meters worth of DNA (if measured linearly), which makes storing and replicating this genetic material a difficult task.[4] In order to package DNA in a way that fits into cells, it is organized into chromosomes. Humans have 46 chromosomes within a somatic cell and 23 within reproductive cells. Within the chromosomes DNA is tightly packed around proteins called histones, and the DNA/protein complex is then called chromatin.[5] In order for DNA replication to occur, the chromatin and helices both need to be unwound to make the individual strands of DNA accessible. A depiction of DNA organization can be seen in Figure I.2. DNA replication occurs within the S (synthesis) phase of the cell cycle. The cell cycle is divided into G_1 in which the cell is growing, S phase; in which cellular DNA is duplicated, G_2 when the cell is growing and preparing for division, and M (mitosis) phase, in which chromosomal condensation and nuclear division occur. There are checkpoints during the cell cycle which are used to control the cell cycle, and either causes it to continue or to pause. G_1/S is the first checkpoint, if the cell continues through this checkpoint then it is committing to proceeding through the cell cycle. The G_2/M checkpoint stops after synthesis and before mitosis to check for accuracy of the DNA replication and can pause to repair the DNA if it has been damaged.[6-7]

When the cell is getting prepared to enter S phase, proteins must be assembled in preparation of replication. The origin replication complex (ORC), a multi-subunit protein serves as the initiator protein for replication; meaning that it binds to a recognition start site in DNA in an ATP dependent manner. ORC is also responsible for the start of protein assembly for the pre-replicative complex (pre-RC) by interacting with CDC6.[7] CDC6 is one of the most important proteins for assembling proteins onto the DNA for replication. CDC6 protein levels are regulated by the cell cycle and are at high expression in M-G1 transition and the G1-S transition. Without CDC6, cells are unable to replicate their DNA, and with too much CDC6 they replicate it overly abundantly without stopping for mitosis.[7] From this it appears that ORC when chromatin bound recruits CDC6, and then the ORC/CDC6 complex in turn recruits minichromosome maintenance (MCM) proteins in this case MCM2. MCM2-7 in eukaryotes is likely the helicase responsible for unwinding the DNA helix.[7-8] The pre-replicative complex of the ORC, CDC6 and MCM2 are assembled during G1 phase, however replication does not begin until the cells have entered S phase. The control of DNA replication appears to be initiated by cyclin-CDKs which phosphorylates and causes the disassembly of the pre-RC. In order for replication to begin, the pre-RC must be disassembled and the pre-IC must become assembled.[7, 9]

As the cell transitions to S phase, MCM10 is loaded onto the chromatin which is likely facilitated by phosphorylation of human ReqQ4 helicase which is a target for CDK and has a binding site for MCM10. This phosphorylation also allows the binding of Cdc45 and GINS to form the pre-initiation complex (pre-IC). Next, the pre-IC turns into the CMG complex (CMG stands for Cdc45, MCM2-7 and GINS) by the addition of MCM2-7 to Cdc45

and GINS.[9] The CMG complex encircles the DNA and is the active replicative helicase responsible for unwinding the double stranded DNA helix, and is the core of the replisome progression complex (RPC).[10-11] A summary of the basic steps to initiate replication as described above is depicted in Figure I.3. Additional components of the RPC include Tof1-Csm3 complex which is used to allow the complex to pause at protein-DNA barriers, along with FACT, a histone chaperone; Mrc1, a checkpoint mediator, Top1 a type I topoisomerase, Mcm10 and Ctf4 which are proteins bound to DNA polymerase α-primase (pol α).[10] The GINS complex is also able to associate with DNA polymerases α, δ and ε. DNA is only replicated in a 5' to 3' manner; therefore one strand is replicated continuously—known as the leading strand, while the other is done in a non-continuous manner—known as the lagging strand, this is termed semi-conservative replication.[1, 12] DNA polymerase (pol) α primase is utilized to prime the leading and lagging strands with RNA making a DNA-RNA primer hybrid to use as template for replication by creating a 30-40 nucleotide sequence of DNA-RNA with a 3'-OH group.[8, 10] Once the template is made, replication factor C (RFC) facilitates polymerase switching from pol α to proliferating cell nuclear antigen (PCNA); PCNA is the sliding clamp that holds the replicative polymerase onto the DNA template.[8, 10]

There are three major stages to DNA replication: initiation, elongation and termination. Initiation, described above prepares the replisome for actual DNA copying to occur. Elongation is the act of the replisome processing along the DNA, inserting nucleotides which makes the daughter strand of DNA.[13] In order to maintain genomic integrity, DNA replication must be very quick and accurate; the error rate of replication is ~1 x 10^{-6} (i.e. the replicative polymerases make 1 error for every million bases they copy) but the addition of

proofreading activity and mismatch repair (MMR) lowers this error rate to ~1 x 10^{-10} for any given replication cycle, as shown in Figure I.4.[8, 14] MMR is a repair process which removes normal bases that are not in the correct pairing, helping correct DNA replication errors. This process uses strand discrimination to remove the base from the newly synthesized strand instead of the parental strand.[15-16] One of the reasons for this low replicative error rate is the differences in free energy between a correct base pair and an incorrect base pair, as well as the proofreading exonuclease activity associated with some of the replicative polymerases all help ensure the correct base is inserted lending to the low spontaneous mutation rate of replication. The estimated rate of spontaneous replication error is about ~1 x 10^{-10}, or 1 in every 10,000,000,000 per nucleotide per cell replication.[8, 14, 17-19] While this rate (i.e. < 1 mutation per genome per cell generation) may seem like a small number, the number of cells that are replicating and the number of times cells replicate over the human life span add up, leading to consequences such as aging and cancer.

DNA pol α, δ, and ε are all part of the B family of polymerases, whose protein structures are shaped to strongly select for the correct Watson-Crick nucleotide pairs into the active site. The geometric structure of a normal Watson-Crick base pair is different than that of a non-Watson-Crick mispair, in which the glycosidic dihedral bond angles are different as well as the C1'-C1' distance and H-bonding locations vary, all of these help the polymerase select the correct base for insertion.[20] Leading strand synthesis is replicated in a continuous manner by DNA pol ε, however, the lagging strand is discontinuous and occurs in patches of about 250 base pairs at a time called Okazaki fragments. Each of the Okazaki fragments is initiated by DNA pol α-primase and then is extended by pol δ.[8] The lagging strand is

inherently more complicated due to its fragmented replication. Replication protein A (RPA) coats the single stranded DNA region of the lagging strand to prevent reannealing while it waits to be replicated by pol δ.[8, 21] The DNA polymerases add the 5'-phosphate group of the incoming nucleotide to the 3'-OH group on the existing DNA, thus migrating in a 5' to 3' direction.[22] A simplified cartoon model of the process of eukaryotic replication can be visualized in Figure I.5.

After initiation and elongation, termination is when replication has been completed and the replisome is disassembled.[13] Termination is promoted from converging replication forks, and it is facilitated by 71 chromosomal termination regions (TERs) which influence how fast the replication forks progress and therefore merge. Then Rrm3 which is a DNA helicase and DNA topoisomerase 2 (Top2) help facilitate the fusion of the replication forks at the TERs.[23] DNA must then be rewound and packaged back into chromatin. This occurs in a replication-coupled (RC) nucleosome assembly, where new and parental H3-H4 are deposited followed by the H2A-H2B dimer onto the DNA, and this is all regulated and assisted by multiple histone chaperone proteins.[24] After DNA replication is complete, the cell cycle can move onto mitosis and cytokinesis.

DNA Damage

As previously mentioned, replicative errors can occur, leading to mutations. However there are many other ways that mutations can occur. One of the main spontaneous mutations within cells is base depurination.[17] Depurination occurs when the N-glycosylic bond between a purine and its deoxyribose sugar is cleaved, which releases the base and causes an apurinic

site.[17, 25] Depurination is very mutagenic as it can occur in physiologic conditions and happens with a high frequency, with an estimate of 10,000 depurinations per cell per day.[17] One of the reasons depurination is so mutagenic is the seeming preference for the insertion of deoxyadenosine across from the abasic site.[17] Abasic sites can also occur at pyrimidines (apyrimidinic sites) but they do so with less frequency than apurinic sites. Abasic sites can also be caused by base excision repair (a repair mechanism detailed later). Abasic sites can cause fork stalling leading to either fork collapse or mutations when they are bypassed by translesion synthesis (TLS), a tolerance mechanism.[25] Base deamination is the loss of an exocyclic amino group which can occur spontaneously on cytosine, adenine or guanine but occurs with greatest frequency on cytosine. Deamination of cytosine leads to a uracil paired with adenine—this can result in a C to T mutation, but cells have a robust repair mechanism to prevent this error.[15]

UV radiation is a common exposure due to sunlight. UV is broken down into three subdivisions: UV-A (320 to 400 nm), UV-B (295 to 320 nm) and UV-C (100 to 295 nm). UV-C has historically been used in the DNA damage field due to its potency caused by the 254 nm emission being very close to the peak absorption of DNA which is 260 nm as well as its ability to generate cyclobutane pyrimidine dimers (CPDs). However, most UV-C is filtered out of the atmosphere by the stratospheric ozone layer, and human exposure consists of mainly UV-B and UV-A.[16] CPDs occur when two adjacent pyrimidines become linked by a four member cyclobutane ring, caused by the saturation of the pyrimidine 5,6 double bond. CPDs can exist in multiple conformations but most often are *cis-syn* within normal double-stranded B DNA.[16] CPDs are most frequently two thymine's connected, giving the classic

term “TT dimer”, however they can also occur as TC, CT, or CC which are influenced by the DNA sequence of the irradiated region. CPDs are unable to be bypassed by replicative polymerases and cause a replication fork block. CPDs can also be bypassed by translesion synthesis (TLS), a tolerance mechanism that is thought to exist to allow a cell to potentially have an incorrect base inserted across from a lesion rather than end up with a prolonged replication fork blockage which would likely cause a strand break, almost assuredly leading to either cell death or extensive mutagenesis. TT dimers have been visualized by the help of crystal structures which shows that the DNA helix is distorted, bending approximately 30° towards the major groove and also unwound by 9°.[15] C containing pyrimidine dimers are much less stable, often deaminating to uracil.[15] Another major UV related lesion is a pyrimidine-pyrimidone (6-4) photoproduct (6-4PP); which links the C6 of a 5' pyrimidine to the C4 of the neighboring pyrimidine. 6-4PP usually occurs in TC or CC and occasionally in TT. This 6-4PP lesion only is formed in one stereoisomer and it causes a major distortion in the DNA helix due to the 3' pyrimidine ring being almost parallel to the DNA helix axis and being perpendicular to the 5’ pyrimidine ring, this lesion is usually repaired by nucleotide excision repair although if TLS is performed on this lesion, it usually inserts a G.[15-16] A correctly paired TT (6-4) photoproduct has been analyzed by NMR and shown that it causes the DNA to bend towards the major groove by 44° and become unwound by 32°.

Additionally, DNA can be damaged by a variety of chemical exposure. One example is *cis*-diamminedichloroplatinum (cisplatin); originally used as a mustard gas in the world wars, it was later modified and utilized as a chemotherapeutic agent.[16] Cisplatin’s mechanism of action is crosslinking DNA strands; if the crosslinking occurs on the same strand it is

called an intrastrand crosslink, and if it occurs on two separate strands then it is called a interstrand DNA cross-link. Interstrand crosslinks are caused by cisplatin, and are important because they prevent the DNA from separating and therefore blocks DNA replication and transcription. Additionally, cisplatin also causes 1,2-intrastrand linkages between adjacent guanines on N7.[16] Cisplatin causes mutations mainly in the form of G:T and A:T transversions. Pol η can help suppress mutagenesis across from cisplatin-GG intrastrand crosslinks by inserting the correct C pair.[15] *N*-methyl-*N*'-nitro-*N*-nitrosoguanidine (MNNG) is another chemical agent. MNNG causes methylation of the DNA, and its major lesion is O^6-methylguanine (O^6-MeG). MNNG is an S_N1 alkylating agent, and defects in MMR can lead to increased resistance of such agents. MNNG normally leads to S phase checkpoint followed by MMR-dependent G_2/M arrest and apoptosis. O^6-MeG inhibits DNA replication and triggers repair through MMR. O^6-MeG is recognized by MSH2-MSH6 heterodimer and then signals downstream checkpoints.[16]

Another naturally occurring way to get DNA damage and mutagenesis is oxidative stress. Reactive oxygen species (ROS) is naturally occurring due to cellular metabolism—with the major source being the mitochondrial electron transport chain, but it also occurs from phagocytosis, cell injury and metabolism or detoxification of chemicals.[15, 17, 26] All of these mechanisms generate various forms of oxygen species that can damage DNA, RNA, and proteins.[17] This production of ROS from oxygen is considered the "oxygen paradox", in that it is necessary for energy production yet it is dangerous and can lead to attacks on DNA from ROS.[16] Reactive oxygen species can come in the form of radicals such as superoxide anion (O_2^-) and hydroxyl radical ($HO^\cdot$) as well as non-radical forms such as hydrogen

peroxide (H_2O_2). These different ROS have varying deleterious effects; superoxide anion can produce hydrogen peroxide, and can either cause damage or produce hydroxyl radical. Hydroxyl radical is the most toxic ROS, and is reactive on DNA, although it must be produced within 1-2 molecular diameters of DNA in order to react with it due to its high reactivity.[15-16] The hydroxyl radical attacks DNA in two main ways; it attacks the double bonds that are within the DNA bases, or by removing a hydrogen from the deoxyribose sugar attached to the DNA base. Hydroxyl radical attacking the sugar can result in fragmentation of the sugar, or it can cause the loss of the base and a strand break if it occurs on a terminal sugar residue.[16] Examples of the chemical reactions that cause and mediate ROS can be seen in Figure I.6. ROS causes oxidative stress when there becomes an imbalance in cellular processes, either from an increase in ROS or from a decrease in antioxidants. Oxidative stress can induce damage, to DNA in the form of lesions as well as cause lipid peroxidation and protein oxidation or degradation, as well as change signaling patterns within the cell.[26-27] DNA oxidation in the form of oxidative lesions can lead to errors in replication and possibly mutations. DNA protein crosslinks can also occur between carbon radicals and the carbon chains of the amino acids, and this causes DNA replication errors as well as interferes with the structure and function of the protein.[15] While the amount of ROS generation appears overwhelming, cells have developed many protective mechanisms to combat the imbalance that could occur by their generation. ROS can be mediated by antioxidant enzymes such as superoxide dismutase (SOD) which can turn superoxide into hydrogen peroxide. Hydrogen peroxide in turn can be converted to water and oxygen by catalase. There are also other mechanisms to reduce hydrogen peroxide using glutathione or cytochrome c, for example.[16]

Imbalance of oxidative stress, and accumulation of oxidative damage can lead to mutations and increase in certain cancers.[16]

In addition to naturally made ROS from cellular processes, there are many chemicals that can interact with these cellular processes causing an increase in the amount of ROS produced, two examples are menadione (MD) and methylene blue plus light (MBL). Methylene blue (MB) is a redox dye which carries a positive charge and is reduced on the cell surface before being transported into the cell membrane. Once within the cell membrane, MB is re-oxidized and therefore it cannot escape the cell. MB within the cell can then interact directly with oxygen or with heme-containing proteins.[28] MB can also activate the pentose phosphate pathway within the cell which is the pathway utilized to make nicotinamide adenine dinucleotide hydride (NADH) and some precursors of nucleic acid. One way this pathway might be activated is by the reduction of NADPH to $NADP^+$ caused by MB.[28] MB is utilized as a way to generate oxidative stress in the laboratory, specifically a lesion called 8-oxo-guanine (8-oxoG), but it is also utilized in the clinic for numerous reasons including a treatment for methemoglobinemia and as an antidote for paraquat poisoning.[28-29] Menadione (MD) is a chemotherapeutic agent which can be reduced at the Complex I of the mitochondrial respiratory chain and lead to the production of O_2^-. MD can activate apoptosis through a Ca^{2+} -dependent mitochondrial pathway.[30-31]

8-oxo-guanine

8-oxoG is a highly mutagenic oxidative lesion because it can rotate around its axis and Hoogsteen base pair with adenine instead of base-pairing normally in a Watson-crick

base pair with cytosine. When 8-oxoG is in the *syn* conformation it can base pair in a 8-oxoG:A pair which looks very similar to a normal T:A base pair making it hard to detect and repair and can lead to a transversion mutation.[16, 32] Eukaryotic replicative polymerases can replicate 8-oxoG by inserting an A across from it, causing a G:C to T:A transversion.[33] This is a very common place lesion and bypass error, however eukaryotes have multiple mechanisms to try and prevent and repair 8-oxoG from being mutagenic.

In addition to damage to guanine after the incorporation into DNA, damaged guanines can be directly incorporated into DNA. 8-oxoG also denoted in some of the literature as 8-oxo-dGTP, can come from oxidation of dGTP, or from the oxidation of 8-oxo-dGDP and then nucleoside diphosphate kinase can convert the nucleoside diphosphate to a triphosphate. In order to try and prevent the incorporation of 8-oxoG into DNA, cells utilize 8-oxo-dGTPase which are used to hydrolyze 8-oxo-dGTP to 8-oxo-dGMP which helps to reduce the 8-oxo-dGTP pool. This GTPase is encoded by MTH1. Once the pool is reduced to 8-oxo-dGMP, it is unable to convert back to dGDP or dGTP as human guanylate kinase is not able to phosphorylate dGMP. This leads to the further dephosphorylation of dGMP to 8-oxo-deoxyguanosine which can then be excreted in the urine.[15-16]

Since it has been established that 8-oxoG can occur either by oxidative damage onto the dGTP pool or to already utilized dGTP within the DNA strand, there are multiple pathways to try and repair the damage once it is within the DNA. One protein within *E.coli* termed formamidopyrimidine-DNA glycosylase, or Fpg, also known as MutM can directly remove 8-oxoG from the DNA strand due to its glycosylase activity. Additionally there is

another glycosylase within *E.coli* that can help remove 8-oxoG if it is mispaired to an A, it is called MutY. MutY does not directly remove 8-oxoG but rather removes the incorrect A from the undamaged strand, BER then usually inserts a C leading to a GO: C pair which can then be acted on by MutM which can in turn remove the 8-oxoG. One more enzyme, termed MutT helps to prevent the incorporation of 8-oxoG by hydrolyzing 8-oxodGTP as previously described. Humans are known to have a homolog to MutY called MYH.[15-16]

Mutagenesis

DNA damage does not inherently mean mutations. In order for DNA damage to turn into a mutation, the damage must occur, must be unsuccessfully repaired and must be replicated incorrectly, therefore imprinting it into the DNA. Many chemicals and environmental stressors such as UV light are considered mutagens in that they increase the prevalence of mutation generation. Mutagenesis, which is the process of mutation generation, can be caused by mutagens or by spontaneous means such as replicative error as previously described.[16, 18] There are different types of mutations within DNA which include point mutations, insertions and deletions. Point mutations are mutations that occur either as a single base insertion or deletion, or by a single base substitution. A base substitution is the changing of one base to another, for example a G becomes an A. There are two types of base substitutions: transitions and transversions. A transition base substitution is a substitution within the same class of base, for example one purine is exchanged with another purine (A and G), or a pyrimidine exchanged for another pyrimidine (T and C); whereas a transversion mutation is a base substitution mutation in which a purine is substituted for a pyrimidine and

vice versa (e.g. G to T).[16] Base substitution mutations can be further categorized by their effect. If a base substitution results in a change from one amino acid to another amino acid, then the mutation is called a missense mutation. This type of mutation is frequently responsible for changes in gain or loss of function mutations which drive carcinogenesis. A nonsense mutation occurs when a point mutation changes the original amino acid to a stop codon, which usually leads to early termination and a non-functional protein. There are also silent mutations, in which the nucleotide sequence changed due to the mutation but the codon still reads for the same amino acid therefore the mutation goes unnoticed physiologically.[16] Mutations do not only occur at a single point, or single base; often there are insertions or deletions of more than one base in a row, as well as tandem base substitutions and complex base substitutions. When one of these types of mutations occurs, specifically insertions and deletions of greater than one base, then it often leads to (but not always) a frameshift. A frameshift occurs when there is an insertion or deletion of 3*n* +/- 1bp, resulting in the amino acid sequence which is used for translation is shifted, this can lead to alterations in the function of the protein or lead to a non-functional protein.[16]

The location of mutations can cause a difference in the molecular effects within the cell. Mutations within the promoter can vary the level of the gene expression and mutations within the regulatory sequence of the gene can alter the regulation of gene expression. Mutations within the 3' of the protein-coding region can cause of defect in transcription termination or alteration of mRNA stability, mutations within the intron can change mRNA splicing and mutations within the origin of DNA replication can cause a defect in DNA replication initiation.[16]

Translesion Synthesis (TLS)

Translesion synthesis is a tolerance pathway used to bypass lesions that block the replication fork. Once the replication fork is stalled, specialized polymerases called TLS polymerases are brought in, they insert a nucleotide across from the damage, and extend past the damage—thus allowing replicative polymerases to return and continue replicating DNA, giving the term "lesion bypass". TLS can insert the right base and be high fidelity, but often times it inserts the wrong base which leads to mutagenesis. TLS is a tolerance pathway and not a repair pathway because it does not take out the lesion, but rather inserts a base whether correct or incorrect across from the lesion and extends past the damage in order to allow DNA replication to continue. This occurs when replication is occurring and replicative polymerases stall.[8, 15-16, 34-43]

The TLS polymerases include DNA polymerase η, encoded by Rad30A, DNA polymerase ι (pol ι) encoded by *Rad30B*, DNA polymerase κ (pol κ) encoded by *DINB1*, and dCMP transferase Rev1 encoded by *UmuC* all of the Y family of polymerases as well as DNA polymerase ζ, of the B family of polymerases. Each of these polymerases has varied cognate lesions which they are able to bypass with differing fidelities based on which polymerase is bypassing which lesion.[15-16, 19]

TLS polymerases lack the 3' – 5' exonuclease activity associated with normal replicative polymerases, and they have much higher error rates than replicative polymerases, on the magnitude of 10^{-2} to 10^{-4}. Although the lack of exonuclease activity contributes to this high error rate, it is not the only reason. TLS polymerases characteristically have large, open

active sites which allow for the accommodation of large bulky lesions. This structural difference allows for variability in what nucleotide is incorporated, as it is not a geometrically constrained fit like in a replicative polymerase.[15, 38] All polymerases contain a finger, palm and thumb domain.[44] The A-, B- and Y-family polymerases all share highly conserved palm domain, but the secondary structures of the thumb and finger domains are vastly different between these families. The Y-family polymerases thumb and finger regions are considerably smaller than that of the A- and B- families. Y-family polymerases all contain four domains, a palm, finger, thumb and little finger (LF), with the thumb and LF constituting the active site (see the structure in Figure I.7).[36] Within these regions, the Y-family polymerases all have a conserved catalytic active site within the N-terminal polymerase which is approximately 350-450 residues, of which about 100 of the residues are only in the Y-family and make up the little finger domain. The little finger, in combination with the thumb domain is used to hold the DNA substrate, and this is where the flexibility lies allowing for the flexibility to accommodate varying lesions. On the opposite side, the C-terminal side contains an appendage which is used for regulatory protein-protein interactions which varies in size depending on the polymerase. Human and mouse Rev1 contains an extra N-terminal BRCT domain not found in the other Y-family polymerases.[45]

There are multiple models for TLS in which might all be accurate depending on the circumstances due to the use of different polymerases and these are illustrated in Figure I.8. TLS can be either a one or two polymerase system. In the one polymerase mechanism, a single TLS polymerases is used and it inserts across from the lesion, as well as extends past the lesion. In the two polymerase system, one polymerase is used to insert a base across the

lesion but a second polymerase then is used to extend past the lesion. Whether the system is either one or two polymerases is based on the type of lesion and which polymerase(s) are used.[15] An example of each mechanism is: the bypass of a TT dimer by pol η is likely a one polymerase system, but bypass of AP sites by Rev1 and pol ζ is likely a two polymerase mechanism.[15] Due to the low fidelity of these polymerases they are highly regulated and kept at low levels during normal replication in order to keep mutagenesis to a minimum and are recruited when needed to damaged DNA during fork stalling. These polymerases are likely regulated transcriptionally and post-transcriptionally in order to keep them at low levels until needed.[15]

POLH, also known as *hRAD30A*, is the gene that encodes for human DNA polymerase η, one of the TLS polymerases. It was first discovered in *S. cerevsiae* in 1999 and is found in mice, drosophila and humans.[38] POLH contains 11 exons over 40 kilobases and is located on human chromosome 6p21.1-6p12, with one of the 11 exons is untranslated.[34, 38] Human pol η is 713 amino acids long and 78 kDa. Protein complementation studies found that the addition of pol η into a xeroderma pigmentosum variant (XP-V) cell line, discussed below, was able to restore the cells ability to bypass CPDs.[38] Based on further *in vitro* replication and biochemical studies of pol η, it is known that pol η bypasses CPDs well.[34] Bypass of CPDs by pol η is more accurate than other polymerases, and less mutagenic than double strand breaks (DSBs) which would occur if the lesion was unable to by bypassed, however bypass by pol η still produces errors approximately 1 out of 30 times, at least *in vitro*.[42] Pol η is able to bypass damaged bases, TT dimer and 8-oxoG with better fidelity than across from their undamaged counterparts.[42, 46-47] Single nucleotide kinetics has

shown that dATP is inserted across from both the 3' and 5' T in the TT dimer. When TT dimers were studied biochemically in a nucleotide competitive environment it showed that dimer bypass fidelity was relatively low. This study by McCulloch et al. showed that pol η bypasses the 5' T of the dimer 4.4 times more accurately than on undamaged T ($32x10^{-4}$ versus $140x10^{-4}$). The most frequent insertion was of G across from the 5'T with an error rate of $32x10^{-4}$ which created a T to C transversion, whereas the 3'T has an error rate of $390x10^{-4}$. This experiment shows that there is a bias on the lesion position for the fidelity and it was determined that this was due to the lesion and not the sequence content as the experiment analyzed multiple sequence contexts. The difference in fidelity by placement is likely due to base pair energetics and base pairing stability.[46] In order to better understand how the fidelity of pol η works, the crystal structure of the catalytic domain (amino acids 1-432) was solved in 2010. See Figure I.9 for the structure of pol η. The structure of pol η acts as a molecular splint in which it keeps the damaged DNA section straight due to the high positive charge on the DNA-binding surface, this allows it to interact with four upstream template nucleotides above the active site. The LF domain (aa 316-324) has a β-strand which is almost parallel to the template strand and this LF domain also interacts with the template and primer in the minor groove.[16, 36] Based on the interaction of pol η with the template strand, it leads to the ability of pol η to extend past the lesion 3 base pairs, after which the major-groove interactions with the lesion (CPD) is too far away and are no longer stabilized leading to the natural dissociation of the polymerase from the template.[36, 41] Pol η is localized in the nucleus by its nuclear localization signal that occurs within the C-terminal end. Following DNA

damage by UV, pol η is recruited into foci and it was determined that the N-terminal zinc finger motif is required for this foci formation[16].

Rev1 is considered a dCMP transferase because it preferentially inserts a C no matter what the template is. Therefore, if Rev1 is replicating on a run of G's it puts in the correct base of C, however it continues to put in C's even across the other bases and lesions. The reasoning for its choice of base was discovered to be due to the use of Arg324 within its own protein as the template instead of using the DNA template.[15, 45, 48] Pol κ is the TLS polymerase known for its bypass ability of (-)-*trans*-*anti*-BPDE-N^2-dG adduct, although it can also bypass the (+)-*trans*-*anti*-BPDE-N^2-dG adduct which are both adducts formed by benzo[a]pyrene, and pol κ is able to insert the correct C nucleotide across from these adducts.[16] Pol κ also can bypass AP sites but does so in a potentially error prone manner, often inserting an A opposite the AP site. Pol ι preferentially inserts G across from an undamaged T template instead of the appropriate A. However when confronted with a TT (6-4) photoproduct, pol ι usually incorporates the correct A pair. When attempting to bypass TT dimer, pol ι struggles, and when it is able to bypass it does so by inserting a T, leading to increased mutagenesis.[15] To show how specific each polymerase is for their specific lesions, it should be noted that the TT dimer blocks the activity of pol κ and ζ, therefore they cannot insert across from 3'T of the dimer, however if pol ι inserts across the 3'T, it usually cannot extend, and pol κ or ζ is able to do the extension step. With this pol η helps to suppress mutagenesis across from TT dimers, as it can sometimes accurately bypass it, and in its absence there is a great increase in mutagenesis.[15-16]

One of the other uses for TLS in addition to damage bypass is somatic hypermutation. Somatic hypermutation is the production of antibodies by B cells which is accomplished by base substitutions within the DNA of the V regions of Ig genes. This process is started by cytosine deamination followed by replication using TLS polymerases, specifically Rev1, and pol ζ with some implications of pol η and ι also might be involved.[15, 44] This process creates around one billion antibody variants for the immune system.[48]

Regulation and availability of the polymerases

One of the main regulatory mechanisms known for TLS is the ubiquitination of PCNA. After DNA damage occurs, a DNA damage response is triggered including the monoubiquitination of PCNA by Rad6-Rad18 on Lys164, which leads to the recruitment of TLS polymerases.[19, 49] Rad18 binds to single stranded DNA, which may be the trigger to cause its ligase activity for PCNA. When replication is blocked, Rad18 binds to ssDNA, once bound it recruits Rad6 and together they monoubiquitinate PCNA.[50] Once monoubiquitinated, PCNA has a higher affinity for pol η and other TLS polymerases, which provides a good mechanism for potential polymerase switching.[50-51] The PCNA-interacting protein domain (PIP1 domain) within pol η appears to be required for its TLS ability; and even though there are two PIP domains, 1 and 2, functional PIP2 is not sufficient for performance of TLS, PIP1 is therefore required for functional TLS.[52] In addition to the necessity of the PIP1 region, there is also a ubiquitin binding zinc finger domain (UBZ) and the nuclear localization signal (NLS) that are required for pol ηs function in TLS. NLS is important in the regulating the interaction between pol η and PCNA though cycling of

monoubiquitination and deubiquitination of this region. The UBZ is important due to the fact that it binds to the K164 ubiquitin on PCNA. Polyubiquitination of K63 on PCNA is thought to be involved in restarting the stalled replication fork by recruiting ZRANB3/AH2.[19, 49]

Pol η after UVC damage localizes into nuclear foci. This was investigated also in pol ι and was found that after UV-C treatment, pol ι also localizes into nuclear foci but only in the presence of pol η; in cells lacking pol η, pol ι was unable to localize. The interaction of pol η and pol ι is through a direct interaction using the residues 492-715 of the C-terminal end, which is not the catalytic region, of pol ι.[53] The region of pol η necessary for the interaction with pol ι is likely between aa 352-595, although the experiment could not rule out the residues 595-713 also being necessary. This direct interaction is only a fragment of the overall pol η within the cell, but is likely the reason for the co-localization within the nuclear foci.[53] The C-terminal region of pol η, amino acids 595-713 is region responsible for pol η's localization to replication foci.[54] While it is well known that the two interact, this leads to questions as a lot of the mutagenesis data in the field suggests that pol ι is a backup mechanism for pol η.[55-56] This being said, it appears that pol ι, although highly dependent on pol η to localize to the nucleus, can also interact with PCNA and PCNA can help pol ι localize, albeit at a lower amount. There is also evidence that some TLS is able to occur without the formation of foci.[57] Once localized, PCNA, RFC and RPA help pol ι in the TLS process.[58] The action of RFC and RPA alone do not appear to be enough to increase the activity of pol η, but in combination with PCNA the activity increases about 12 fold.[59-60]

The human relevance of DNA polymerases is in their involvement in cancer; whether by creation of mutations, or their involvement in possible chemotherapeutic resistance. Although the levels of the various polymerases appear to vary widely depending on the patient and the tumor, there is the possibility of predicting the outcome of treatment if the investigator would analyze for the level of the polymerases before and after treatment. Previous research has shown TLS polymerases ι and η are often over expressed in cancers, however pol κ is usually down regulated, except for its increase in lung cancer.[61-63] Additionally, a few other polymerases including pol β, which is involved in NER are also overexpressed in many cancers.[63] The overexpression of these polymerases can lead to increased mutagenesis and help fuel cancer progression, as well as cause resistance to chemotherapy. A very pertinent example is the presence of pol η during treatment with cisplatin. Based on a structural analysis, as well as a retrospective analysis of tumors analyzed for pol η mRNA levels determined that higher levels of mRNA was correlated with response to platinum based therapy: with low levels of pol η showing a greater response to platinum based therapy, and higher levels of pol η more likely failing, or having recurrence.[62, 64-65] This leads to the potential to either check for expression before chemotherapy treatment to determine whether platinum agents should be used or avoided; as well as the potential for a therapeutic inhibitor targeting pol η to be used in complement with traditional chemotherapy.

Repair Mechanisms: Nucleotide Excision Repair

Nucleotide excision repair (NER) is used for the removal of many types of DNA damage including bulky adducts. NER recognizes damage by looking for distortions within the helix instead of looking at the lesion itself.[15-16] NER is one of the most complex repair mechanisms but it can be broken down into six main steps. First it must find the damage, and in humans it is believed that the protein complex NPC-RAD23B is responsible for recognition. Second it must be able to get access to the lesion by unwinding the DNA in the local region, which is done by TFIIH. Third, it must make incisions on both sides of the lesions which are performed by XPF on the 3' and ERCC1-XPF on the 5'. The fourth step is the release of the DNA region containing the lesion, fifth is DNA synthesis by pol ε or δ in the excised region and sixth is ligating the newly synthesized region to the previously synthesized region by DNA ligase. These steps are summarized in Figure I.10. NER is usually a post-replication repair model, but there is also transcription-coupled NER (TC-NER) which is triggered when the RNA polymerase complex is blocked at a damage site. TC-NER is useful in that it helps transcription continue and not stop, therefore it helps prevent cell death. TC-NER is a fast and efficient repair model. One other type of NER is global genome repair (GGR) which is responsible for the repair of nontranscribed strands and unexpressed regions of the genome. GGR is therefore helps prevent mutagenesis by searching the helix for structural distortions. TC-NER and GGR have the same steps except for damage recognition since GGR is not initiated by RNA polymerase stalling.[15-16, 66]

Repair Mechanisms: Base Excision Repair

Base excision repair (BER), is one of the major repair pathways to get rid of damaged DNA bases. It uses enzymes called DNA glycosylases which recognize the damaged base and makes an incision/cleaves the N-glycosidic bond which is what connects the base to the deoxyribose-sugar backbone. Once the base is removed, it creates an AP site, next whether using an AP site caused by BER or from spontaneous base loss, a protein called an AP endonuclease hydrolyzes the phosphodiester bond on the 5' side of the AP site. DNA synthesis then occurs in either a one base, short-patch BER, or multiple bases which displace some of the previously synthesized strand, long-patch BER. For short-patch BER dRpase modify the ends and DNA ligase ligates the bases together. In long-patch BER, FEN1 is used to cleave the flap that was created from the displacement of some of the previously synthesized DNA, and then it is ligated by DNA ligase.[15-16, 44, 67] See Figure I.11 for a rendition of BER. The polymerase used to fill in the patch varies depending on the length, for short-patch, pol β is used, where in long-patch usually pol δ or ε synthesizes the patch. There are many different glycosylases which are utilized within the first step of detecting the damaged bases. Of interest to this research would be Fpg also named MutM which removes 8-oxoG in addition to other oxidized and ring-opened purines, as well as MutY which removes adenine when it is paired with 8-oxoG. MutY and MutM are both isolated from *E.coli*. Humans have OGG1 instead of MutM which also removes oxidized, ring-opened purines and 8-oxoG, as well as they have MYH which is the MutY homolog.[15-16, 67]

Cancer

The study of mutations is valuable because mutations are the start of what can turn into cancer. Cancer is a disease that needs a mutation which has a growth advantage over normal cells, leading to proliferation of the mutated cell. The first step towards cancer termed initiation or mutagenesis is the focus of this research. Initiation is the generation of a "stable, heritable change", and is usually the result of unsuccessfully repaired DNA damage.[15-16, 18, 68] Once initiated, the mutated cell might die if the mutation makes it unviable, it could also stay in a static state based on the conditions and normal cells around it, or it could contain a selective advantage resulting in cell proliferation. The second stage, promotion, can be brought on either by the selective advantage growth of the mutated cell on its own, or by the use of a tumor promoter.[68] Two endogenous mechanisms for the promotion of growth are either by the activation of a proto-oncogene or by the loss of function of a tumor suppressor gene. Proto-oncogenes are usually involved in positively regulating cell proliferation and help to ensure cell survival so mutations within this type of gene lead to a gain in function oncogene which often block apoptosis and stimulates cell survival. Tumor suppressor genes are usually negative regulators of proliferation and positive regulators of apoptosis, so this gene tends to have a loss of function mutation which leads to unregulated cell growth[69] In either case, the initiated cell begins to clonally expand which can create a preneoplastic lesion. Progression is the next and final step leading to carcinogenesis, and this is when the preneoplastic lesion which was benign, now converts into neoplastic cancer. During progression there is an increase in DNA synthesis due to the increased proliferation, this in turn can lead to additional mutations within the population of the tumor.[18, 68-69] The order and

timing are crucially important in the model of initiation through promotion; without initiation there will be no mutagenesis even if there is promotion, and without promotion even the mutation from the initiation event will not turn into cancer.[15, 69]

DNA damage as described previously is hard to avoid in life due to exposure to chemicals, radiation and oxidative stress. The main categories of DNA damaging agents are (1) direct-acting carcinogens, which are chemicals that do not need metabolically activated such as *N*-methyl-*N'*-nitro-*N*-nitrosoguanidine (MNNG). (2) There are also indirect-acting carcinogens which do need metabolically activated before they can react with DNA such as benzo[a]pyrene. (3) There is radiation and oxidative damage which can occur both directly and indirectly and (4) inorganic agents which have unknown mechanisms such as arsenic. UV light which is studied here, is recorded to cause around one million new cases of skin cancer each year, not including melanomas.[15, 69]

Carcinomas make up the majority of human cancers. These are tumors derived from epithelial cells in the various organs. The other types of cancers which are slightly less common are sarcomas which are derived from mesenchymal tissues, leukemia which are derived from blood forming stem cells and lymphomas which come from B and T lymphocytes.[15] This risk of developing some cancerous lesion within a human lifespan is 1 in 2 for men and 1 in 3 for women, with approximately 65-80% of cancer development being related to environmental exposures.[15]

Xeroderma Pigmentosum

Xeroderma pigmentosum (XP) is a sun sensitive, cancer prone disease phenotype that can be comprised of 8 varying subsets of the overall disease which are labeled XP-A through XP-G and XP-V. XP-A through XP-G all have varying deficiencies within NER, while XP-V is deficient in functional pol η. XP is an autosomal recessive disorder which is more prevalent in some populations: for example cases are rare in Caucasians approximately 1 in 250,000 people, however populations such as Japan and Egypt have increased rates at about 1 in 40,000 people.[34] Often patients with XP have parents who are consanguineous. There are a number of clinical hallmarks for XP including severe photosensitivity which is presented as especially painful sunburns in early childhood, skin dryness, premature skin aging, and malignant tumors including squamous cell carcinoma, basal cell carcinomas and melanoma on the face, head and neck. Some subsets of XP also have a neurological component.[34] Table I.1 illustrates the breakdown of the various subtypes by their effects and gene affected. The risk of tumors in XP is 1000 times greater than in the normal population and it starts much earlier in life.

The neurological involvement is thought to be due to neuronal death from oxidative stress induced DNA damage—leading to irreversible progressive symptoms. Some neurological symptoms include lowered IQ, spasticity, peripheral neuropathy and ataxia.[34] Additionally, approximately 40% of XP patients have ophthalmological symptoms including blepharitis, ectropion, and corneal abnormalities. They also have increased risk of neurological cancers and ocular neoplasias. Diagnosis of XP involves a series of serologic,

metabolic and genetic tests, unfortunately there is no cure for the disease and treatment includes treating the symptoms and preventing sun exposure.[34] XP-A through G patients often develop their tumors in their very early years with an average around age 8, and have a life expectancy into their 20s. XP-V is a more mild phenotype that does not have a neurological component, and they develop their tumors slightly later, in the mid-teens, and therefore can sometimes live into their 40s.[34]

XP-A through G constitutes 80% of XP patients, however XP-V is approximately 20% just on its own. XP-A patients are deficient in the NER protein XPA which is also utilized in transcription coupled repair (TCR), and therefore have some of the most severe clinical manifestations of the disease. XPB and XPD are helicases which are utilized in both NER and TCR. XPC is the largest subgroup of XP, and XPC is only deficient in global genome repair and not in TCR, they are free of neurological symptoms and only manifest in the severe UV sensitivity and skin tumors. XP-E, F and G are more rare then the other subsets. XP-E is deficient in the DNA damaging binding gene (DDB2), which is associated with helping repair CPDs. XP-F and XP-G are proteins used in NER, but at a lesser capacity than some of the other proteins and therefore present with a mild phenotype of XP and these patients have a slightly longer life expectancy. XP-V patients have functional NER but are deficient in functional pol η which is necessary for the TLS of CPDs.

The major clinical manifestation of XP is skin cancers, of which when evaluated, C to T and tandem CC to TT UV specific mutation spectrum is found. Approximately 50% of XP patients develop non-melanoma skin cancer (NMSC) by the age of 10, and while basal cell

carcinoma (BCC) is most prevalent in the normal population, there seems to be a higher proportion of squamous cell carcinomas (SCC) within the XP population. Part of the difference can be attributed to the mechanisms of BCC versus SCC: the major risk factor for BCC is childhood exposure to UV and then intense intermittent exposure to UV throughout life versus SCC being associated with more chronic cumulative exposure.[34] They also work through different mechanisms, in that BCC is mitigated through sonic hedgehog (SHH) whereas SCC works more through p53.

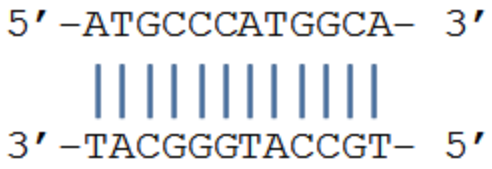

Figure I.1 – Example of a double strand DNA sequence. This is a simplified example of a double stranded DNA sequence. This image is used to illustrate standard base pairing.

Figure I.2 – Depiction of DNA organization within chromatin. A. This is a simplified depiction of DNA within the chromatin structure. With the lowest level of organization being the nucleosome which has two superhelical turns of DNA around a histone octamer. These nucleosomes are then connected by short linker DNA regions. At the next level these nucleosomes are folded into a fiber and then the fibers are further folded into chromosomes. **B.** This is an X-ray diffraction image of a structure of the nucleosome at resolution of 2.8Å showing the DNA double helix wound around the central histone. Figure reprinted and legend adapted from Felsenfeld and Groudine.[70]

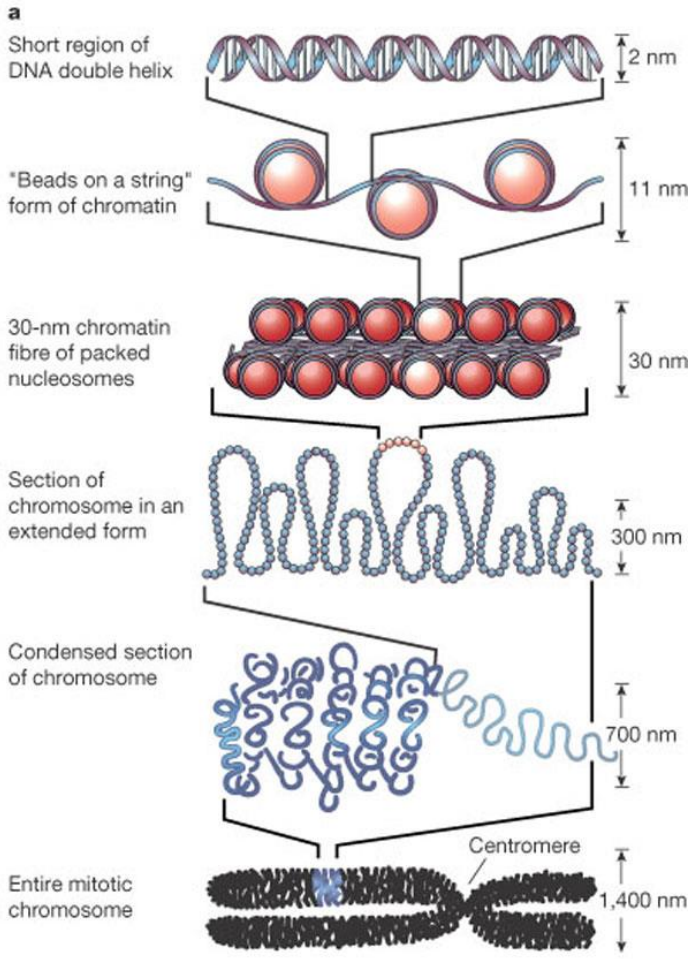
a
Short region of DNA double helix
2 nm
"Beads on a string" form of chromatin
11 nm
30-nm chromatin fibre of packed nucleosomes
30 nm
Section of chromosome in an extended form
300 nm
Condensed section of chromosome
700 nm
Centromere
Entire mitotic chromosome
1,400 nm
b

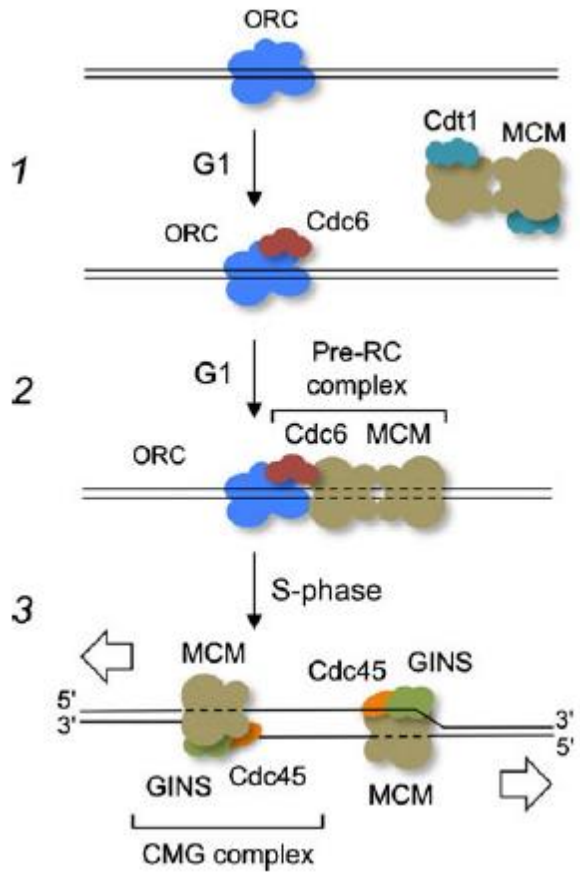

Figure I.3 – Assembly of the proteins at the replication origin. A. A simplified depiction of the steps leading to replication origin unwinding in yeast which has the same steps as in humans. Replication origins are bound by ORC, and during G1 phase, ORC recruits Cdc6 (step 1). This in turn recruits Cdt1/MCM complex forming the pre-RC complex (step 2). MCM is loaded onto double-stranded DNA. S phase beings when MCM is activated by GINS and Cdc45 (step 3). One CMG complex functions at each replication fork. Figure reprinted and legend adapted from Onesti, MacNeill 2013.[9]

.

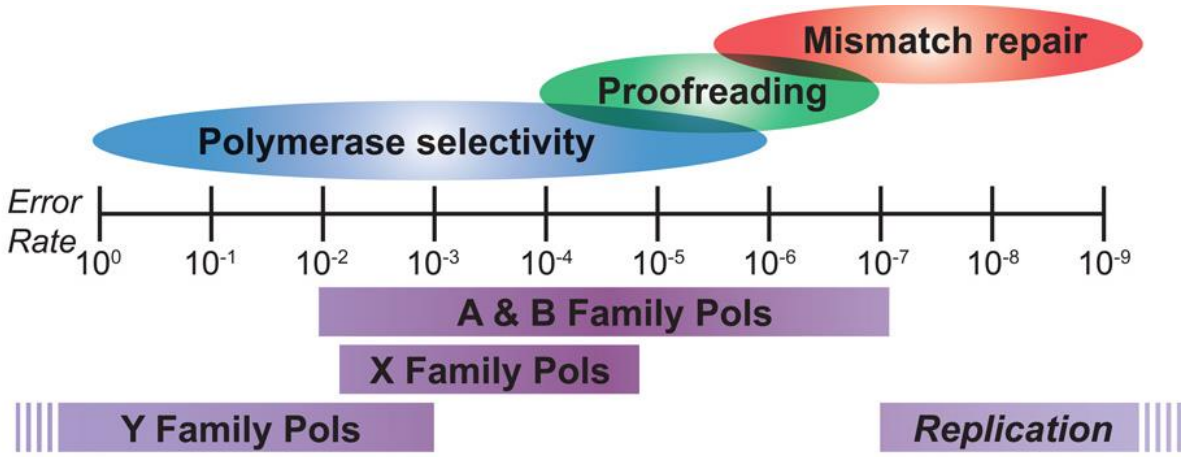

Figure I.4 – Replication fidelity. This is a depiction showing the relative contribution of the three main factors of replication fidelity. The ranges are overlapping due to the fact that there are multiple mechanisms to increase the level of fidelity, and within each family of polymerases the error rates vary. Figure reprinted and legend adapted from McCulloch and Kunkel.[8]

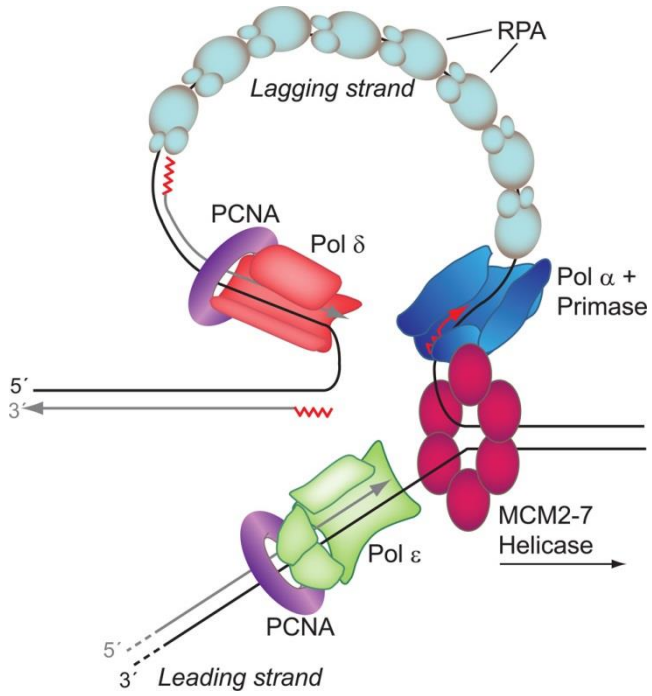

Figure I.5 Replication fork model. This is a simplified cartoon model of the eukaryotic replication fork. This model shows pol ε processing along on the leading strand while pol δ is assigned to the lagging strand. There is a helicase hexamer (magenta); RPA (light blue ovals); PCNA (purple torus); pol α-primase (blue); RNA-DNA hybrid primer (red zig-zag and arrow) and newly synthesized DNA (gray lines). Figure reprinted and legend adapted from McCulloch and Kunkel.[8]

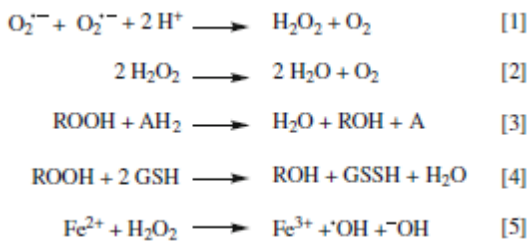

Figure I.6 – Main biochemical mechanisms for producing ROS. 1. Superoxide dismutase reacts with superoxide anion to form hydrogen peroxide and oxygen. 2. Hydrogen peroxide is converted to water and oxygen by catalase. 3. Catalase can react with various hydrogen donors using 1 mol of peroxide. 4. Glutathione peroxidase catalyzes the reduction of varying hydroperoxides using glutathione. 5. Fenton reaction produces hydroxyl radical. Figure reprinted and legend adapted from Mátes et al.[27]

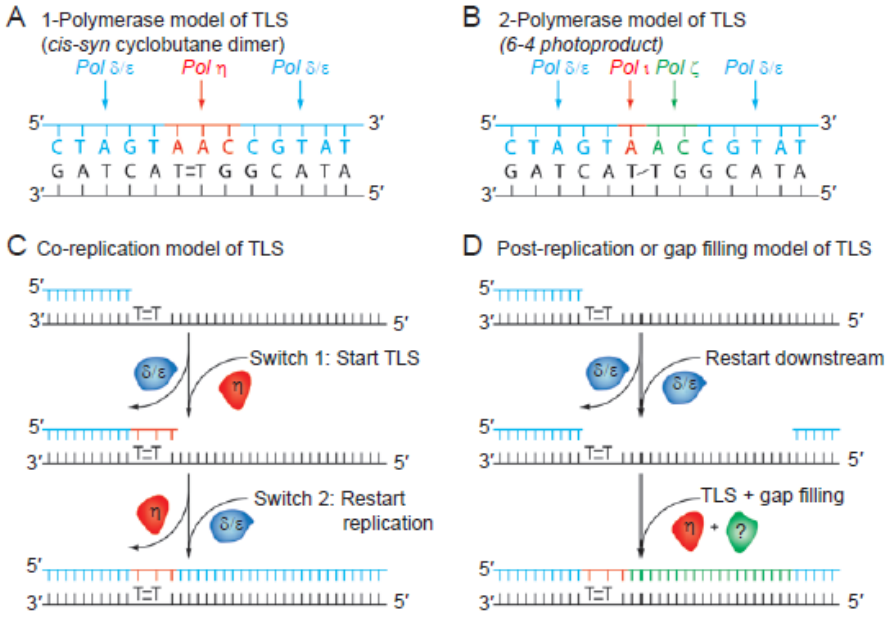

Figure I.7 – Varying models of TLS. (A) A one-polymerase model of TLS illustrated over a TT dimer. This shows a single polymerase being responsible for both the insertion and extension past the lesion. (B) Illustrated here is a two-polymerase model of TLS over a 6-4PP showing that different polymerases are responsible for the insertion versus extension step. In this model it shows that pol ι inserts across from the 5' lesion, and pol ζ inserts across from the 3' lesion and extends past the lesion. Both A and B are completing TLS within a relatively close proximity to replicative polymerases. (C) This is a model of TLS that occurs during ongoing DNA synthesis. (D) This is a gap-filling model of TLS in which TLS occurs away from the main replication. Both C and D can be utilized in either the one or two polymerase model of TLS as illustrated in A and B. A and B are models of the actual TLS process while C and D shows the timing of TLS and therefore there is overlap between the models. Figure reprinted and legend adapted from McCulloch and Kunkel.[8]

Figure I.8 – Structure of human pol η. (a) This figure illustrates the ternary complex of human pol η in complex with normal DNA. Protein domains are labeled and color coded. The DNA template is orange and the primer template is yellow. Oxygen atoms are red and nitrogen atoms are blue. dAMPNPP is illustrated as a ball-and-stick representation with Mg^{2+} as purple spheres. **(b)** This is an image of the active site Mg^{2+} coordination is shown by pale yellow dashed lines. The 3'-OH of the primer strand is 3.2 Å from the α-phosphate which is shown by the red dashed line. **(c)** Human pol η-DNA interactions in the active site. The protein side chains from the finger domains are light blue and the palm domain are pink sticks. **(d)** Illustration of the upstream interactions with DNA. The LF domain, shown as light purple ribbon, contacts both the template and the primer. The thumb domain, shown in green, only makes 3-4 hydrogen bonds with the primer strand. Side chains which contact DNA are highlighted and labeled. Figure reprinted and legend adapted from Biertümpfel et al.[36]

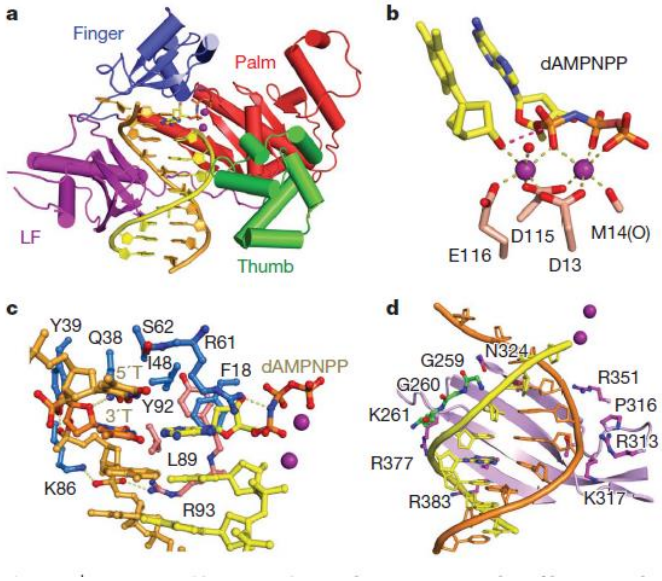
a
Finger
Palm
LF
Thumb
b
dAMPNPP
E116
D115
M14(O)
D13
c
Y39
Q38
S62
R61
I48
F18
dAMPNPP
5′T
Y92
3′T
L89
K86
R93
d
N324
G259
G260
K261
R351
P316
R313
R377
R383
K317

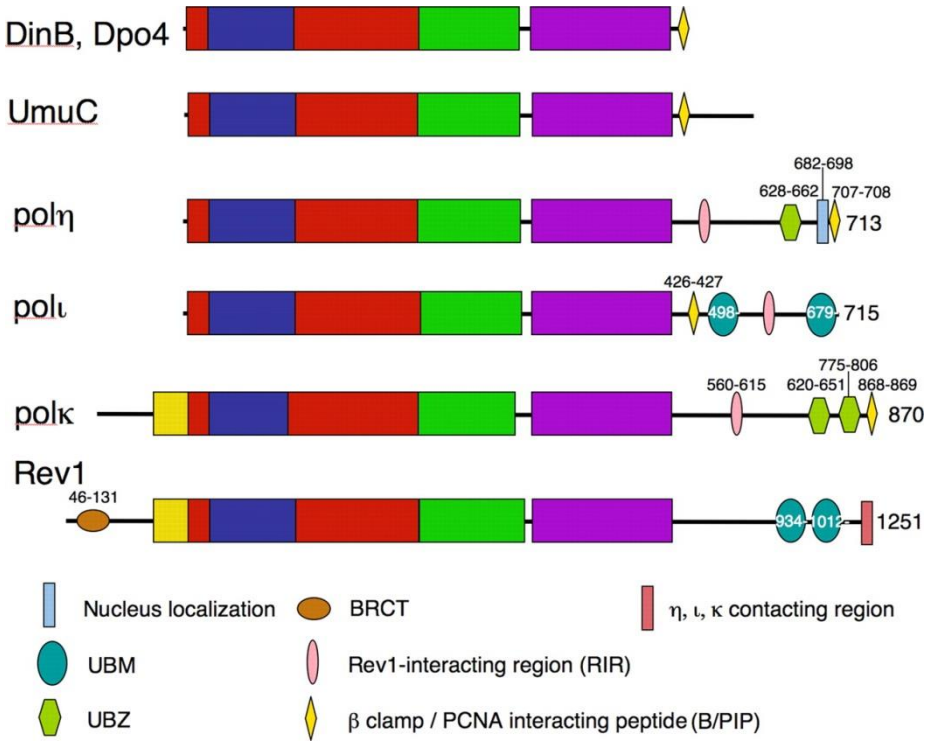

Figure I.9 – Structure Domains of the Y-family polymerases. The polymerase domains are labeled in the following colors: red (palm), blue (finger), green (thumb), purple (LF) and yellow (N-terminal addition for pol κ and Rev1). The regulatory units are listed in a legend within the figure. Abbreviations include: UBM for ubiquitin-binding motif, UBZ for ubiquitin-binding zinc finger and BRCT for Brca1 C-terminal domain. Figure reprinted and legend adapted from Yang and Woodgate.[45]

Figure I.10 – Nucleotide Excision Repair. This figure illustrates the sub pathways of GG-NER versus TC-NER using UV damage as a model. In GG-NER on the left the damage sensor XPC works with the UV excision repair protein RAD23B and centrin 2 (CETN2) which constantly probes the DNA helix for helix distorting lesions which are recognized by the help of UV-DNA damage-binding protein (UV-DDB). Once the XPC complex binds to the damage, RAD23B dissociates. In TC-NER on the right, damage is recognized indirectly due to stalling of RNA polymerase II (RNA pol II). During transcript elongation UV-stimulated scaffold protein A (UVSSA), ubiquitin-specific-processing protease 7 (USP7)and Cockayne syndrome protein WD repeat protein CSA-CSB complex is formed which causes the reverse translocation, or backtracking, of RNA pol II which allows the DNA lesion to be accessible for repair. After damage recognition TFIIH (transcription initiation factor IIH_) is recruited to the lesion in both pathways. XPG endonuclease binds to the pre-incision NER complex. TFIIH causes the unwinding of the DNA and XPD then verifies that the lesion is present with the assistance of the ATPase activity of TFIIH XPB and XPA subunits. Replication protein A (RPA) is recruited to coat the undamaged strand. XPA recruits XPF-ERCC1 heterodimer creates a 5' incision around the lesion. XPG then cuts a 3' incision around the lesion which causes a 22-30 oligonucleotide to be released. PCNA is then loaded onto the 5' incision which recruits DNA pol δ, ε, or κ to complete the gap filling. Finally NER is completed by the ligation of the nicks by DNA ligase 1 or 3. Figure reprinted and legend adapted from Marteijn et al.[66]

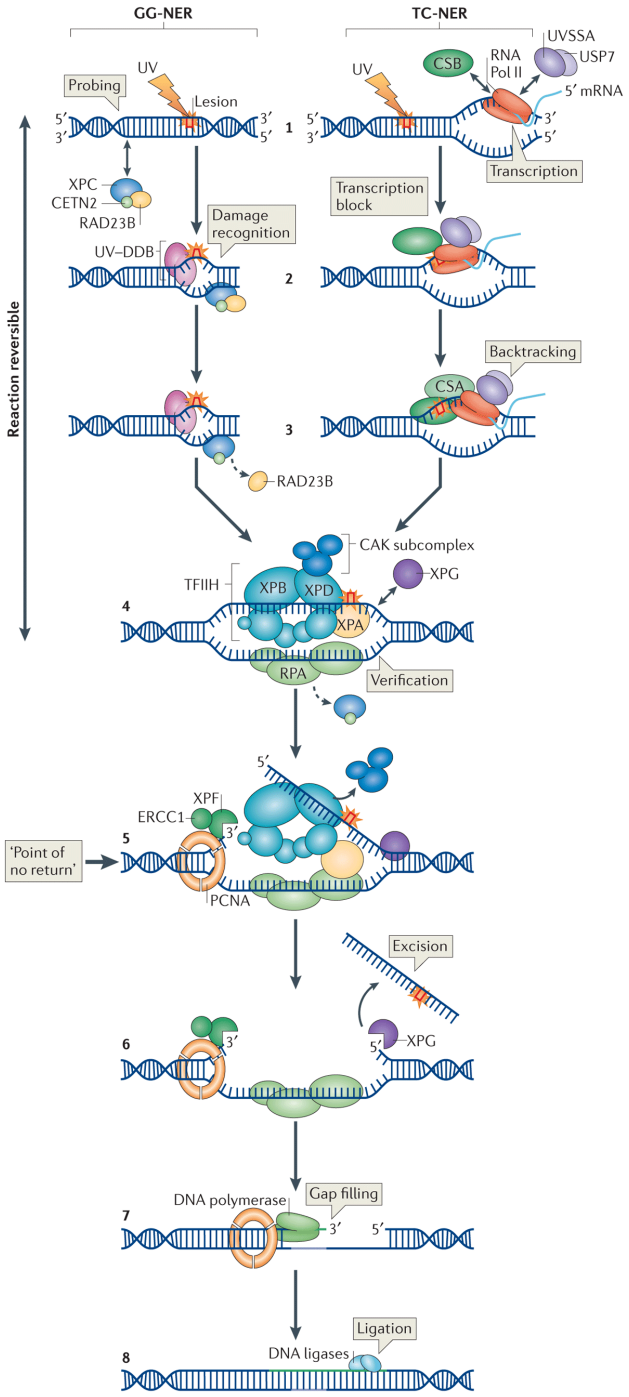

Nature Reviews | Molecular Cell Biology

Figure I.11 – Base Excision Repair. This figure is showing the effects of oxidative stress which causes 8-oxoG or an abasic site. DNA glycosylase OGG1 removes 8-oxoG and leaves an AP site. APE1 incises at the 5' side of the AP site sugar leaving a 5'-sugar phosphate which is either native (non-oxidized) or oxidized. A native 5'-sugar phosphate can be repaired by short patch (single nucleotide) BER (SN-BER) but the oxidized sugar phosphate group must be repaired by long-patch BER (LP-BER). SN-BER proceeds after the incision by APE1, pol β dRP lyase removes the 5'-sugar phosphate. Pol β then fills in the gap and the nick is ligated by ligase. In LP-BER when there is an oxidized phosphate group, the oxidation causes its resistance to pol β dRP lyase so instead pol β synthesizes and fills in the gap, and FEN1 excises the nucleotide flap before it is ligated together. If the oxidized sugar phosphate can occur by alternate LP-BER in which the DNA strand displacement synthesis is completed by pol β, δ or ε followed by FEN1 flap cleavage. This LP-BER process is the replacement of three or more nucleotides. Figure reprinted and legend adapted from Liu and Wilson.[71]

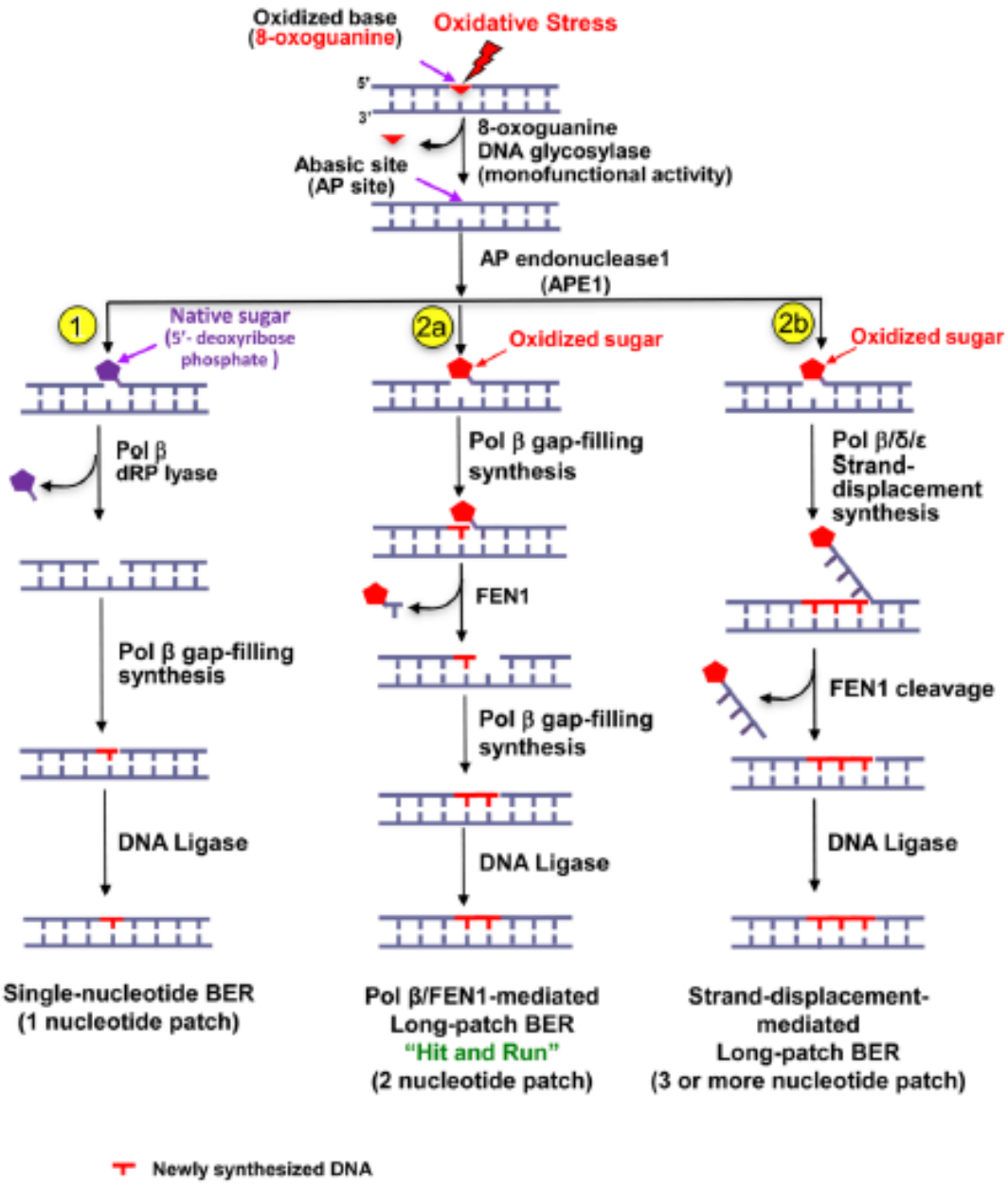
Oxidized base
(8-oxoguanine)
Oxidative Stress
5'
3'
8-oxoguanine
DNA glycosylase
(monofunctional activity)
Abasic site
(AP site)
AP endonuclease1
(APE1)
1
Native sugar
(5'- deoxyribose
phosphate)
Pol β
dRP lyase
Pol β gap-filling
synthesis
DNA Ligase
Single-nucleotide BER
(1 nucleotide patch)
2a
Oxidized sugar
Pol β gap-filling
synthesis
FEN1
Pol β gap-filling
synthesis
DNA Ligase
Pol β/FEN1-mediated
Long-patch BER
"Hit and Run"
(2 nucleotide patch)
2b
Oxidized sugar
Pol β/δ/ε
Strand-
displacement
synthesis
FEN1 cleavage
DNA Ligase
Strand-displacement-
mediated
Long-patch BER
(3 or more nucleotide patch)
Newly synthesized DNA

Table I.1 – Categorization of XP subtypes by gene and complementation group. This table gives a breakdown of the complementation group to their frequency, their major clinical effects, and the gene defect that causes the manifestation of the disease. Table reprinted from Ahmad and Hanaoka.[34]

Table 2. Characteristics of xeroderma pigmentosum complementation groups

Comple-mentation Group	Frequency (%)	Skin Cancer	Neurological Involvement	Ophthalmological Involvement	Gene Defect
A	30	+	+++	+	XPA
B	0.5	+	+	+	XPB/ERCC3
C	27	+	–	+	XPC
D	15	+	+++	+	XPD/ERCC2
E	1	+	–	+	DDB2/XPE/p48
F	2	+	–	+	XPF/ERCCC4
G	1	+	+	+	XPG/ERCC5
Variant	23.5	+	–	+	XPV/hRAD30

Research Hypothesis and Rationale

DNA damage can lead to stalling of the replication fork, and if not immediately repaired it can lead to prolonged fork stalling and eventually fork collapse and either cell death or gross chromosomal changes caused by double strand breaks.[16] In order to prevent this, cells have developed a process, termed translesion synthesis (TLS), which utilizes specialized DNA polymerases with wide open active spaces able to accommodate the large bulky lesions created by damaging events and agents. This allows the polymerases to insert a base, either correct or incorrect across from the lesion and allows replication to continue.[35, 39, 44] In this process the correct base can help prevent mutagenesis, whereas an incorrect base can lead to mutagenesis; however by utilizing TLS the cell accepting the potential base substitution as compared to gross chromosomal changes.[16, 72] One of the main polymerases involved in TLS is pol η which is characteristically known to bypass CPD dimers created by UV-C. In this study we wanted to expand on the literature which describes the effects of the presence and absence of pol η when bypassing dimers induced by UV-C. Therefore, we evaluated the effects of UV-B on mutagenesis in the presence and absence of pol η. We also wanted to investigate another cognate lesion that pol η is able to bypass, 8-oxoG. We did by this by measuring ROS levels in cells, the effect of oxidative stress on proteins and mutagenesis. We then evaluated the mRNA expression levels of the TLS polymerases in a time course following treatment with DNA damaging agents. Our hypotheses are:

1. That UV-B will cause DNA damage mainly in the form of CPDs and the presence of pol η will suppress mutagenesis across from these lesions.

2. That pol η will help suppress oxidative stress induced mutagenesis.
3. That pol η expression will increase after DNA damaging agents that cause CPDs, or platinum based cross-links, and that in the absence of pol η we will see an increase in a backup polymerase expression, most likely by pol ι.

The means of testing these three hypotheses will be described in three distinct chapters to follow. Briefly, since most previous work has been done biochemically or with plasmids; therefore we chose to investigate these hypotheses utilizing a mammalian cell culture model with matched cell lines either with or without functional pol η.

CHAPTER 1

Detrimental effects of UV-B radiation in an XP-Variant cell line*

Kimberly N. Herman[1], Shannon Toffton[1], Scott D. McCulloch [1,2]

[1] Department of Biological Sciences, Environmental and Molecular Toxicology Program

[2] Center for Human Health and the Environment

North Carolina State University, Raleigh, NC 27695

* Running Title: *Effects of UV-B radiation on XP-V cells*

Corresponding Author:

Scott McCulloch

850 Main Campus Drive

Campus Box 7633 Raleigh, NC

scott_mcculloch@ncsu.edu

Key Words: DNA damage, DNA polymerase η, mutagenesis, translesion synthesis, ultraviolet radiation

Published In:

Environmental and Molecular Mutagenesis. June 2014; Volume 55, Issue 5: Pages 375-384.

http://onlinelibrary.wiley.com/doi/10.1002/em.21857/abstract

Abstract

DNA polymerase η (pol η), of the Y-family, is well known for its *in vitro* DNA lesion bypass ability. The most characterized bypass event for this polymerase is that of cyclobutane pyrimidine dimers (CPDs) caused by ultraviolet light. Historically, cellular and whole animal models for this area of research have been conducted using UV-C (λ100-280 nm) due to its ability to generate large quantities of CPDs and also the more structurally distorting 6-4 photoproduct. While UV-C is useful as a laboratory tool, exposure to these wavelengths is generally very low due to being filtered by stratospheric ozone. We are interested in the more environmentally relevant wavelength range of UV-B (λ 280-315) for its role in causing cytotoxicity and mutagenesis. We evaluated these endpoints in both a normal human fibroblast control line and a Xeroderma pigmentosum variant (XP-V) cell line, in which the POLH gene contains a truncating point mutation leading to a non-functional polymerase. We demonstrate that UV-B has similar but less striking effects compared to UV-C in both its cytotoxic and mutagenic effects. Analysis of the mutation spectra after a single dose of UV-B shows a majority of mutations can be attributed to mutagenic bypass of dipyrimidine sequences. However, we do note additional types of mutations with UV-B that are not previously reported after UV-C exposure. We speculate these differences are attributed to a change in the spectra of photoproduct lesions rather than other lesions caused by oxidative stress.

Introduction

Human exposure to solar radiation is constant due to its large array of wavelengths, varying from the infrared down to short wave ultraviolet and beyond. Exposure to ultraviolet radiation has been shown to cause detrimental effects to human skin; including sunburns and skin cancer.[73] Interestingly, some clinical and epidemiological studies have shown a correlation between sunscreen use and an increase in some forms of skin cancer.[74] While this may seem paradoxical, increased sunblock use tends to correlate with increased sun exposure. For decades, commercially available sunblock has primarily contained ingredients that block both UV-C and UV-B radiation, even though nearly all UV-C is filtered by the stratospheric ozone layer and only ~5% of ultraviolet exposure coming from UV-B wavelengths.[75] Despite this, UV-C has most often been used for research due to its potency and ability to generate cyclobutane pyrimidine dimers (CPD) and other photoproducts.[76] There is ample evidence that both UV-B and UV-A radiation can also generate CPDs;[75, 77] however they also make other secondary lesions through their ability to generate reactive oxygen species (ROS).[16, 77-80] The ability to generate multiple types of lesions adds relevance to the study of UV-B and UV-A radiation with respect to mutagenesis.

The photoproducts caused by UV light include 6-4 photoproducts (6-4 PP) and CPDs. Both lesions occur between adjacent pyrimidines, but the 6-4 PP is structurally more bulky and is readily repaired by the nucleotide excision repair (NER) pathway.[81] CPDs are generally less bulky and while they can be recognized and repaired by the NER system, the kinetics of their repair is slower. Because of this, it is much more likely CPDs will be

encountered during replication and therefore require translesion synthesis (TLS), making them primarily responsible for the mutagenesis that occurs after UV light exposure.[82] There are multiple types of CPD dimers based on the identity of the adjacent bases (i.e. CC, TC, CT, or TT). DNA polymerase η (pol η) is able to readily bypass at least the thymine-thymine dimer (TT dimer) with high efficiency and moderate fidelity.[83] It is assumed that pol η is able to bypass all of the dimer combinations (and also the corresponding uracil containing lesions created by deamination of the cytosine base) with similar properties. There is *in vitro* experimental support for bypass of a TU (thymine-uracil) dimer[84-85] and genetic evidence that in yeast the CC and TC lesions are preferentially processed by pol η.[86]

The potency of UV-C has led to its popularity as an investigative tool for UV photoproduct mutagenesis. However, UV-C is not the only wavelength spectra that can cause photoproduct lesions. UV-B and UV-A, although less energetic, are much more abundant and environmentally relevant than UV-C,[75-76, 80, 87] and they can produce photoproduct lesions as well as generate significant levels of reactive oxygen species (ROS).[84, 88] ROS can lead to a wide variety of DNA lesions,[89-90] at least one of which, 7-8-dihydro-7,8-oxoguanine (8-oxoG) is also bypassed by pol η.[33, 42-43, 91] Therefore, investigating the types of mutations generated after exposure to UV-B and UV-A radiation may provide clues as to what types of lesions are commonly generated and which of the multiple polymerases available in human cells are involved in their bypass.[44] In this study, we sought to understand the role of CPDs compared to other potential lesions caused by environmentally relevant exposures of ultraviolet light in relation to their mutagenesis. To begin, we used a moderate dose of UV-B radiation and analyzed its effects on cells both proficient and deficient in the main CPD

bypass polymerase, pol η. We have evaluated the cytotoxicity in the presence and absence of caffeine, as well as mutation rates and spectra after single dose of primarily UV-B exposure. We compare our results to previously published work using UV-C and simulated sunlight sources of radiation.

Materials and Methods

Cell lines, growth conditions and treatments protocols

GM02359-hTERT (XP-V strain XP115LO) Clone 1B, denoted here as XP-V (containing a non-functional DNA polymerase η due to a truncating mutation at ORF position 1117) has been previously described.[92-93] We use as a control, an apparently normal neonatal foreskin fibroblast line (NHF1-hTERT), denoted here as NHF, which has been previously characterized.[93-94] These cell lines were a generous gift from Dr. Marila Cordiero-Stone (University of North Carolina). All media and supplements were obtained from Sigma-Aldrich (Saint Louis, MO) or Gibco-Life Technologies (Grand Island, NY). XPV cells were maintained in Dulbecco's MEM with 2mM L-glutamine, 10% FBS and 2x MEM Non-Essential amino acids. NHF cells were maintained in Eagle's MEM with 10% FBS and 2 mM L-glutamine. Some expansion cultures for HPRT sequence analysis were maintained with the addition of 100 U penicillin/100 µg streptomycin. All cultures were maintained in 37°C with 5% CO_2. UV-B treatments were performed by removal of growth media and addition of HBSS to cells. P100 plates used 3 ml HBSS and 96-well plates were dosed using 100 µl of HBSS per well. The lamp used has been described previously.[95] Exposure to either

a 5 or 10 mJ/cm^2 final dose was performed with no lid and took ~10 and ~20 seconds, respectively.

Cell Viability

Cell viability after UV-B treatment was determined using the CellTiter-Glo Luminescent Cell Viability Assay Kit (Promega, Madison, WI). Cells were plated into 96 well, flat bottom plates (655083; Greiner Bio-one, Austria) at 5,000 cells per well based on preliminary plating studies as suggested by the manufacturer. 24 hours after plating, cells were treated with UV-B, UV-B plus caffeine or no treatments. UV-B dosing was as described above. For treatments using caffeine (1 mM final), a 1 hour pre-treatment was used, it was removed with the media for UV-B treatment and replaced after treatment; then it was left in the media until viability was measured. At 24 and 48 hours, cells were lysed and luminescence was measured using a FLUOstar Omega plate reader (BMG Labtech, Offenburg, Germany) using the protocol recommended by the manufacturer.

Mutation Frequency

The HPRT mutation assay was conducted essentially as previously described.[94] Briefly, cells were preselected for functional HPRT by growth in 1x HAT (hypoxanthine, aminopterin, thymidine) media (H0262; Sigma-Aldrich, Saint Louis, MO) for 10 days. Cells were then expanded and plated at 15-20% confluence and grown for 24 hours, followed by treatment of 10 mJ/cm^2 UV-B, or no treatment. These cells were then maintained in logarithmic growth for 14 days. Selection for loss of HPRT function was performed by re-plating 4 x10^4 cells per P100 plate in growth media + 40 μM 6-thioguanine (A4882; Sigma-

Aldrich, Saint Louis, MO). Cells were given fresh media/6-TG on day 7 of selective growth day. Mutants were counted and collected on the 14th day of selective growth. Colony forming efficiency was determined at the time of mutant selection by plating 750 cells per P100 plate in non-selective media (normal growth media). Colony forming efficiency plates were counted on the same day as mutant collection. Mutation frequencies were calculated as previously described.[94] For colonies not destined for mutation spectra analysis, colonies were fixed with methanol/acetic acid (vol:vol 3:1) and stained with crystal violet prior to counting. Statistics for HPRT mutation frequencies were conducted using a one-way ANOVA with the Tukey post test, performed using GraphPad Prism version 5.00 for Windows, GraphPad Software, San Diego California USA, www.graphpad.com.

Analysis of HPRT mutation spectra

Mutation spectra analysis used a modified protocol based on previously published work.[96] Mutant colonies were first identified by inverted light microscopy without crystal violet staining. Colonies were harvested as described.[97] Briefly, the plates were rinsed with PBS or HBSS, an 8 mm sterile plastic cloning ring was placed around them, trypsin solution was added to the ring and incubated at 20 seconds at room temperature, and then at 37°C for 15 minutes after trypsin was removed. Complete media was used to collect the cells and they were re-plated for continued growth. Expansion of these cells was performed in selective 6-thioguanine containing media. RNA was collected using the Qiagen RNeasy Mini Kit (Qiagen, Louisville, KY). cDNA was produced using the High Capacity cDNA Reverse Transcription Kit from Applied Biosystems (Life Technologies, Grand Island, NY). After

cDNA production, PCR amplification of the HPRT gene was done using LongAmp Taq DNA Polymerase (New England Biolabs, Ipswich, MA), and PCR primers 5′-CTGCTCCGCCACCGGCTTCC and 5′-GATAATTTTACTGGCGATGT (Primers 1 and 2)[96] with the cycling parameters: 95°C for 5 min, 35 cycles of 95°C for 1 minute, 48°C for 1 minute, 65°C for 2 min, with a final extension of 65°C for 2 minutes. PCR cleanup was performed using a QIAquick PCR Purification Kit (Qiagen, Louisville, KY), followed by a second round of PCR using 1:100 dilution of PCR product, and primers 5′-CCTGAGCAGTCAGCCCGCGC and 5′-CAATAGGACTCCAGATGTTT (primers 3 and 4).[96] Sequence analysis was performed using Geneious Pro Version 5.4.4(Biomatters, Auckland, New Zealand). Analysis of the POLH gene in both cell lines was performed by PCR amplification using primers 5′-CCTCACCTCTCCAGACCTGC and 5′-GAGGAGACCATTCTGTCTGGA and the cycling parameters: 95°C for 1 min, 30 cycles of 95°C for 30 sec, 45°C for 1 minute, 68°C for 1.5 min, with a final extension of 68°C for 5 minutes using Quick-load Taq 2X Master Mix (New England Biolabs, Ipswitch, MA). This amplifies a product of ~750 base pairs that flanks the altered position. Sequencing was performed by Genewiz (Research Triangle Park, NC) using the same primers as the PCR reaction.

Results

Verification of Cell Lines and Dosing

In order to determine the effect of an environmentally relevant level of UV-B radiation on cells, we dosed a pair of hTERT immortalized cell lines. The cells were an apparently normal

human foreskin fibroblast and a dermal fibroblast line deficient in DNA polymerase η activity, in which the deficient cell line contains a point mutation leading in the POLH gene at codon 373, leading to a truncation in the protein that results in a complete loss of DNA polymerase η activity.[92-93] First we verified the genotypes of both cell lines and found the expected mutation in the XP-V cell line (Figure 1.1A). We then exposed exponentially growing cells to doses of biologically relevant UV-B radiation.[95] These doses can be achieved by relatively short exposure to direct sunlight (Dr. Jonathon Hall, personal communication) and with the lamp used and a monolayer of cells in culture, required only ~21 seconds for the highest dose. While the peak output of this lamp occurs at 312 nm, it likely does have a minor output in the UV-C range as it emits between 280-350 nm wavelengths (according to manufacturer literature). Based on preliminary studies, we chose 5 and 10 mJ/cm^2 as doses which were not overly cytotoxic to cells (data not shown). The goal of these experiments was to examine if relatively low levels of primarily UV-B radiation were able to affect cells in a manner similar to the potent UV-C exposures that characterize many studies involving pol η.[55, 93, 98]

Cell Proliferation and Effects of Caffeine

The CellTiter Glo™ assay was used to measure ATP levels in whole cell lysates. This correlates with cell number and preliminary studies verified that we were in the linear detection range for total cell number (data not shown). We plotted the luminescence value (i.e. surrogate for cell number) for irradiated cells relative to the same value for non-irradiated cells and defined this ratio as the proliferation index (Figure 1.1C; raw

luminescence values are shown in Figure S1.1). In each experiment, multiple replicate wells were used and the values averaged. Each value plotted is the average of multiple independent experiments. As can be seen in Figure 1.1C and 1.1D, exposure to both 5 and 10 mJ/cm^2 UV-B radiation was not overly cytotoxic to NHF cells in the presence or absence of caffeine (solid lines). At 1 day and 2 days post radiation exposure, cell numbers were at least 90% those of un-irradiated cells with no striking difference noted. Figure S1.1 shows that luminescence values increased with time, indicating that cells were indeed proliferating. This demonstrates that the dose is not excessively cytotoxic. That caffeine does not have any noticeable effect suggests that whatever damage is occurring is not enough to activate the ATM/ATR pathway in response to stalled replication forks. In contrast, we do see a noticeable effect of adding caffeine to the XP-V cells. At day 1, there is no apparent difference in cell number, but by day 2 we see a decrease in the number of cells exposed to combination treatment of both caffeine and UV-B radiation. The drop in total luminescence over time seen in Figure S1.1 also supports the conclusion that in XP-V cells, the combination of UV-B light and caffeine caused an increase in cell death. This phenotype is the same as previously described after UV-C radiation and is considered diagnostic of XP-V cells.[98-99] It suggests to us that UV-B radiation is capable of causing a replication block in cells lacking pol η that is exacerbated by caffeine, possibly by inducing the G1 cell cycle block.[100] Based on these results, we were interested in whether XP-V cells exposed to UV-B radiation would display increased mutagenesis as they do after UV-C exposure.

Mutagenesis of UV-B

To investigate this, we employed the hypoxanthine-guanine phosphoribosyltransferase (HPRT) mutagenesis assay (Figure 1.2A). While this assay requires selection of mutants and is therefore not an idle locus, it has been used extensively to look at UV light mutagenesis in multiple cell lines, including those used here.[93] NHF and XP-V cells were dosed with 10 mJ/cm^2 of UV-B light and then selected for growth in 6-thioguanine to select for loss of HPRT activity. Importantly, we saw no difference in the low cell density cloning efficiency of the two cell types (12-15%; Table 1.1). We observed that the background mutation rate for both cell types was similar (0.55 x 10^{-5} and 0.98 x 10^{-5} for NHF and XP-V cells, respectively; Figure 1.2B; Table 1.1). These results agree with data from a mouse model in which animals lacking pol η showed no increase in tumors under non-exposed conditions; as well as a cellular study in which pol η is overproduced, but no increase in spontaneous mutations were observed.[93, 101] Our data did show a statistically significant increase in the mutation frequency after UV-B exposure (compared to no exposure) in both cell types (~18 and ~25 fold, for NHF and XP-V cells, respectively). Importantly, the observed mutation frequency of NHF and XP-V cells after UV-B exposure were significantly different from each other (Figure 1.2B; 8.56 x 10^{-5} and 25.8 x 10^{-5} for NHF and XP-V cells, respectively). These observed mutation frequencies after UV-B exposure show a similar trend to the increased mutagenesis after UV-C exposure in XP-V cells. This data is consistent with a lack of pol η dependent lesion bypass in these cells. It also demonstrates that even at doses that do not cause excessive cytotoxicity, mutagenesis above background levels occurs even when pol η is present, and that loss of pol η further

magnifies this phenotype. We acknowledge that these cell lines are not isogenic and therefore the difference could be due to factors other than pol η. However, at 1 and 24 hour post irradiation, we saw no evidence of different levels of TT dimer lesions by dot blot analysis (Figure S1.2). This suggests that both initial levels of and overall repair rates for this lesion are comparable in these two lines.

Mutation Spectra Evaluation

Since UV-B and UV-C radiation can produce multiple different types of lesions,[80, 87] we were interested in how the spectra of mutations caused by UV-B radiation compared to those observed after UV-C exposure. To investigate this, we generated spectra of mutations caused by UV-B light in pol η proficient and deficient cells by isolating RNA from 6-TG resistant clones, PCR amplifying the HPRT open reading from cDNA and then sequencing these products. Tables 1.2, 1.3 and Figure 1.3 show a marked difference in the types of mutations observed in NHF and XP-V cells. The most obvious difference is the relative levels of base substitutions to insertion/deletions. In NHF cells, insertions/deletions account for 67% of the total mutations, compared to only 26% for XP-V cells. We also observe more variability in the types of insertion/deletion mutations in NHF cells. In NHF cells, we detected 3 different insertions at 2 different locations and 6 different types of deletions ranging from a single base up to over 100 bases deleted. These occurred at 7 separate locations in the gene (Table 1.3). All but one of the insertions/deletions are predicted to cause a truncation of the HPRT protein (Table 1.3). In XP-V cells, no insertions were observed and

the deletions were of a much more limited scope (a single 1 base deletion and 3 separate instances of a 77 base deletion) (Table 1.2).

The most striking difference was observed in the numbers and distribution of base substitutions mutations. In NHF cells, all of the base substitutions can be attributed to dipyrimidine sites in one of the two strands (Table 1.3). These mutations account for a minority of total changes in the NHF cells, though. Four of the 6 sites are either TT or CC sequences while only 1 is of a mixed base sequence (the last could be either TT or CT). Of the photoproduct associated mutations, there were 3 changes each at C and T bases. In XP-V cells, there is a similar trend of most base substitutions occurring in dipyrimidine photoproduct sites, but we also detected 2 changes that cannot be attributed to such sequences (Table 1.2). Of the photoproduct sites, 5 are at either CC or TT sites and 6 are at TC or CT sites, a different distribution than that seen in NHF cells. But like in NHF cells, the mutations at photoproduct sites also occur equally at T and C residues (5 and 6 changes, respectively). Taken together, the results presented here suggests to us that in NHF cells, functional pol η helps suppress mutagenesis caused by UV-B light, with the majority of changes being more complex insertion/deletions. In XP-V cells lacking functional pol η, an increase in overall mutagenesis is noted as well as a specific increase in base substitutions at dipyrimidine sequences and also mutations at other non-photoproduct associated sites. While we have not determined the genotype of the pol ι gene, we assume it to be wild type and therefore expect that in our XP-V cells, the majority of photoproduct induced mutations are caused by low fidelity bypass by this protein, as has been shown previously.[55]

Discussion

It is generally believed that most non-melanoma skin cancers are caused by UV-B and/or UV-A radiation. Most of UV-C radiation is filtered by stratospheric ozone before reaching the ground level, leading to the composition of UV irradiation we are normally exposed to being ~95% UV-A and UV-B.[75, 102] We were interested in how these less energetic but more environmentally relevant wavelengths of solar radiation affect human cells with respect to cytotoxicity and mutagenesis. A study of yeast strains proficient or deficient for either the *rad30* (pol η) or rev3 (pol ζ) genes was conducted comparing UV-C to simulated sunlight (SSL; UV-B and UV-A in proportions that mimic solar radiation).[103] Their results suggested that the lesions created by UV-C are more mutagenic. Similarly, we found that UV-B did indeed cause an increase in mutagenesis in normal cells, it was less than the reported values for this line using UV-C.[93] Interestingly, they saw little to no effect on mutation rate when pol η was missing using only SSL. This differs somewhat from our results in that our XP-V line showed a further increase in mutation rate compared to normal cells (Figure 1.2). One explanation could be the different types of radiation used. Another explanation could be the lack of pol ι in yeast, as it is known to be involved in UV light dependent mutagenesis in the absence of pol η.[55]

Pol η is considered to be the main polymerase involved in lesion bypass of products caused by UV-C radiation. As we limited ourselves to a comparison of mostly UV-B to UV-C radiation, we reasoned that if the less energetic UV-B was working by a mechanism similar to UV-C, we should observe similar effects. Therefore, we decided to evaluate for

cytotoxicity both in the presence and absence of caffeine, as a specific enhancement of cytotoxicity by caffeine is a well described phenotype of XP-V cells.[100, 104] We also were interested in whether pol η deficiency would cause an increase in mutations after UV-B radiation and if so, whether the types of mutations found was similar to or different from that reported after UV-C radiation. To this end, we performed the HPRT mutagenesis assay and sequenced the coding sequence of 6-TG resistant mutants.

Our results show that normal human fibroblasts do not exhibit significant sensitivity to killing by 5 and 10 mJ/cm^2 UV-B. These doses are low and environmentally relevant, able to be absorbed in only a few minutes of direct, mid-day sunlight. However, XP-V cells do exhibit cytotoxicity at these doses but only in the presence of caffeine (Figure 1.1C). Based on previous reports that used UV-C radiation, we hypothesize that this increased cytotoxicity is result of collapsed replication forks due to inefficient or absent TLS. In normal cells and in the absence of caffeine, these collapsed forks should trigger the ATR-dependent damage response pathway.[100] Caffeine is a known ATM/ATR inhibitor.[95] It has been previously shown that in response to UV-C irradiation, XP-V cells show a significant inhibition in proliferation in the presence of caffeine.[55, 93, 104] Those studies used UV-C doses that kill the majority of cells. Our results suggest that even lower doses of radiation that kill only a small percentage of total cells causes the same phenotype. This suggests that the response to DNA damage is very sensitive and finely tuned. It does not require high doses that kill most cells. It also shows that cells respond in the same fashion to both UV-C and UV-B radiation.

We were also interested in understanding how specifically UV-B could affect mutagenesis, and whether the protective effect of pol η extended to these wavelengths of radiation. We determined mutation frequencies and spectra for UV-B treated normal and XP-V cells in order to begin to understand the role that pol η plays in this process. We started this work assuming that the mutation rates would likely be lower than that of UV-C treated cells, but that there would be a similar trend in terms of mutagenicity and sensitivity in the XP-V line. This indeed was the case. In previously published work by Bassett *et al*, UV-C doses ranging from 4-8 J/m^2 (equivalent to 0.4-0.8 mJ/cm^2) on NHF cells gave mutation frequencies ranging from 11 to 19.3 x 10^{-5}.[94] In XP-V cells, which is the same cell line we used, they used doses of 2-4 J/m^2 of UV-C (0.2-0.4 mJ/cm^2) giving mutation frequencies ranging from 31 to 46.9 x 10^{-5}. These doses may appear to be relatively small compared to ours (0.2-0.8 mJ/cm^2 versus 5-10 mJ/cm^2 used in our studies), but it is important to keep in mind that UV-B radiation is overall less energetic and that the peak wavelength of the emission source we used was 312 nm, significantly higher than the peak absorption maximum of DNA.

As Table 1.1 shows, NHF cells dosed with 10 mJ/cm^2 UV-B gave a mutation frequency of 8.56 x 10^{-5}, compared to XP-V cells with a frequency of 25.8 x 10^{-5}. These values are significantly different than untreated cells for each cell line, i.e. UV-B radiation is mutagenic in both cell lines. We also see a statistically significant difference in the mutation frequency of UV-B light when comparing NHF and XP-V cells. The values observed are somewhat lower than those reported for UV-C, perhaps due to the above noted potency of light with a peak emission of ~254 nm, very close to the maximum absorption wavelength of

DNA. Due to this difference in wavelengths of the light sources used in these various studies, it is possible that a completely different set of DNA lesions are being generated by each exposure.[80, 87] Initially, we assumed that UV-B would cause more mutations at non pyrimidine dimer sites as it is frequently stated that UV-B can cause oxidative stress at relevant levels. We saw only limited evidence for this, as only 1 of the 2 non-photoproduct base substitutions we detected could possibly be attributed to 8-oxoguanine, the most abundant oxidative lesion. This is consistent with Kozmin et al, who reported that that pol η can accurately bypass 8-oxo-guanine after SSL exposure in yeast cells.[103] However, we have not observed an increase in 8-oxoguanine levels in the DNA after this much UV-B exposure (data not shown), suggesting that the mutagenic effect of the UV-B light used here is largely photoproduct dependent, although a minor contribution by oxidative damage cannot be ruled out completely.

Comparison of the mutation spectra of NHF and XP-V cells caused by UV-B light was very interesting. The most notable observation was the striking difference in the number of insertion/deletion mutations versus base substitutions when comparing the two cell lines. In NHF cells, we observed 50% deletions, 17% insertions and 33% base substitutions. However, in XP-V cells no insertions were found and only 26% of the changes were deletions, with the remaining 74% of mutations being base substitutions. The most likely explanation for this difference is that in NHF cells, the presence of functional pol η allows for bypass of CPDs in a more efficient manner and in way that is more accurate. It is interesting to note, however, that even in NHF cells, all the detected base substitutions were at dipyrimidine photoproduct sites. Possible explanations for this are that TLS of CPDs by

pol η is not completely error free, as has been suggested before,[46] or that other polymerases (likely pol ι) also play a role in normal TLS of UV light generated lesions.[55] We do note that a published report (compiling both previous work and new data)[55] showed that in 'wild type' cells (i.e. both pols η and ι present) the majority of base substitutions caused by UV-C were transitions (87%; T→C or C→T) while our results show that only ~33% of base substitutions were transitions (Table 1.2). It is entirely possible that this is caused by the distribution of photoproduct lesions after UV-C versus UV-B radiation.[77, 105]

Breaking down the base substitutions observed in XP-V cells, we see a similar distribution of changes at photoproduct sites when compared to published reports[55] (Table 1.2; Figure 1.3). Specifically, roughly 63% of the changes were transversions, here either T→A or C→A changes. This matches the 55-70% value reported in Wang *et al* for two different XPV cell lines that were dosed with UV-C light (see Tables 1.1 and 1.2).[55] Results from Kozmin et al also confirm that UV-C causes predominantly transversions, but they report that simulated sunlight caused only 50% transitions and 28% transversions.[103] We speculate that for our results, the absence of pol η, even with the less cytotoxic UV-B, the same replication blocking lesions are produced as in UV-C, albeit possibly in lower overall levels. When these lesions are bypassed in a pol ι dependent manner, they cause the same types of errors. More evidence that the mutagenic response to UV-B light is similar to that of UV-C is the fact that we see roughly equal mutations on the transcribed and non-transcribed strands of HPRT (45%/55% split) in XP-V cells, similar to the 44%/56% split observed in XPB4E and XP115LO cells from Wang et al using UV-C radiation.[55] While no data is

presented in that report regarding strand specificity in wild type cells, we also observed no difference in our NHF cells (50%/50% transcribed and non-transcribed strand, respectively).

Our data shows that UV-B acts in a very similar fashion to UV-C, albeit with somewhat lesser effects with regards to cytotoxicity. The fact it can induce mutagenesis even in the presence of pol η lends support to the notion UV-B exposure is a risk factor for skin cancer. Our data suggest that the majority of the mutations are associated with photoproduct sites. That mutation frequencies increase in the absence of pol η suggests that CPDs are the main culprit of the mutagenesis. As UV-B is the minor component of the UV radiation we are exposed to, it will be important to extend these studies to the UV-A range of wavelengths, and also to study the combined effects of various wavelengths (i.e. using 'simulated sunlight' lamps). Some of these studies have been performed in yeast cells,[103] but the relevance to human health cannot be determined, given the differences in TLS polymerases and repair systems available to each organism.

Figure 1.1 – Sequence Verification and Cell Viability. A. Results of sequencing a portion of the POLH cDNA in NHF and XP-V lines, confirming C1117T change in the latter. B. Schematic of cell viability assay as determined by CellTiter-Glo Luminescent Cell Viability Assay Kit (Promega). NHF and XP-V cells were seeded at 5,000 cells/well. Caffeine was added to 1 mM final concentration 23 hours post plating to appropriate wells. 24 hours post plating, media was removed and replaced with HBSS, and cells were treated with UVB or no treatment. HBSS was removed and fresh media was then added +/- 1 mM caffeine. Viability assay was performed at 24 and 48 hours post treatment. C. Graph of relative cell viability (compared to no UV-B treatment) as measured at 24 hours post treatment. Cell number is proportional to luminescence as measured by the amount of ATP present in cell lysates. C. Graph of relative cell viability as measured at 48 hours post UVB treatment.

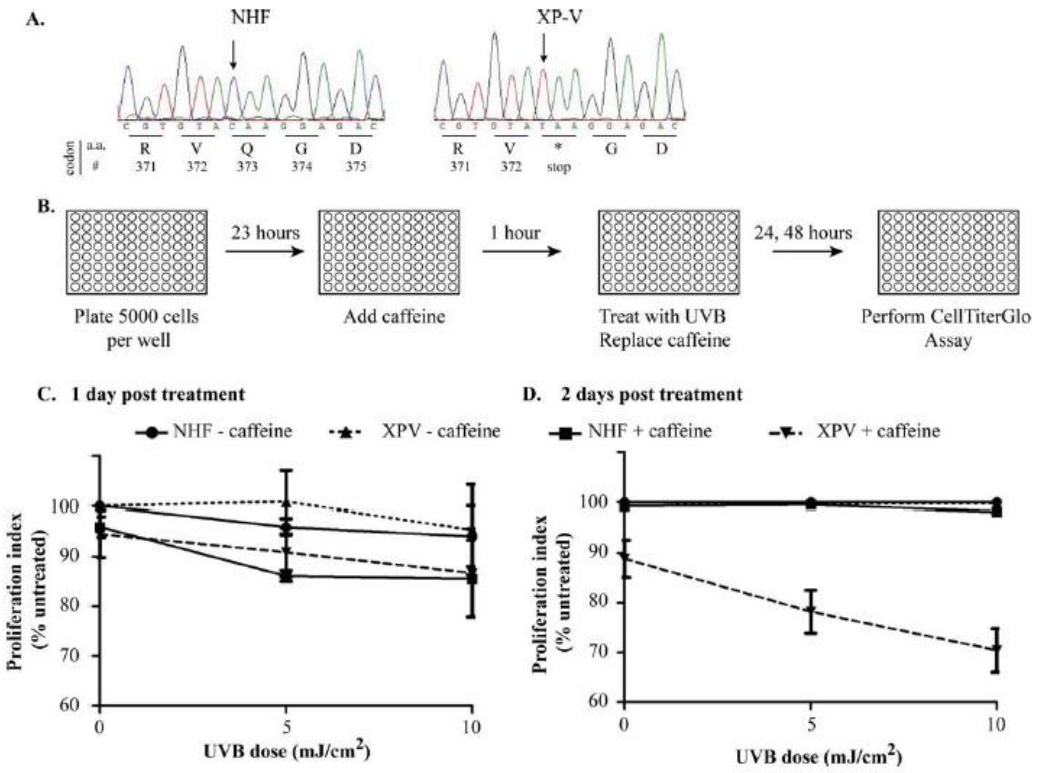
A.
NHF
XP-V
codon
a.a.
#
R 371
V 372
Q 373
G 374
D 375
R 371
V 372
* stop
G
D
B.
23 hours
1 hour
24, 48 hours
Plate 5000 cells per well
Add caffeine
Treat with UVB
Replace caffeine
Perform CellTiterGlo Assay
C. 1 day post treatment
NHF - caffeine
XPV - caffeine
Proliferation index (% untreated)
UVB dose (mJ/cm2)
D. 2 days post treatment
NHF + caffeine
XPV + caffeine
Proliferation index (% untreated)
UVB dose (mJ/cm2)

Figure 1.2 - A. Schematic diagram of HPRT mutation assay. Cells were plated at 15-20% confluency, grown for 24 hours and then treated with UV-B (or no treatment). Cells were kept in exponential growth for 14 days then plated at 40,000 cells per plate for selection plates or 750 cells per plate to determine plating efficiency. After 14 days in selective media (D-MEM or E-MEM + 40 μM 6-thioguanine), plates were stained with crystal violet and visually examined by microscope to count colonies. For plates that were used to expand cultures for cDNA analysis, colonies were counted without the aid of crystal violet staining. B. Mutation frequencies were calculated as in Bassett *et al*.; MF= [(number of colonies)/(number of cells plated)]/(CFE). Mutation frequencies were calculated for each separate experiment, with a minimum of 3 experiments for each treatment. The averages of multiple trials are shown on the graph ± SEM. The graph was generated using GraphPad Prism 5.0. Statistics used an ANOVA with a Tukey Multiple Comparisons test (* $P \leq 0.05$, ** $P \leq 0.01$, *** $P \leq 0.001$, **** $P \leq 0.0001$). Results show significance between no treatment and treatment in both the NHF and XP-V cells, as well as between the treated XP-V and NHF cells.

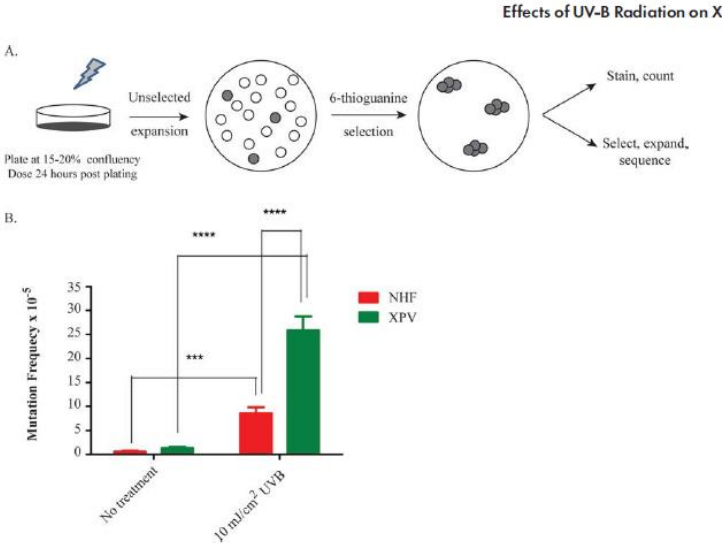
Effects of UV-B Radiation on X
A.
Unselected
expansion
6-thioguanine
selection
Stain, count
Select, expand,
sequence
Plate at 15-20% confluency
Dose 24 hours post plating
B.
****
****
***
Mutation Frequecy x 10^-5
35
30
25
20
15
10
5
0
NHF
XPV
No treatment
10 mJ/cm2 UVB

Table 1.1 – Mutation Rates: Average rates of mutagenesis at the HPRT gene after a single dose of UV-B radiation on NHF and XP-V cells with at least 3 replicate experiments. Mutant colonies were counted by inverted microscope after 14 days of 6-TG selection. Mutation frequency was calculated as (number of resistant colonies)/[(number of cells plated for selection)(CFE)]. Colony forming efficiency is the number of colonies on the unselected low density plates/ total cells plated for plating efficiency.

	NHF		**XP-V**	
	No treatment	**10 mJ/cm^2 UVB**	**No treatment**	**10 mJ/cm^2 UVB**
Mutant colonies	4	97	7	177
Colony forming efficiency	0.13	0.12	0.12	0.15
Mutation frequency	0.55×10^{-5}	8.56×10^{-5}	0.98×10^{-5}	25.8×10^{-5}
Number sequenced	0	18	0	19

Table 1.2 – Mutations observed in the HPRT gene of UV-B irradiated XP-V cells after 6-thioguanine selection. Listed mutations for likely CPD sites are given assuming the dimer was the source of the mutation. The multiple occurrences of mutations at the same position (222, 532, 616) were observed in different experiments, demonstrating they are independent events.

Base substitutions

Position	Mutation	Photoproduct	Strand	Sequence*	Effect
2	A → T or T → A	No		GCC**A**TAA	*No start codon*
617	C → A or G → T	No		ACA**C**AAA	C206F
39,40 **	C → A; A → T	Yes	T	GTT**CA**TCA	Δ14-218
40	C → A	Yes	T	GTT**C**ATC	Δ14-218
62	T → A	Yes	NT	ATT**T**ATT	Δ21-218
222	C → A	Yes	NT	ATT**C**TTT	F74L
222	C → A	Yes	NT	ATT**C**TTT	F74L
259	T → A	Yes	T	TTC**T**ATT	Δ87-218
464	C → T	Yes	NT	ATC**C**AAA	P155L
606	C → A	Yes	T	ATT**C**AAA	L202F
616	T → C	Yes	NT	GTT**T**GTG	C206R
616	T → C	Yes	NT	GTT**T**GTG	C206R
616	T → C	Yes	T	GTT**T**GTG	C206R

Table 1.2 Continued

Insertions/Deletions

Position	Size	Sequence	Effect
18	-1 bp	GCC(**A**)GGG	Δ9-218
531	-77 bp	CAT(**GATTCAAATC…AAATCCAACA**)AAG	Δ183-218
532	-77 bp	ATG(**ATTCAAATCC…AATCCAACAA**)AGT	Δ183-218
532	-77 bp	ATG(**ATTCAAATCC…AATCCAACAA**)AGT	Δ183-218

*Given 5′→3′ of the relevant strand for photoproducts with the altered base in **bold** and the photoproduct site underlined. For non-photoproduct site, the sequence of the transcribed strand is given. Sequences of deleted bases are shown in **bold** within parentheses, with the position listed being the last present prior to the deleted region.

** Tandem base substitution in which only one is within a photoproduct site

Table 1.3 – Mutations observed in the HPRT gene of UV-B irradiated NHF cells after 6-thioguanine selection. Listed mutations for likely CPD sites are given assuming the dimer was the source of the mutation. The multiple occurrences of mutations at the same position (18, 609) were observed in different experiments, demonstrating they are independent events.

Base substitutions

Position	Mutation	Photoproduct	Strand	Sequence*	Effect
34, 36 **	A → T, C → A	Yes	T	ATC**A**T**C**ACT	D12Stop
62	T → A	Yes	NT	AT**T**ATT	L21Stop
208	C → T	Yes	T	CC**C**CTT	G70R
209	C → T	Yes	T	CC**C**CCA	G70E
223	T → A	Yes	NT	TC**T**TTG	F75I
623	T → A	Yes	NT	TCA**T**TAG	V208N

Insertions/Deletions

Position	Size	Sequence	Effect ***
453	+1 bp	CTG(**A**)CCT	Δ154-218
609	+14 bp	ATG(**CTATAAAAAAAAAT**)ATT	****
609	+15 bp	ATG(**CTATAAAAAAAAAAT**)ATT	Δ208-218
18	-1 bp	GCC(**A**)GGG	Δ9-218
18	-1 bp	GCC(**A**)GGG	Δ9-218
27	-107 bp	GTC(**CTGTCCATAA…CATCACTAAT**)CAC	Δ10-218
384	-18 bp	ATC(**TTCCACAATCAAGACATT**)CTT	Δ129-134
399	-4 bp	TAT(**CTTC**)CAC	Δ135-218
403	-1 bp	TAT(**C**)TTC	Δ136-218

Table 1.3 Continued

485	-47 bp	CAA(**AGTCTGGCTT…CACCAGCAAG**)CTT	Δ166-218
532	-77 bp	ATG(**ATTCAAATCC…AATCCAACAA**)AGT	Δ183-218
535	-77 bp	AAC(**ATGATTCAAA…TCAAATCCAA**)CAA	Δ182-218

* Given 5′→3′ of the relevant strand for photoproducts with the altered base in **bold** and the photoproduct site underlined. For non-photoproduct site, the sequence of the transcribed strand is given. Sequences of inserted or deleted bases are in **bold** inside parentheses, with the position listed being the base prior to the inserted or deleted position.

** This sample contained 2 base substitutions separated by a single base. Only one of the changes is in a potential photoproduct site.

*** The numbers given indicate the size of the truncated protein (i.e. Δ182-218 indicates the mutated protein was 181 amino in length). Most of the deletions also contained changes in amino acids at the C-terminal end of the truncated protein compared to wild type sequence.

**** This mutation changes amino acids starting from residue 204 and takes the normal stop codon out of frame, giving a new reading frame of at least 223 amino acids.

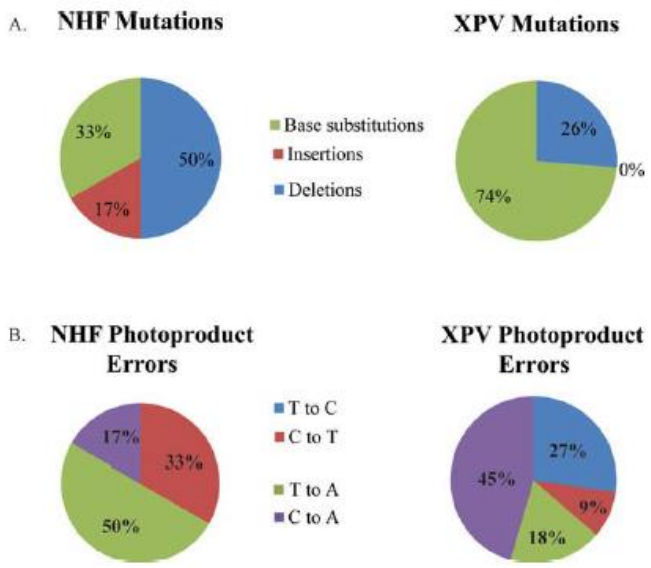

Figure 1.3 – Visualization of specific error types: 6-thioguanine resistant colonies were collected by ring cloning, expanded and mRNA harvested to produce HPRT cDNA. Sequencing of nested PCR products was performed and compared to the wild type HPRT cDNA sequence. Analysis of sequences was performed using Geneious Pro Version 5.4.4 software. All changes were recorded and categorized by type of mutation (base substitution, insertion, deletion). A. Breakdown of the types of changes observed in NHF and XP-V cells. B. Breakdown of the types of base substitutions assumed to be photoproduct errors in NHF and XP-V cells.

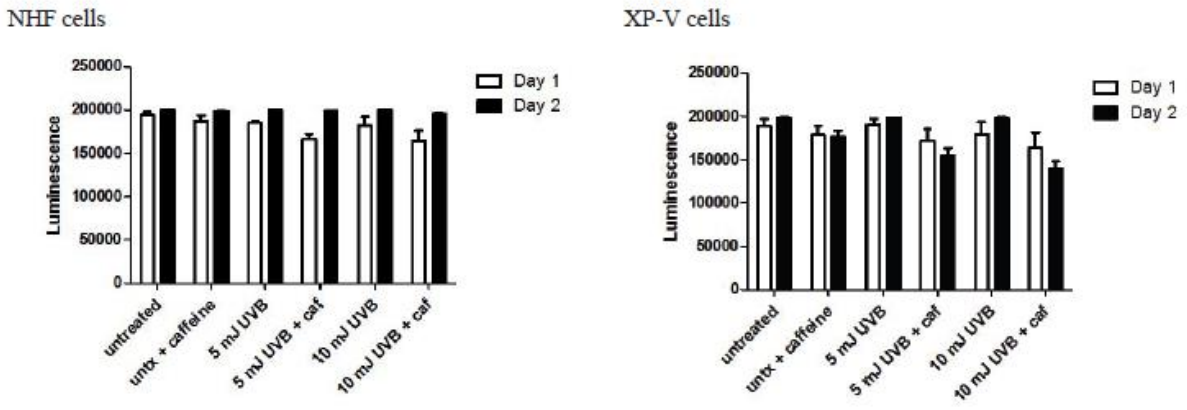

Figure S1.1-Raw data for luminescence values 1 and 2 days post treatment. Data was obtained as described in Materials and Methods. Values are the average of at least 3 independent experiments with error bars showing standard deviation of averages (themselves derived from 5 replicates per condition). An increase in luminescence from Day 1 to Day 2 indicates that cells are continuing to proliferate, while a decrease in luminescence suggests cells are either stagnant or decreasing in number.

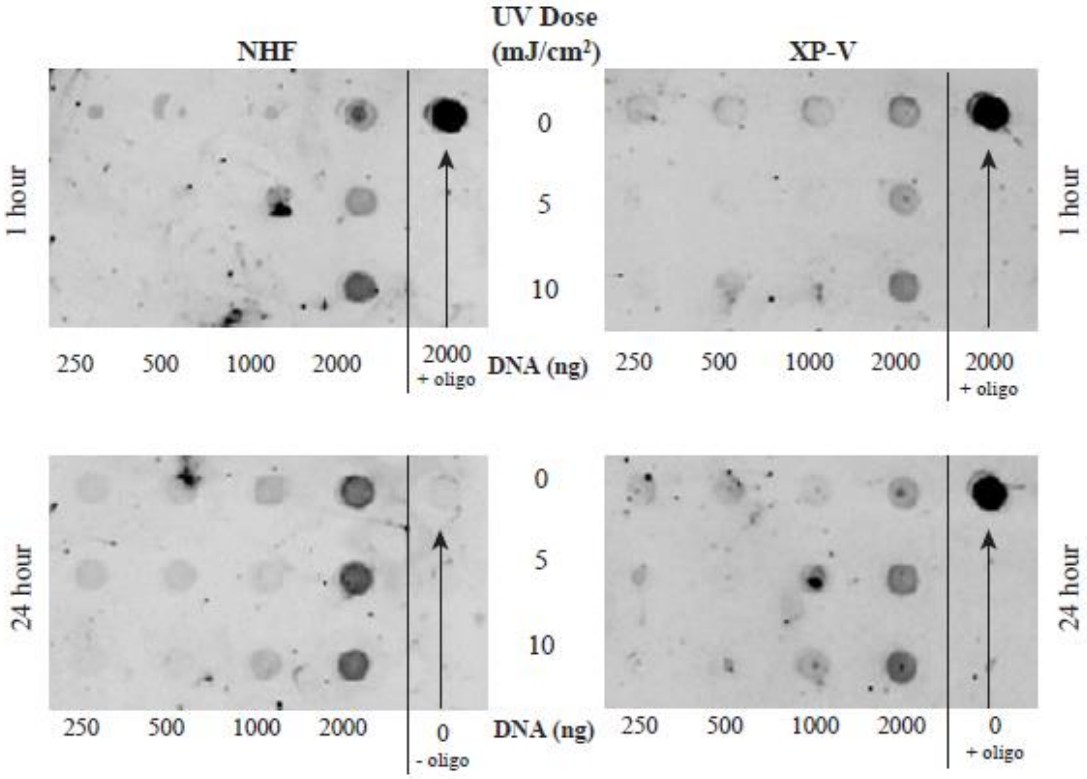

Figure S1.2- Dot blot of genomic DNA collected 1 and 24 hours after UV-B irradiation. Cells were treated and DNA samples were collected and purified as described in Materials and Methods. After quantification by UV absorption, they were processed using the Bio-Dot apparatus from BioRad (Product number 170-6545) using protocols described previously,[76, 81] and as recommended by the manufacturer. The primary antibody was from Sigma-Aldrich (St. Louis, MO; T1192) and was used at 0.8 μg/ml final concentration. The upper right dot in each 1 hour blot contained 2000 ng untreated DNA that was spiked with 0.38 pmoles of a TT dimer containing 75-mer as positive control. The right lane of the bottom blots contained no DNA as negative control (left) or oligo only as another positive control.

CHAPTER 2

Minimal Detection of Nuclear Mutations in XP-V and Normal Cells Treated with Oxidative Stress Inducing Agents *

Kimberly N. Herman[1], Shannon Toffton[1], Scott D. McCulloch [1, 2]

[1] Department of Biological Sciences, Environmental and Molecular Toxicology Program

[2] Center for Human Health and the Environment

North Carolina State University, Raleigh, NC 27695

* Running Title: *Oxidative stress and nuclear mutagenesis*

Corresponding Author:

Scott McCulloch

850 Main Campus Drive

Campus Box 7633 Raleigh, NC

scott_mcculloch@ncsu.edu

Key Words: DNA damage, DNA polymerase η, mutagenesis, translesion synthesis, oxidative stress

Published In:

Journal of Biochemical and Molecular Toxicology. December 2014; Volume 28, Issue 12: Pages 568-577

http://onlinelibrary.wiley.com/doi/10.1002/jbt.21599/abstract

Abstract

Elevated levels of reactive oxygen species (ROS) can be induced by exposure to various chemicals and radiation. One type of damage in DNA produced by ROS is modification of guanine to 7,8-dihydro-8-oxoguanine (8-oxoG). This particular alteration to the chemistry of the base can inhibit the replication fork and has been linked to mutagenesis, cancer and aging. *In vitro* studies have shown that the translesion synthesis polymerase, DNA polymerase η (pol η), is able to efficiently bypass 8-oxoG in DNA. In this study we wanted to investigate the mutagenic effects of oxidative stress, and in particular 8-oxoG, in the presence and absence of pol η. We quantified levels of oxidative stress, 8-oxoG levels in DNA, and nuclear mutation rates. We found that most of the 8-oxoG detected were localized to the mitochondrial DNA, opposed to the nuclear DNA. We also saw a corresponding lack of mutations in a nuclear encoded gene. This suggests that oxidative stress' primary mutagenic effects are not predominantly on genomic DNA.

Introduction

Oxidative stress is defined as an excess of reactive oxygen species (ROS) over antioxidants. ROS can occur as a consequence of normal respiration, as well as from external sources; it is a relevant challenge to normal homeostasis and human health. ROS takes many forms including the radical species superoxide anion ($O_2^{\cdot -}$) and hydroxyl radical ($^{\cdot}OH$), in addition to such non-radicals including H_2O_2.[26, 106-107] ROS can cause cellular damage by attacking DNA directly, or indirectly, as well as damaging lipids and proteins. All of these processes can lead to various diseases, aging and cancer.[26, 106]

One of the most abundant and mutagenic oxidative alterations is 7,8-dihydro-8-oxoguanine (8-oxoG), which can be formed by ROS directly attacking guanine bases within double stranded DNA. 8-oxoG can potentially Hoogsteen base pair with adenine, instead of forming a normal Watson-crick base pair with cytosine. This mispair causes a GC →TA transversion. Due to the structural similarity of 8-oxoG:A base pair to that of the T:A base pair, this mispair can be refractory to proofreading and possibly some repair mechanisms as well.[91, 108-109] There are, however, multiple mechanisms to try and reduce the effects of 8-oxoG on the genome. One of these is 8-oxoguanine glycosylase (hOGG1) which is responsible for excising the damaged 8-oxoG base, thus initiating base excision repair. Additionally, there is human Mut T homolog (hMTH1) which hydrolyzes free 8-oxoG nucleotide triphosphate in the nucleotide pool and human Mut Y homolog (hMYH) which removes the mispaired A from the 8-oxoG:A pair.[106] The 8-oxoG remaining in the DNA

during DNA replication is then able to inhibit progression of the replication fork and becomes a candidate for translesion synthesis (TLS).[110]

Studies have shown that the Y-family of DNA polymerases (pol) (DNA polymerase η, ι, κ and Rev1) have some ability to bypass the damaged 8-oxoG base, usually inserting A.[91, 111-112] *In vitro* lesion bypass assays and cell based plasmid replication assays have been used to evaluate pol η, showing it can bypass 8-oxoG, and that it does so with better efficiency than past normal guanines, but with very low fidelity.[42, 91, 113] For this reason, we decided to evaluate a cellular response of oxidative stress on nuclear DNA, in particular evaluating for effects of 8-oxoG in cells proficient in known DNA repair pathways (normal human fibroblast) and in cells deficient in functional pol η (Xeroderma pigmentosum variant (XP-V) cell). The goal was to evaluate the role of pol η in oxidative stress induced nuclear mutagenesis.

In order to evaluate for nuclear mutagenesis we chose to use the hypoxanthine-guanine phosphoribosyltransferase (HPRT) nuclear mutation assay with two chemicals which are known oxidative stress agents. Menadione (MD) is a general oxidative stress agent which affects complex I of the electron transport chain, causing the production of superoxide anion.[30-31, 114] Methylene blue plus light (MBL), causes redox cycling and the production of superoxide. MBL has previously been shown to preferentially produce 8-oxoG in the treatment of plasmids.[29, 113, 115-116] In addition to HPRT mutation rates, we also evaluated the level of oxidative stress and 8-oxoG generated during these treatments.

Materials and Methods

Cell lines, growth conditions and treatments protocols

Cell lines used were GM02359-hTERT (XP-V strain XP115LO; referred throughout as XP-V), a pol η deficient line; and NHF1-hTERT (referred to as NHF), a normal fibroblast control line, both previously described.[56, 92-93] Conditions for growth were as described previously.[56] Treatment conditions were determined by literature review in conjunction with preliminary cell viability studies. Menadione (USB Corporation, Cleveland, OH) was used at 125 μM. Stock solutions of 1 mM were made in HBSS (Sigma-Aldrich, Saint Louis, MO) and filtered sterilized with a 0.2 μm filter (Genesee Scientific, RTP, NC) and diluted immediately prior to use in HBSS. Cells were treated for 20 minutes at room temperature.[30, 114, 117] Methylene blue plus light treatments were completed as follows: methylene blue (Calbiochem, EMD Biosciences, La Jolla, CA) stocks of 1 mM were prepared in ppH2O and filter sterilized (0.2 μm). Cells were treated based on McBride *et al* and Lee and Pfeifer.[29, 113] Briefly, cell growth media was removed and replaced with 10 mM sodium phosphate buffer (pH 6.9) (Fischer-Scientific, Fair Lawn, NJ) containing deferoxamine mesylate (Calbiochem, EMD Biosciences, La Jolla, CA) at a concentration of 0.1 mM.[29, 113] Methylene blue was added to the phosphate buffer at a final concentration of 5 μM, then culture plates were exposed to an LED light (warm white 800 lumens, equivalence to 60W incandescent) at a distance of 18 inches for 15 minutes at room temperature.[29, 113, 115] For exposure to ultraviolet A radiation (UV-A), a dose of 400 mJ/cm^2 was used, from a 360 nm monochromatic lamp (EN-280L; Spectroline). The setup is a dual 8-watt tube with a 2F082 filter. Fluence was

determined by a SEL033 (#SEL0339663) detector from International Light technologies attached to a phototherapy UVA measurement system ILT1400SEL033. Ultraviolet B radiation (UV-B) was used at 10 mJ/cm^2 as previously described.[56] Addition of caffeine for specific treatments were as previously described.[56] The positive control for the flow cytometry was t-butylhydroperoxide (tBHP) (Sigma-Aldrich, Saint Louis, MO) at final concentration of 1 mM, treated for 1 hour at 37^{o}C, as recommended by the manufacturer.

Total Cellular ROS detection

Cells were plated at 0.5x10^6 cells per P10 plate (Genesee Scientific, RTP, NC), incubated for 24 hours and then treated (as described above). Immediately after treatment, cells were washed with HBSS (Sigma-Aldrich, Saint Louis, MO) and then 3 mL of HBSS was added to the plates. CM-H_2DCFDA (DCF) (Gibco-Life Technologies, Grand Island, NY) dye was added to the HBSS to a final concentration of 1 μM (as pre-determined by preliminary background fluorescence studies). Plates were incubated for 30 minutes at 37^{o}C in the presence of DCF. The cells were then washed again with HBSS and trypsinized, harvested in 5 mL polystyrene round-bottom tubes (BD Falcon, BD Biosciences: Franklin Lakes, NJ), washed again in HBSS, harvested and the cell pellet was brought up in 0.5 mL of HBSS and kept on ice in the dark until analysis by flow cytometry. Data was acquired on a Becton Dickinson LSRII cytometer (BD Biosciences, Franklin Lakes, NJ) using Diva 6.1 software. Data analysis was performed using FlowJo software.

Protein ROS detection

Detection of oxidized protein was performed as previously described with slight modifications.[118-122] Cells were plated at 80% confluency and grown for 24 hours. Cells were then treated and collected at 0, 4 or 24 hours after treatment. Treatments were as described above. Cells were trypsinized, washed with HBSS, and cell pellets collected. Cell pellets were lysed as described previously.[95] An equal volume of 20% trichloroacetic acid (TCA) was added to the lysate, followed by vortexing and centrifugation at 800*g* for 5 minutes. The supernatant was discarded and 250 μL of 2N hydrochloric acid (HCL) was added to re-suspend the pellet. Then 250 μL of 2,4-Dinitrophenylhadrazine (DNPH) (Sigma-Aldrich, Saint Louis, MO) in 2N HCL was added and the mixture was rotated for 1 hour at room temperature. 500 uL of 20% TCA was added and the tubes vortexed to mix. Protein pellets were harvested by centrifugation at 800*g* for 5 min. Pellets were washed with ethanol:ethylacetate (1:1) three times. The pellet was then dried and resuspended in 8M urea. This mixture was centrifuged at 13,400*g* for 5 minutes and the upper phase was collected. Protein concentrations were determined by Bio-Rad protein assay as described.[95] Samples (3 μg) were separated using 12% SDS-PAGE. Gels were wet transferred to nitrocellulose and Western blot analysis was performed. Antibodies used were used: Anti-DNP (D9656, Sigma-Aldrich, Saint Louis, MO); anti-β-actin (A5441). Imaging was on a Storm 865 (GE Life Science) using Cy5 labelled secondary antibodies:ECL Plex Goat anti rabbit Cy5 (PA45011V) and ECL Plex goat anti mouse Cy5 (PA45009V).

8-oxoG detection by alkaline gel

Replicative form plasmid DNA, M13mp18, from XL1 blue cells was purified by Qiagen miniprep kit. It was then treated with either: no treatment, methylene blue only, light only or methylene blue plus light. Samples were treated in 10 mM phosphate buffer, and underwent three ethanol precipitations to remove residual methylene blue. Two μg of treated plasmid was digested with FPG (New England Biolabs) under conditions recommended by the manufacturer. FPG was deactivated by heating for 10 minutes at 60°C, and samples were separated through a 1.5% alkaline gel as described.[123]

8-oxo-dG detection by 2D Mass Spectrometry

5×10^6 cells were treated as described above and harvested for cell pellets at either 1 hour or 24 hours post treatment. Total cellular DNA was prepared from cells by the addition of lysis buffer (Qiagen 1045696) to which was added 20 mM 2,2,6,6-Tetramethylpiperidinooxy (Tempo) to prevent additional 8-oxoG production. Proteins were precipitated using neutralization solution (Qiagen 1045697). Samples were vortexed and centrifuged at ≥16,000*g* for 15 minutes. Supernatant was collected and DNA/RNA precipitated with isopropanol. The pellet was resuspended in lysis/20 mM Tempo buffer, RNaseA (Sigma-Aldrich) was added and incubated for 30 minutes at 37°C. Protein precipitation solution was again added the sample was centrifuged at ≥ 16,000*g* for 15 minutes, followed by a second isopropanol precipitation. DNA was resuspended in 30 μL of ppH_2O with 1 mM Tempo. 2D chromatography was performed as in Boysen *et al*.[124] See Supplemental Figure 3 for description of mitochondrial DNA preparation. 2D mass

spectrometry was performed by Leonard Collins at the University of North Carolina Biomarker Mass Spectrometry Facility.

Mutation Frequency

The HPRT mutation assay was conducted as previously described.[56, 93-94]

Analysis of mutations at the ura3-29 locus after MBL dosing

The wild-type (proficient in both OGG1 and RAD30 (pol η) base yeast strain used is the same as generated in a previous report (7B-YUNI300; *MATa CAN1 his7-2 leu2-Δ::kanMX ura3-29:agp1 trp1-289 ade2-1 lys2-ΔGG2899-2900*).[125] OGG1 and/or RAD30 were deleted separately or in combination as described previously.[125-126] They are referred to here as OGG1 RAD30, *ogg1Δ* RAD30, OGG1 *rad30Δ*, and *ogg1Δ rad30Δ*. Each strain contains a non-functional *ura3-29* locus (codon 86, TCT) which reverts to a functional state after GC→AT mutations. This change is suggestive of 8-oxoG dependent mutagenesis.[33] For one day treatments, cultures (10 ml) of each strain were grown from a single colony overnight at 30°C, 250 RPM in YPD. Cells were harvested by centrifugation, washed once in PBS, resuspended in 10 ml PBS, and methylene blue (Calbiochem, EMD Biosciences, La Jolla, CA) was added to final concentration of 5 μM. Cells were transferred to a P10 culture dish and exposed to an LED white light source as described above and previously.[113, 115] Cells were then harvested and washed twice with 10 ml PBS. After the final wash, cells were re-suspended in 0.5 ml PBS and plated onto either complete synthetic media (CSM) or CSM -Uracil (CSM -Ura) to obtain total cell numbers and numbers of mutants at the URA3 locus, respectively. Mutation frequency was calculated as (Number of mutants/Total number of

cells). Experiments were performed at least 3 times. For three day treatments, after the final wash a 100 µl aliquot of cells was added to 9.9 ml YPD and grown overnight at 30°C, 250 RPM. The dosing step was repeated on day 2 and again on day 3 before plating cells onto CSM/CSM -Ura as described above.

Results

Production of Cellular Oxidative Stress

In order to verify that our treatments were creating oxidative stress, we performed flow cytometry using 2'-7' dichlorofluorescin (H2DCF) dye which becomes oxidized to the fluorescent dichlorodihydrofluorescein (DCF) in the presence of ROS.(omori non-canonical 2011) Controls included cells which were both untreated and undyed, and cells that were untreated but dyed with H2DCF to give baseline values to compare against for increases in fluorescence caused by increased ROS. The positive control used was *tert*-butyl hydroperoxide (tBHP) at a dose of 1 mM for one hour at 37°C. Oxidative stress treatments evaluated included 125 µM MD, 5 µM MBL, 10 mJ/cm^2 UV-B, and 400 mJ/cm^2 UV-A. As expected, untreated, undyed cells displayed the lowest levels of fluorescence, and tBHP treated cells displayed the highest levels of fluorescence (Figure 2.1A and B; Table 2.1). The shift from left to right for untreated, dyed cells (Figure 2.1A and B, Clear curves; Supplementary Figures 2.1 and 2.2) indicates background fluorescence of the dye and/or basal levels of ROS. From this we see that there may be slightly different levels of ROS in the NHF compared to the XPV line under normal growth conditions, or that the cells have intrinsically different background fluorescence. The large increase in fluorescence caused by

tBHP (Figure 2.1A and B, red curves) suggests a very high level of ROS production. This is consistent with the severe cytotoxicity observed by tBHP at this treatment level (data not shown). Surprisingly, despite using agents and doses that have been reported in the literature to cause oxidative stress, in our hands the treatments generated ROS at roughly the same levels as observed in untreated cells (Figure 2.1A and B, orange, green, purple curves). The exception to this is MBL, which in the NHF cells did cause a detectable increase in DCF fluorescence (Figure 2.1A). Although additional dyes to test for cell death were not done in conjunction with ROS staining, it seems likely that MBL treatment has affected cell survival, as suggested by the decrease in the percentage of the parent population for MBL compared to Untreated (Table 2.1). This holds true for both NHF and XPV cells, and is similar to the effect seen with tBHP exposure. This suggest that despite the overall FITC-A level (i.e. level of detected ROS) for MBL being only slightly elevated in NHF cells and somewhat lower in XP-V cells compared to untreated samples, the treatment is in fact affecting the cell population in other ways.

Effects of oxidative stress - Protein Oxidation

In addition to direct detection of ROS we were interested in evaluating possible effects of oxidative stress within the cells. First, we chose to look at protein oxidation using a Western blot assay. After increased ROS, an antibody that recognizes a DNP conjugate to carbonylated proteins will show increased numbers of bands and a streakier appearance of lanes. Consistent with the flow cytometric detection of ROS results, Figure 2.1D-G shows moderate increases in oxidized proteins after most of the treatments and time points. The

most prominent increase in oxidized protein is after MBL treatment, which correlates well with the above described flow cytometry based data.

8-oxoG detection by alkaline gel

Replicative form DNA of M13mp18 bacteriophage was used as a model to test the efficacy of MBL in generating 8-oxoG. DNA was exposed to MBL treatment, purified, and then treated with FPG, a protein that cleaves 8-oxoG from the DNA, leaving an abasic site. Separation of the DNA in an alkaline gel causes strand breaks at abasic sites, producing an increase in smaller fragments, or smear of DNA instead of discrete bands (Figure 2.2A). Figure 2.2B shows that only in the presence of both MB and white light, rather than each treatment alone, are detectable levels of 8-oxoG generated. The smear evident in the right most lane, confirms that the methylene blue plus light treatment creates 8-oxoG in greatly elevated levels compared to no treatment.

8-oxoG detection by 2D mass spectrometry

While the above assay shows that MBL can cause 8-oxoG in DNA in solution, we were also interested in whether our treatments were capable of generating 8-oxoG in DNA within cells. To test for this, we collected DNA from cells after treatments and analyzed it using mass spectrometry. We dosed cells with 125 μM MD, 10 mJ/cm^2 UV-B, 400 mJ/cm^2 UV-A or 5 μM MBL and collected DNA 1 hour post treatment. We also collected DNA 24 hours post treatment for the MBL dose. As shown in Table 2.2 and Figure 2.2, we were unable to detect elevated 8-oxoG levels with MD, UV-B or UV-A treatments. However, we did observe a roughly 10 fold increase in 8-oxoG from the MBL treatment. This was

observed in both cell lines, suggesting a similar mechanism of formation. Additionally, 8-oxoG levels 24 hours after treatment show that repair of the damage is occurring, and that the rate is similar in both cell lines (Figure 2.2C). Due to the fact that menadione uses Complex I of the mitochondrial respiratory chain for reduction and is known to interfere with mitochondrial respiration, and that methylene blue causes redox cycling of NADPH and NADH within the mitochondria,[28, 30] we also looked at 8-oxoG levels specifically in DNA fractions highly enriched for mitochondrial DNA (Supplementary Figure 2.3). As seen in Table 2.2 and Figure 2.2D, once separated out from the total cellular DNA, we observed that most of the detected 8-oxoG is localized in the mitochondrial DNA and not in nuclear DNA fractions.

Evaluation of Nuclear Mutations using the HPRT locus

The fidelity of pol η has been assessed in numerous biochemical experiments and studies. Many of these studies have confirmed pol η performs low fidelity bypass of 8-oxoG *in vitro*,[42-43, 47, 91, 113, 127] while other studies have suggested that this bypass is "error free" (for lack of a better term).[33, 128-129] In addition to biochemical experiments, pol η also has been evaluated using damaged plasmids transfected into cells. This work suggests that the presence of pol η suppresses mutagenesis.[113] With this background of biochemical and plasmid based data, we wanted to transition into a cell based assay to investigate whether the presence of pol η would affect nuclear mutagenesis rates after oxidative stress. Unexpectedly, we found that our oxidative treatments seemingly had no effect on nuclear DNA mutation frequencies, as measured by the HPRT assay (Table 2.3). Untreated XP-V

cells had a mutation frequency (MF) of 0.98 x 10^{-5}. Treatment with menadione (MF 2.33 x 10^{-5}; 2.4X) and MBL (MF = 1.01 x 10^{-5}; 1.0X) gave nearly identical frequencies. Similarly, untreated NHF cells gave a MF value of 0.55 x10^{-5}, with menadione (1.65 x10^{-5}; 3X) and MBL (1.27 x10^{-5}; 2.4X) again causing very little difference. This is in comparison to our previously published work using environmentally relevant levels of UV-B (10 mJ/cm^2) in which the MF of XPV cells was 25.8 x10^{-5} (26X higher than untreated) and for NHF cells the MF was 8.56 x10^{-5} (15.6X untreated).[56] In addition we attempted alternative treatment protocols in an attempt to exacerbate the effects, in case a single, short oxidative stress inducing treatment was insufficient to generate damage/mutations at levels detectable in this assay. Repeated, low dose MD treatments caused cell death, regardless of the levels used. Repeated MBL treatments did not alter the mutation frequency, but did result in extremely low colony forming efficiencies (CFE). Treatments with H_2O_2 produced highly variable results (both within replicates and within different experiments) and were therefore unable to be used. We also attempted the addition of caffeine after MBL treatment (similar to as has been used to increase cytotoxicity effects of XP-V lines under UV-C and UV-B treatments),[56, 98, 100] but again this lowered the CFE (less than 1%) to a point that the mutation frequencies obtained were unreliable. These additional treatments are described in Supplementary Note 2.1. In total, we were unable to find treatment levels/conditions that balanced survivability with mutations.

Oxidative stress dependent Ura3-29 mutations in yeast cells

In order to further explore the effects of MBL in cells, we used a set of yeast strains that were deficient in OGG1, RAD30, or both. OGG1 is the sole 8-oxoG repair enzyme in *S. cerevisiae* cells, and RAD30 (pol η) is the only Y-family member with significant lesion bypass ability. It has previously been shown that spontaneous mutations at the Ura3-29 locus are increased in an *ogg1*mutant strain, and that deletion of *rad30* further increases this mutation frequency.[33] Here, we performed similar experiments, but instead dosed cells either once or on 3 consecutive days with 5 μM MBL (20 minute exposure). Consistent with our results described above, deletion of pol η alone did not affect the mutation frequency at a nuclear locus (Figure 2.3). We do see, however, that both deletion of either OGG1 alone or both OGG1 and RAD30 gives a large increase in the mutation frequency at the Ura3-29 locus. This is true after either a single exposure or 3 separate days of treatment. Determination of the sequence of functional Ura3 genes in mutants from the double knockout strain showed that they were all GC→AT changes (data not shown), as expected if errors when bypassing 8-oxoG were the cause. These data suggest that when increased levels of 8-oxoG are present, the mutagenic propensity of it are partially mitigated by pol η, at least in yeast. They also suggest that the repair of 8-oxoG is more important in preventing mutagenesis than lesion bypass; whether or not a similar phenomenon is occurring in human cells remains to be seen. It is important to keep in mind that human pol η has a much greater *in vitro* error rate when bypassing 8-oxoG as compared to yeast pol η.[91]

Discussion

Numerous studies have evaluated the role of human polymerases encountering oxidative lesions; including plasmid replication assays and *in vitro* biochemical studies. In addition, studies assessing oxidative stress cytotoxicity have been performed, but none have combined both. Therefore, we treated cells with MD and MBL, in hopes of gaining a broader understanding of lesion bypass after oxidative stress. We chose MD for its properties as a general oxidative stress agent, and MBL for its defined ability to produce 8-oxoG in DNA.[115] Additionally, UV-B and UV-A were used for their well-known mutagenic effects in conjunction with their general consideration as oxidative stressors.

First, we tested for oxidative stress by flow cytometry. Our treatments, despite being published as oxidative stress agents, showed relatively low levels of detectible ROS (Figure 2.1A-C). However, these particular doses were chosen for their relatively minor cytotoxic effects to allow for evaluation with the long term mutagenicity assay; higher levels of the treatments could have produced larger quantities of ROS, but, it would enhance cytotoxicity, reducing the effectiveness of the HPRT assay. Our MD and MBL treatments show clear signs of oxidative stress, as evident through production of oxidized proteins (Figure 2.1D-G; Table 2.1), as well as detectible 8-oxoG lesions in DNA (Figure 2.2; Table 2.2). Despite seeing effects of oxidative stress throughout the cell, our nuclear mutation frequencies (assayed at the HPRT locus) of these treatments were disappointingly low and not significantly different from untreated cells. Attempts to exacerbate oxidative stress to increase mutation levels (Supplementary Note 2.1) were unsuccessful. Despite our additional

efforts, we were unable to find conditions that balanced longer term survivability with detection of mutations, with many possible contributing factors. The first possibility is that the oxidative stress treatments used here were not enough on their own to cause detectable mutations. Under more 'real world' conditions exposure to multiple different agents simultaneously is more realistic, including combined exposures of sunlight, chemicals within food or water, and other sources of stress. Another possibility suggested by our yeast data and other previously published results[33, 91, 113] is, a pol η deficiency on its' own is insufficient for 8-oxoG damage to cause mutations, and instead, there would need to be a concomitant deficiency in OGG1 or other repair factors to increase the 8-oxoG load. In addition, it is interesting to note that our MBL treatment caused 8-oxoG to be mainly localized in the mitochondria. MBL and MD both use the electron transport chain in order to create ROS, so it is perhaps not surprising to see effects in the mitochondria DNA; however it was unexpected to not see more general cellular effects caused by the increased ROS. This lack of effect could be due to the diffuse nature of ROS compared to a more direct damaging agent such as UV light. These results suggest that more research is needed to determine when the cells robust repair mechanisms become overwhelmed by ROS, therefore permitting TLS to bypass the DNA damage caused by ROS and creating the potential for mutagenicity. Lastly, it is entirely possible that the HPRT assay has insufficient sensitivity to detect low levels of mutations, and therefore another method may be more suited to detecting these changes; including the potential for deep sequencing.[130]

Figure 2.1 - ROS and Oxidative Stress Analysis - (A) Flow cytometric analysis of ROS levels, NHF cells. (B) Flow cytometric analysis of ROS levels, XP-V cells. For both A and B the peak the negative control is an untreated, undyed cell sample. (C) Color code key for Panels A and B. (D) Protein extracts from NHF cells were analyzed by Western blot with an α-DNPH antibody to detect oxidized protein, as a measure of oxidative stress. Treatments and times of analysis are as indicated. (E) Protein extracts from XP-V cells were analyzed by Western blot with an anti-DNPH antibody as described for Panel D. (F) Western blot for β-actin on gel from Panel D. (G) Western blot for β-actin on gel from E. (*) Indicates a sample that was not conjugated to verify the anti-DNPH antibody was specific.

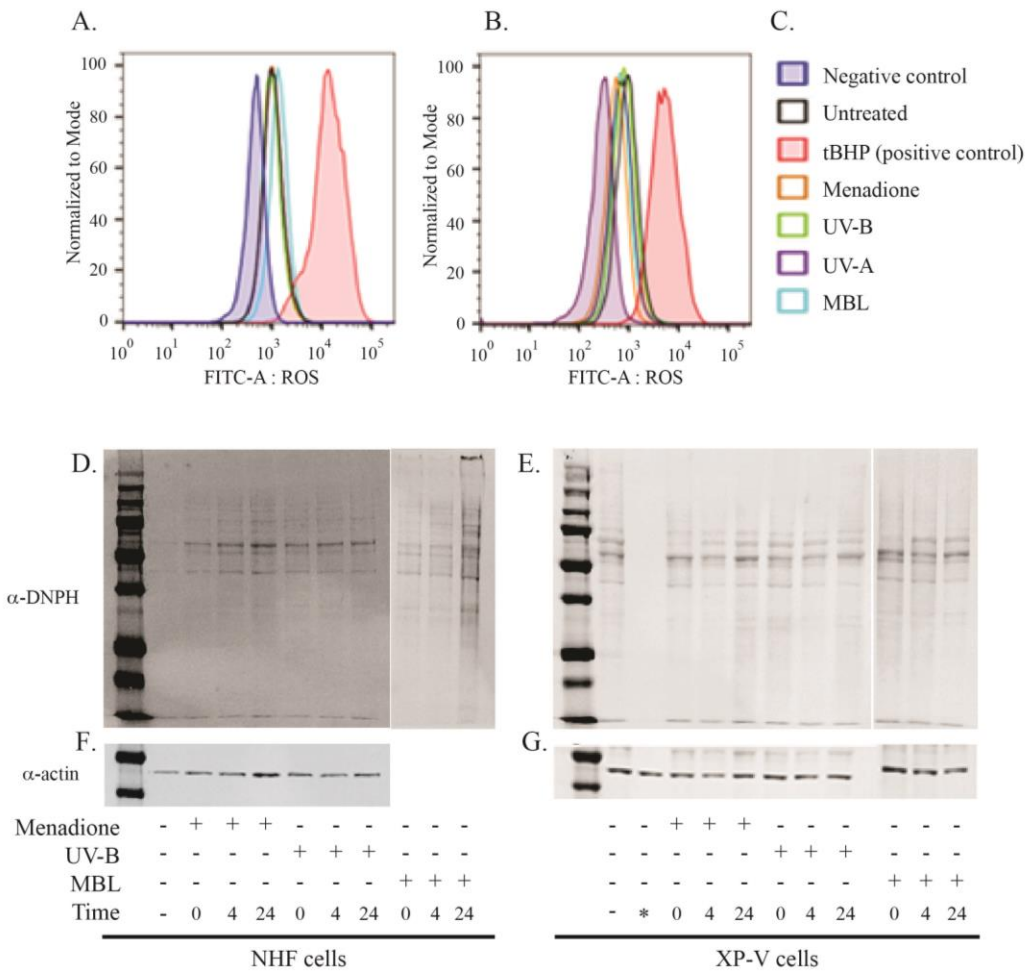
A.
B.
C.
Normalized to Mode
FITC-A : ROS
Negative control
Untreated
tBHP (positive control)
Menadione
UV-B
UV-A
MBL
D.
E.
α-DNPH
F.
G.
α-actin
Menadione
UV-B
MBL
Time
NHF cells
XP-V cells

Table 2.1 - Oxidative Stress Flow Cytometry - Statistical analysis using FlowJo software for calculating ROS detection. The value of "FITC-A" indicates fluorescence which is correlated with ROS level. "Freq of Parent" indicates the percentage of cells gated and analyzed from the total population, a measure of cell viability.

	NHF		XP-V	
	Freq of Parent	**FITC-A**	**Freq of Parent**	**FITC-A**
No dye	93.7	470	61.2	304
tBHP	68.6	15922	25.6	6003
Untreated	93.8	1106	58.5	976
125 µM Menadione	92.5	1075	53.8	571
10 mJ/cm^2 UV-B	94.6	1014	67.0	869
400 mJ/ cm^2 UV-A	94.8	1091	68.3	738
5 µM MBL	74.7	1388	27.1	786

Figure 2.2 - 8-oxoG analysis - (A): Schematic of 8-oxoG detection assay in plasmid DNA. The presence of 8oxoG is revealed by cleavage with FPG, generating a smear of DNA during alkaline agarose gel electrophoresis. Replicative form M13mp18 DNA was used with: no treatment, methylene blue only, light only or methylene blue plus light. (B): Alkaline gel after FPG treatment indicating that the MBL treatments generate ample 8-oxoG lesions. (C): Analysis of 8-oxoG levels in total DNA isolated from NHF cells after the treatments listed. Whole cell DNA was isolated from NHF cells (black bars) and XP-V cells (white bars) and sent for mass spectrometry. (D.): Enriched mitochondrial DNA was also isolated and analyzed. The results indicate that MBL preferentially damages mitochondrial DNA.

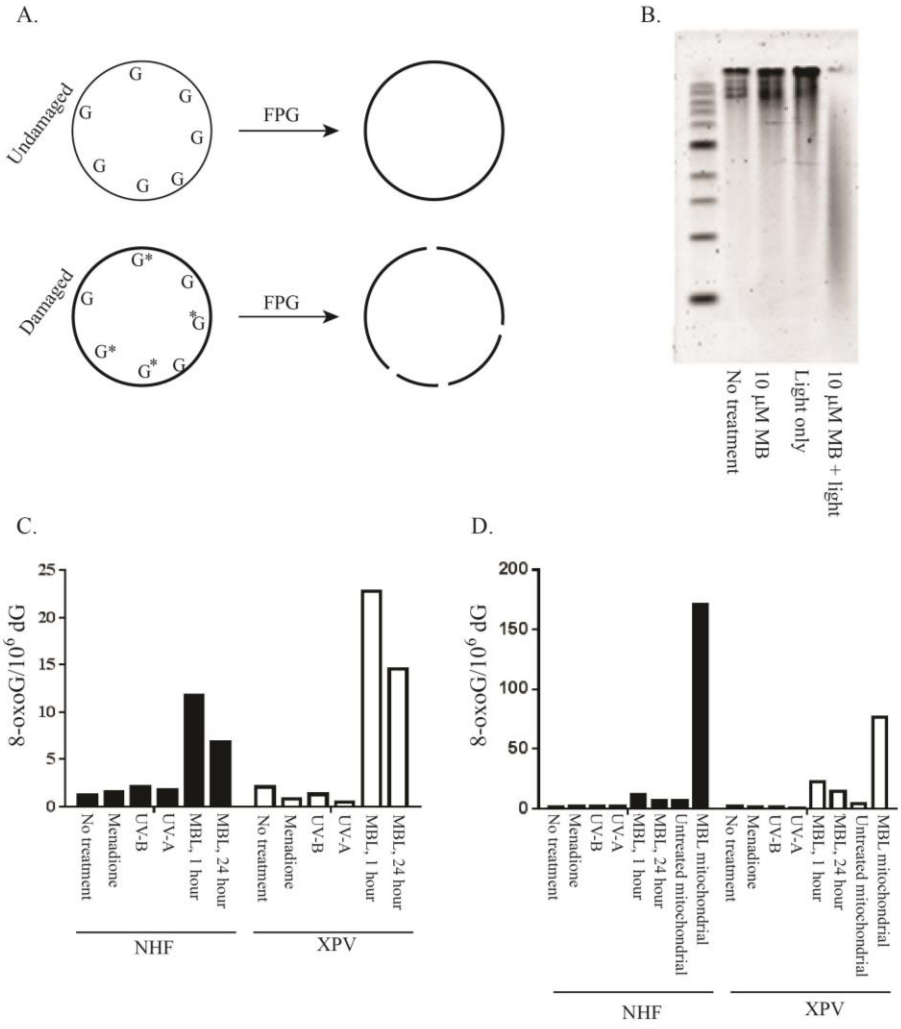
A.
Undamaged
FPG
Damaged
FPG
B.
No treatment
10 μM MB
Light only
10 μM MB + light
C.
8-oxoG/10^6 dG
No treatment
Menadione
UV-B
UV-A
MBL, 1 hour
MBL, 24 hour
NHF
XPV
D.
8-oxoG/10^6 dG
MBL mitochondrial
Untreated mitochondrial

Table 2.2 - Analysis of 8-oxoG damage in nuclear and mitochondrial DNA - Levels of 8-oxo-dG were measured in total DNA and fractions enriched for mtDNA using mass spectrometry. Values given are levels of 8-oxo-dG per $1x10^6$ dG. Times given indicate when DNA was harvested after treatment. Untreated samples were similarly harvested 1 hour after mock treatment.

	8-oxo-dG/10^6 dG	
	NHF	**XP-V**
Untreated	1.2 (1)	2.1 (1)
125 µM Menadione: 1 hr	1.5 (1.3x)	0.8 (0.7x)
10 mJ/cm^2 UV-B: 1 hr	2.1 (1.8x)	1.3 (0.6x)
400 mJ/cm^2 UV-A: 1 hr	1.8 (1.5)	0.5 (0.2x)
5 µM MBL: 1 hr	11.8 (10x)	22.8 (11x)
5 µM MBL: 24 hr	6.8 (5.7x)	14.5 (6.9x)
Untreated mtDNA	4.0 (3.3x)	6.1 (2.9x)
5 µM MBL: 1 hr, mtDNA	76.4 (63.7)	170.9 (81.3x)

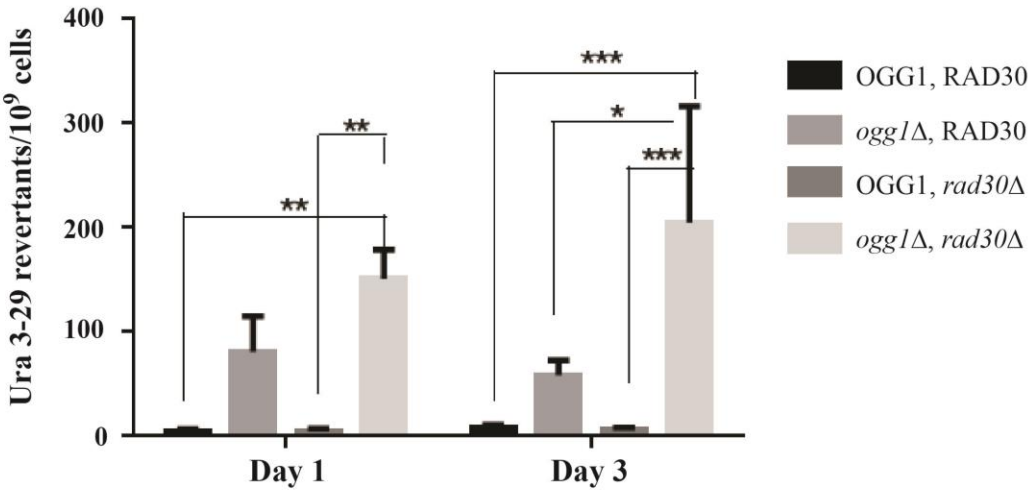

Figure 2.3 – Oxidative stress induced mutation frequency at the URA3-29 locus is dependent on OGG1 and RAD30 activity - Yeast strains proficient or deficient in either OGG1, RAD30 (pol η), or both were treated with MBL (5 μM, 20 minutes) for 1 or 3 days. Reversion of the TCT Ura3-29 allele to TAT confers growth in the absence of uracil and suggests mispairing of A opposite 8-oxoG in the opposite strand.[33, 91] The statistics were run with Graphpad Prism 6 using a 2way anova with a Tukey post test. Significance is as follows: *= $p \leq 0.05$, **= $p \leq 0.01$, ***= $p \leq 0.001$.

Supplementary Note 2.1- Additional Mutation Frequency Treatments - Due to the fact that the results from the nuclear mutation assay were lower than anticipated, we wondered whether the doses and treatments were not sufficient on their own to create the oxidative stress. Additional treatments were evaluated by HPRT in order to help exacerbate the effects that we were thought were lacking. We tried multiple different approaches, including a long term MD treatment at various lower doses; however, cells did not survive long enough for mutation assessment. We also tried multiple doses of methylene blue plus light over a longer period of time; however, this did not affect the mutation frequency, it only lowered the colony forming efficiency of the assay to very low levels (less than 5%). We added caffeine to the MBL treatments in hopes that adding the ATR inhibitor would help any underlying mutations have a greater affect, however, it did not. Other treatments included a 1 mM H_2O_2 treatment for 30 minutes at room temperature in HBSS; and a 400 mJ/cm^2 UV-A treatment. In total, we were unable to find conditions in which a significant fraction of cells survived that were accompanied by increased mutations.

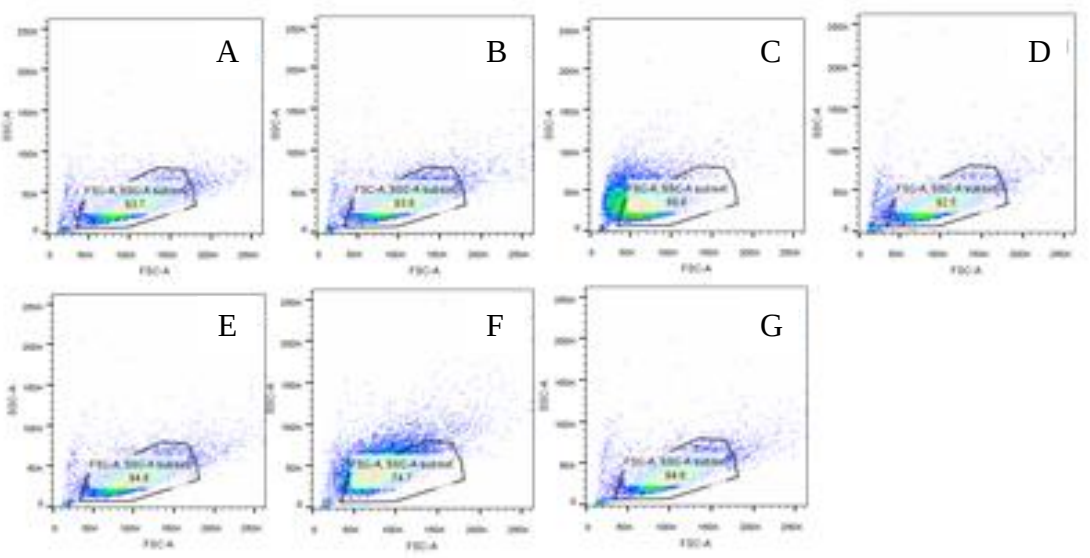

Supplementary Figure 2.1: **Gated regions of forward scatter (FSC; Y-axis) and side scatter (SSC; X-axis) analysis in NHF cell lines.** A: NHF cells, undyed. Used for negative control for flow cytometry. B: NHF cells, untreated. Used to show background fluorescence of dye. C. NHF cell, tBHP. Used as positive control for DCF dye, as suggested by manufacturer. D. NHF cells, 125 µM Menadione. E. NHF cells, 400 mJ/cm^2 UV-A. F. NHF cells, 10 mJ/cm^2 UV-B. G. NHF cells, 5µM MBL.

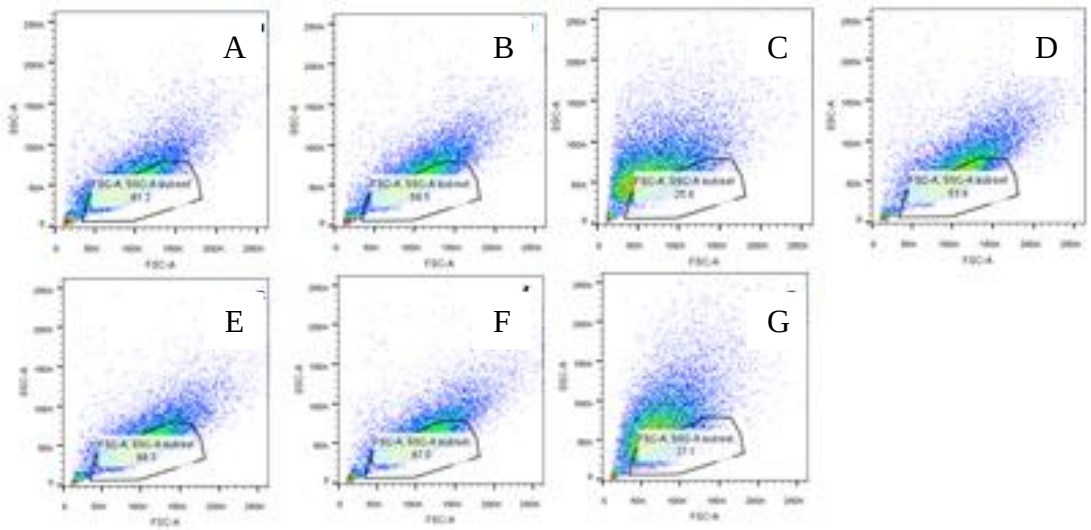

Supplementary Figure 2.2: Gated regions of FSC and SSC analysis in XP-V cell lines A: XP-V cells, undyed. Used for negative control for flow cytometry. B: XP-V cells, untreated. Used to show background fluorescence of dye. C. XP-V cell, tBHP. Used as positive control for DCF dye, as suggested by manufacturer. D. XP-V cells, 125 µM Menadione. E. XP-V cells, 400 mJ/cm^2 UV-A. F. XP-V cells, 10 mJ/cm^2 UV-B. G. XP-V cells, 5µM MBL.

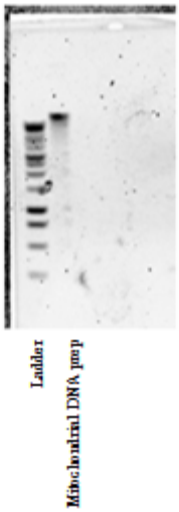

Supplementary Figure 2.3: Electrophoretic analysis of enriched mitochondrial DNA. Cells were collected by centrifugation and a Qiagen plasmid mini kit (Qiagen 27104) was used to collect mitochondrial DNA. 2,2,6,6-Tetramethylpiperidinooxy (Tempo) was added to help prevent 8-oxoG production during DNA isolation: 2.5 µL Tempo to P1; 1 µL Tempo to resuspension ddH_2O. A portion of the purified DNA was separated through 1% agarose gel, stained with SYBRsafe (Invitrogen) and visualized using a GE Life Sciences Storm 865.

CHAPTER 3

DNA polymerase mRNA Expression Changes Following DNA Damaging Agents [*]

Kimberly N. Herman[1], Shannon Toffton[1], Scott D. McCulloch [1, 2]

[1] Department of Biological Sciences, Environmental and Molecular Toxicology Program

[2] Center for Human Health and the Environment

North Carolina State University, Raleigh, NC 27695

[*] Running Title: *DNA damage and polymerase expression*

Corresponding Author:

Scott McCulloch

850 Main Campus Drive

Campus Box 7633 Raleigh, NC

scott_mcculloch@ncsu.edu

Key Words: DNA damage, DNA polymerase η, ι, κ, Rev1, Rev3, translesion synthesis, mRNA expression

Abstract

DNA damage occurs frequently in cells due to exposure to sunlight and chemicals. This damage can affect the cells in terms of cytotoxicity and mutagenesis in addition to other endpoints. In this study we sought to gain further understanding of the response to DNA damage by evaluating the effects of DNA damaging agents on TLS polymerase mRNA levels over time. Here we used two doses of Ultraviolet light B (UV-B) and a single dose of *cis*-diamminedichloroplatinum (cisplatin) and *N*-methyl-*N*'-nitro-*N*-nitrosoguanidine (MNNG) on two cell lines, a pol η proficient, and a pol η deficient cell line. We measured mRNA levels by qPCR at 1, 4, 8, 16 and 24 hours post treatment, and found an overall suppression of mRNA levels across treatments for all polymerases at one hour post treatment. We found a delayed increase in pol η expression at the lower dose of UV-B in pol η proficient cells, and in pol η deficient cells we saw a delayed rise in back up polymerases including pol ι. The high dose of UV-B was very damaging and led to prolonged TLS mRNA suppression. Our results for MNNG were similar to previously reported MNNG—with a delayed rise in pol η and ι message in pol η proficient cells, and a rise in Rev1 in pol η deficient cells. Cisplatin showed a rise in pol η message in pol η proficient cells, and in the pol η deficient cells we saw a subsequent rise in back up polymerases including pol ι.

Introduction

One out of three women, and one out of two men will develop some form of cancerous lesion throughout their lives;[15] and cancer is one of the leading causes of death in the world. There is a strong correlation between many types of cancer and exposure to various environmental contaminants and chemicals. These chemicals work by either directly or indirectly causing DNA damage. If this damage goes unrepaired it has the potential of starting a cell down the path of carcinogenesis.[15, 68] In order to combat the negative effects of DNA damage there are multiple repair mechanisms, including nucleotide excision repair (NER) and base excision repair (BER), as well as damage tolerance pathways such as translesion synthesis (TLS) and non-homologous end joining (NHEJ). Of these mechanisms, the focus of this research is the effects of TLS on DNA damage and mutagenesis.

TLS polymerases are used for bypassing lesions that block DNA synthesis by the replicative polymerases in a process called translesion synthesis (TLS). This process is used to prevent prolonged fork stalling and fork collapse, however bypass by TLS occurs with much lower fidelity than bulk DNA replication. This bypass can occur due to structural features of the TLS polymerases including their large, open active sites which allows for the accommodation of large bulky lesions but does not provide significant discrimination against incorrect base pairing. TLS polymerases also lack the 3' → 5' exonuclease activity associated with normal replicative polymerases, and their error rates are much higher than replicative polymerases.[15, 38-39]

TLS polymerases are vitally important due to their potential to affect cancer by creation of mutations, or with their involvement in chemotherapeutic resistance. Like any enzyme, in order for TLS polymerase to properly do their job, they must first be present, and research evaluating the factors that control the levels of DNA polymerases in cells is lacking. Research to date on patient tumors has shown that levels of non-replicative polymerases vary widely depending on the patient and the tumor, but there appears to be a possibility of predicting the outcome of treatment if the patients TLS polymerases are evaluated before and after treatment. For example, TLS polymerases ι and η are often over expressed in cancers, however pol κ is usually down regulated, except for in lung cancer where it appears to be upregulated.[61, 63] In theory, overexpression of any of these polymerases can lead to increased mutagenesis due to their high error rate, thus helping fuel cancer progression. Based on a structural analysis of pol η crystallized on a platinum adduct, as well as a retrospective analysis of tumors analyzed for pol η mRNA levels, it was determined that mRNA levels was correlated to response with platinum based therapy: where low levels of pol η showed a greater response to platinum based therapy, and higher levels of pol η more likely failing, or having recurrence.[62, 64-65] This leads to the potential to either check for expression before chemotherapy treatment to determine whether platinum agents should be used or avoided; as well as the potential for a therapeutic inhibitor targeting pol η to be used in conjunction with traditional chemotherapy.

Since the available data thus far is limited to polymerase mRNA levels in cancer, we decided to evaluate the baseline levels of TLS polymerases, pol η, ι, κ and Rev1 as well as the catalytic core of the B family polymerase Rev3 to see how they respond to DNA

damaging treatments. We hypothesize that pol η expression will increase after DNA damaging agents that cause CPDs, or platinum based crosslinks, and that in the absence of pol η we will see an increase in a backup polymerase expression, most likely pol ι. In order to test this hypothesis, we evaluated these polymerases in two cell lines, a normal dermal fibroblast line and one pol η deficient, XP-V line, with varying DNA damaging agents, UV-B which causes CPDs; a lesion readily bypassed by pol η; cisplatin, a chemotherapy agent with causes crosslinking which can be bypassed by pol η; and *N*-methyl-*N*'-nitro-*N*-nitrosoguanidine (MNNG) which causes O^6-methylguanine (O^6-MeG), a lesion usually repaired by mismatch repair (MMR), over a time course.

Materials and Methods

Cell lines

Two different cell types were used in this study. One is a dermal fibroblast line immortalized by hTERT, used as a control, the other is a cell deficient in functional pol η (XP-V). The XP-V cell is GM02359-hTERT, denoted XP-V, and the one normal is NHF1-hTERT, denoted NHF. Both of these cell lines are fibroblasts and have been published previously.[32, 56]

DNA Damaging Agent Treatments

UV-B treatment was performed at 10 mJ/cm^2 and 40 mJ/cm^2, using previously published protocols.[56, 95] Exposure times were 21 and 67 seconds for 10 mJ/cm^2 and 40 mJ/cm^2 respectively.[56] 1-Methyl-3-nitro-1-nitrosoguanidine (MNNG); product code M0527

was ordered from TCI America (Portland, OR). MNNG was dissolved in DMSO to 15 mM and then diluted further to 2.5 mM using diH_2O. Aliquots were frozen at -20°C and kept protected from light. Cells were rinsed once with HBSS and then incubated with MNNG at a final concentration of 10 μM in serum free media at 37°C for 1 hour while protected from light. Cisplatin was ordered from Sigma and dissolved at 6.6 mmol/L in 100 mmol/L NaCL, filtered sterilized and stored in the dark at -20°C. To use, cisplatin is thawed at 50°C for 10 minutes, and diluted into serum free media to a working concentration of 11.5 μmol/L and placed in the incubator at 37°C for 1 hr.[94] After treatment, MNNG and cisplatin waste was collected, cells were rinsed three times, then they were collected for the 1 hr time point or the media was replaced until later collection points. The 1 hr time point was collected at the end of treatment due to the varying length of treatments.

RNA collection and processing

To collect RNA, media was removed, cells were washed with HBSS and detached from the plate using trypsin/EDTA and harvested by centrifugation. Cell pellets were processed using Qiagens RNAeasy kit with Qiashredder and DNase (Qiagen, Louisville, KY). cDNA was prepared using 500 ng RNA (as determined by preliminary primer linearity studies) using iScript cDNA Synthesis Kit from BIO-RAD (Hercules, CA). RNA samples were either processed immediately or stored at -80°C. cDNA samples were either used immediately after generation for qPCR analysis were stored at -20°C until used.

qPCR Primer Verification

Prior to qPCR analysis, primers were verified using a 10% linearity test. The amount of RNA used in cDNA generation was varied ranging from 1 μg to 31.5 ng. Then 1 μL of each of these cDNA generation reactions were used for a qPCR trial. Multiple primer sets were tested on untreated NHF and XP-V cells. Primers were considered passing the linearity test if the r^2 was at least over 0.91 with most primers have an r^2 closer to 0.96 or higher. qPCR product was also analyzed on agarose gels to confirm the presence of only one product, at the correct size. Control primers were also evaluated over time courses and dose responses to ensure they would not change more than 10% over the treatment. From this analysis, it was determined that the β2-microglobulin (B2M) transcript would be used as the control for UV-B and cisplatin. β-actin was chosen as the most appropriate control for MNNG dosing.

qPCR

qPCR was performed using iTaq Universal SYBR Green Supermix from BIO-RAD (Hercules, CA) utilizing 20 μM of each primer with a final concentration of 400 nM and 1 uL cDNA as processed above. The qPCR machine utilized was an Applied Biosystems 7300 Real Time PCR System (p/n 4351101). Plates used were MicroAmp Optical 96-well reaction plate with barcode 4306737. Optical adhesive covers (4360954). Nuclease free water (NF-H_2O) (#10977-015) was used for all preparation of RNA, cDNA and qPCR. All of these materials were ordered from Life Technologies/Thermo Fisher Scientific, Grand Island, NY.

Primers were from either IDT (Coralville, Iowa) or Real Time Primers, LLC (Elkins Park, PA).

The thermocycler settings used were: stage 1: 1 repetition: 95°C for 30s, stage 2: 40 repetitions: of 95°C for 15s, 60°C for 60s followed by a dissociation curve for stage 3: 1 repetition: 95°C for 15s, 60°C for 60s, 95°C for 15s, 60°C for 15s. All qPCR reactions were run with 3 biological replicates and 3 technical replicates. Primers used for this study can be found in Table 3.1.

Statistical Analysis

Statistical analysis was performed using a fit linear model in JMP, Pro Version 11, SAS Institute Inc., Cary, NC, for least square means (LSM). The LSM were compared to Tukeys adjustment for multiple comparisons. Data comparing one treatment and one cell type at a time was also analyzed in GraphPad Prism 6.0 for Windows, GraphPad Software, La Jolla California USA, wwwlgraphpad.com; using a one way anova with Tukeys adjustment for multiple comparison when comparing time points, and an unpaired T-test with Welch's correction was used to compare untreated to each time point individually. Significance for these tests are denoted on the graph with * equal to $P \leq 0.05$, ** equal to $P \leq 0.01$, *** $P \leq 0.001$ and **** $P \leq 0.0001$.

Each cell type and treatment had three biological replicates as well as three technical replicates. Technical replicates were averaged for each run. These technical replicate averages were then used as biological replicate value. Each biological replicate was controlled for to a control gene, B2M or β-actin, as well as controlled to untreated level of

the gene of interest. These controls are used to ensure that changes in the CT values are not due to variations in starting RNA levels or differences within background levels of the genes. For the one way anova and T-tests, the values utilized was the $Log_{10}(2^{-\Delta\Delta Ct})$, and the values reported are the average of the biological replicates. For the Fit linear model, the values utilized was the LSM output from JMP from the starting values of $Log_{10}(2^{-\Delta\Delta Ct})$. Due to the internal controls of the linear model, the numbers reported under the linear model are different than that of the one way anova and T-test.

Results

General Information

In the published literature, the vast majority of polymerase expression data available is from clinical tumor samples, with the exception of one group who utilized MNNG in the evaluation of mRNA expression levels of pol η and pol ι. There is available literature on the mutagenesis caused by cisplatin and UV light, as well as the bypass of the lesions caused by these treatments. For this reason we chose UV-B and cisplatin as DNA damaging treatments for this study, we also included MNNG due to these recent reports on expression mentioned above. This study evaluated the independent variables of treatment, time, and cell type, with a dependent variable of mRNA expression level. We did both a global analysis of all of the data combined as well as individual tests. For the individual tests we looked at independent variables of a single cell type and treatment, and the dependent variable of mRNA expression. Comparison of time points to untreated was performed by an Unpaired T-test with Welch's correction, comparison of time points to each other was performed by a one-

way anova with a Tukey multiple comparison test. The global analysis was utilized to compare all variables simultaneously. This was a multi-variant analysis taking into account the four levels: gene, treatment, cell type, and time. This analysis was performed by a fit linear model in JMP, evaluating for least squares means (LSM) with a Tukeys adjustment for multiple comparison.

Values presented here are $\log_{10}$ transformed and therefore a negative number shows a decrease in the genes' expression, and a positive number is an increase compared to the untreated control. Each gene is normalized to its untreated value which is set to zero. Uncontrolled, baseline CT values of the TLS polymerases range from 21 to 27.

One-Way Anova and T-test Analysis

To investigate the effects of UV-B on mRNA expression, we tested two different doses: 10 mJ/cm^2 and 40 mJ/cm^2 in both NHF and XP-V cells. NHF cells treated with 10 mJ/cm^2 showed an initial decrease in all polymerases mRNA levels (-0.319, -0.337, -0.0621, -0.097, -0.170; pol η, pol ι, pol κ, Rev1, Rev3 at 1 hr post treatment respectfully) followed by a delayed increase in pol η (0.307 at 8 hrs) and ι (0.270 at 24 hr) as seen in Figure 3.1. The increase in pol η at 8 hrs post treatment is significant from the initial1 hr decrease (0.307 compared to -0.319) with an approximate 4 fold increase. Additionally, the rise of pol ι at 24 hrs is statistically significant from the decrease at 1 and 4 hrs (0.270 at 24 hr compared to -0.337 at 1 hr, and -0.422 at 4 hr) which is a 4 fold and 5 fold change respectfully. The striking decrease of mRNA expression of pol κ is also noteworthy and significant and every time-point (-0.062, -0.795, -0.584, -0.238, -0.004; 1, 4, 8, 16, 24 hr respectfully). XP-V cells

treated with 10 mJ/cm^2 UV-B exhibited an initial decrease in mRNA levels of pol η, ι, and κ, (-0.801, -0.627, -0.245 respectfully) followed by a delayed increase in pol η (0.035 by 4 hr) and ι (0.044 by 4 hr) mRNA levels with a continued suppression of pol κ message as seen in Figure 3.1. Rev1 and Rev3 levels also appeared to increase slightly in a time dependent manner, however the changes within this cell and treatment are were not considered statistically significant based on the tests we ran. When comparing the response of 10 mJ/cm^2 UV-B to that of the 40 mJ/cm^2 treatment, all polymerases and all time-points except Rev1 in NHF cells and Rev3 in XP-V cell showed suppression of the DNA polymerase mRNA levels. Graphical images of the UV-B analysis can be seen in Figure 3.1.

Next we evaluated the mRNA levels of the TLS polymerases in response to cisplatin. NHF cells had a significant increase of pol η message by 8 hours (0.478 at 8 hrs which is a 2.5 fold change from the 1 hr value 0.081), which remained elevated at 16 hrs (0.287, a 1.6 fold change from 1 hr). There was a rapid increase in pol ι message which is followed by a subsequent decrease in expression which is significant to the elevated levels (0.350 at 1 hr, -0.330 at 8 hr with a continued decrease through 16 hr, -0.5798). XP-V had an initial suppression of the polymerases (-0.204, -0.356, -0.060, -0.125, -0.186 for pol η, pol ι, pol κ, Rev1, Rev3 at 1 hr post treatment respectfully), with a small delayed increase in pol η (0.080 at 16 hr, 0.192 at 24 hr), and a delayed significant increase in the presence of pol ι (0.327 at 16 hr, 0.589 at 24 hr) and Rev3 (0.095 at 16 hr). See Figure 3.2 for graphical images of these results.

Lastly, we evaluated the effects of MNNG on our cell lines. In NHF cells most of the polymerases mRNA levels are increased after an initial suppression, with pol η and ι message being significantly increased at 24 hrs post treatment. The initial 1 hr values are -0.550, -0.290, -0.023, -0.210, for pol η, pol ι, pol κ and Rev1 respectfully, and pol η at 24 hrs is 0.334, while pol ι at 24 hrs is 0.288, which is a 7.7 fold increase in pol η and a 3.8 fold change in pol ι message. XP-V cells have a slight non-significant increase in pol η message (0.114 at 4 hr), a decrease in pol ι (-0.063 at 1 hr and -0.693 at 8 hr) and κ (-0.054 at 1 hr and -0.345 at 8 hr) message as well as a slight significant increase in Rev1 at 4 hr (0.167). A graphical depiction of these results can be seen in Figure 3.2.

Model Statistical Evaluation

We also performed a multicomparitive statistical analysis, allowing us to compare changes that occurred between genes, treatments, time points and cell lines. This is a more complex analysis than the one way anova reported in the above section. The main reason for doing this was to see if any patterns of change were occurring across treatments, time points, and cell types. Values in this section are reported as LSMs, calculated from the initial $Log_{10}(2^{-\Delta\Delta Ct})$ in JMP. No stars were added to these graphs as all significance in this section is based on $p < 0.05$.

We found in UV-B treated XP-V cells, that each gene tested (pol η, pol ι, pol κ, Rev1, Rev3) was significantly different between the two doses at 1 hr post treatment. For example, pol η message levels at 10 mJ/cm^2, was significantly different than the level of pol η message at 40 mJ/cm^2. Additionally, when looking at just the 10 mJ/cm^2 treatment at 1 hr post

treatment in XP-V cells, pol η message levels (-0.119) were significantly different from pol ι message levels (-0.334), and pol ι message levels was additionally significant from Rev1 message levels (-0.135). While this appears to only be a relatively small change in absolute mRNA level: a 2.8 fold change between pol η and pol ι and a 2.9 fold change between pol ι and Rev1, it is still significant due to the multiple levels of comparison within the analysis. This pattern of significance was the same within the 40 mJ/cm^2 treatment, with values of -0.316, -0.531 and -0.332 for pol η, pol ι and Rev1 respectfully at 1 hr (a 1.6 fold change for both). These can be seen graphically on Figure 3.3.

The analysis of NHF cells shows they also responded similarly to the XP-V cells, indicating that there was not a cell type difference, at least with these two samples. Therefore each gene tested (pol η, pol ι, pol κ, Rev1, Rev3) was significantly different between 10 mJ/cm^2 and 40 mJ/cm^2, and when looking at just 10 mJ/cm^2 at 1 hr post treatment; we found that pol η (-0.048) was significantly different from pol ι (-0.263), and pol ι was also significantly different from Rev1 (-0.064), which is a 2 fold difference between pol η and pol ι, and a 2 fold difference between pol ι and Rev1, this can be visualized in Figure 3.3.

When comparing across treatments (UV-B compared to cisplatin, UV-B compared to MNNG, MNNG compared to cisplatin), the 40 mJ/cm^2 treatment as a whole was statistically significant from both MNNG and cisplatin treatments. This means that the pattern of change in the expression levels when cells are treated with 40 mJ/cm^2 UV-B responded very differently than when the cells were treated with the other treatments. This can be seen by the

fact that the 1 hour post 40 mJ/cm^2 is significantly different from cisplatin and MNNG at 1 hr post treatment in all five genes in both XP-V and NHF cells, as seen in Figure 3.3.

Cisplatin and MNNG were not significantly different from each other on a global scale, although there are a few significant points between the two treatments. In XP-V cells cisplatin causes significant changes at the 1 hr time point between pol η (-0.068) and ι (-0.283) a 2.2 fold change, as well as between pol ι and Rev1 (-0.083) a 1.6 fold change. XP-V cells at 1 hr post MNNG treatment had a significant difference in message levels between pol η (0.003) and ι (-0.212), a 1.6 fold change, as well as between pol ι and Rev1 (-0.013), a 1.7 fold change. NHF cells have this same pattern; where cisplatin pol η message at 1 hr was 0.004, pol ι was -0.212 and Rev1 was -0.012 (1.6 fold change between pol η and pol ι; 1.7 fold change between pol ι and Rev1) and NHF MNNG post 1 hr was 0.075, -0.141 and 0.059 for pol η, pol ι and Rev1 respectfully (1.2 fold change between pol η and pol ι; 1.2 fold change between pol ι and Rev1). These graphs can be seen in Figure 3.4.

The 1 hour time point, where the initial polymerase suppression occurs is the only point that is globally significant across treatments and cell lines. This means that across all cell types and all treatments, the polymerases responded in a similar fashion, and if another DNA damaging agent was used the prediction would be that the TLS polymerases would also decrease for that treatment at 1 hr post treatment. A few other significant points are worth noting. One significant point (not shown since it was a lone point) is NHF cells 40 mJ/cm^2 at 8 hrs (-0.958) post treatment, in which pol η message is significantly different from NHF 8 hrs post cisplatin (0.319), a 4.4 fold change which is a very large change given the many

variables within this model. There are two points that have significance between the two cell lines and that is XP-V at 1 hr post 40 mJ/cm^2 (Rev1: -0.332, Rev3: -0.382) compared to NHF MNNG 1 hr post treatment (Rev1: 0.058, Rev3: 0.009), this is a 1.9 fold change between Rev1, and a 2.4 fold change between Rev3. There are multiple other combinations of significance that can be explored in further reports between other genes such as pol η and pol ι across time points or treatments which are not reported here as they are not relevant to our report.

Discussion

Humans are exposed to UV radiation and chemical exposures throughout their lifetime either in the atmosphere, food or water. This exposure can in turn lead to DNA damage and cancer. The cancer can then be treated with chemotherapeutic agents, many of which work by causing DNA damage within the cancer cells, however, these treatments are also able to damage normal cells; leading to the possibility of secondary cancers down the line. Here we studied three DNA damaging agents: UV-B, cisplatin and MNNG. Within this study we evaluated the cellular response with respect to the lesion bypass DNA polymerase mRNA levels and how they changed over time, in multiple cell lines, in response to these varying treatments. We began by investigating UV-B, as we have previously published on the cytotoxicity and mutagenesis of UV-B¸ and we chose to use the same cell lines to allow for a direct comparison. We therefore compared XP-V cells and NHF cells at two UV-B doses, 10 mJ/cm^2 and 40 mJ/cm^2. What we found was a difference in the response at 10 mJ/cm^2, where XP-V TLS polymerases were initially decreased, with a delayed rise in pol ι,

Rev1 and Rev3, however their levels were not significantly different from untreated as determined by T-test. NHF on the other hand showed a significant decrease in DNA pol κ message, and an initial decrease in all of the polymerases followed by a delayed raise of pol η at 8 hrs and a further delayed rise of pol ι message at 24 hrs. These results lead us to the conclusion that the initial decrease in TLS polymerase message levels is likely due to the damage triggering the DNA damage checkpoint. The cell would use the checkpoint to assess the damage and suppress the TLS polymerases, before deciding which polymerase was needed and subsequently recruiting that particular polymerase. The prolonged decrease of pol κ message is explained as the literature demonstrates that pol κ is unlikely involved in the bypass of TT dimers by TLS. The delayed increase in pol η is fascinating, as currently there are no published reports on how these polymerases respond and in what time frame. This is a novel finding that can hopefully lead to the path of further exploration into how the UV-B damage response works.

Our previous work using the HPRT mutation assay showed the mutation frequency and main base substitution changes are: $8.56x10^{-5}$ with mainly T →C and C→ T changes for NHF and $25.8x10^{-5}$ with T→A and C→A changes for XP-V cells.[56] This suppression in mutations in NHF compared to XP-V correlates nicely with the raise in the presence of pol η mRNA as pol η's ability to often bypass TT dimers by inserting the correct AA helps lower the mutation rate, and the T→C and C→T changes are characteristic of pol η when it does make a mistake across from the TT dimer. XP-V cells changes are due to the absence of pol η protein, but the T→A and C→A changes can be attributed to the small rise in pol ι and Rev3 that occurs. Protein levels were not evaluated in this study, as we found the polymerase

antibodies unreliable when using multiple controls, likely due to the homology of the TLS polymerases. We would like in future studies to either use SILAC protein quantification or pull downs aided by mass spectrometry to analyze for protein levels with certainty as to which polymerase is being seen. The great decrease in all of the polymerases across both cell types in the 40 mJ/cm^2 treatment is likely showing a link between the delayed cell cycle checkpoint and the TLS polymerases. This would be a great area to explore further in the future.

Next we evaluated the TLS polymerase response to cisplatin, a chemotherapeutic agent known to make crosslinks. Pol η is known to be able to bypass platinum crosslinks leading to the potential for chemotherapy resistance and cancer resistance.[62, 64] Our mRNA levels for cisplatin treatment are exactly what we predicted: with XP-V having an initial decrease in TLS polymerases message levels, followed by a small delayed increase in pol η, and likely when the cell registered that it was not getting more pol η protein, there was a significant, but delayed increase in the presence of pol ι and Rev3. This is in distinct comparison to the NHF cells which had a significant increase of pol η, and after an initial pol ι increase, there was a subsequent decline in pol ι message levels. We can then compare these results to Bassett et al., in which we used the lower of the two IC_{50} cisplatin levels; 11.5μmol/L cisplatin. For mutagenesis, Bassett et al, evaluated a range of cisplatin doses instead of a single dose per cell. Therefore, they showed that NHF cells at a MF of $8.1x10^{-5}$ at 20μM cisplatin, and XP-V cells MF was $10.9x10^{-5}$.[94] Although there is not a large difference in the MF between the cell lines, the slight difference is possibly attributed to the presence of pol η, whereas the background levels are likely caused by the high cytotoxicity

of the crosslinks and the fact that they block replication. However, the presence of the increase pol η mRNA in our study in NHF cells as well as the delayed increase in pol ι and Rev3 in the XP-V cells can contribute to the differences seen in Bassett et al study.[94] Bassett et al did not do sequencing data on the cisplatin mutations using the HPRT assay, it would be interesting to evaluate the sequence analysis to determine whether the sequences will follow the same pattern as the mRNA expression levels, which would be expected.

We also evaluated for our cellular response to MNNG based on two reports from Shaos group: one by Qi et al, and one by Zhu et al, in that they used 10 μM MNNG but they treated for 2 hours compared to our 1 hour treatment and they used FL cells. Qi et al found a significant increase in pol η mRNA at 6 hours (approximately a 0.6 on a $\log_{10}$ scale) post treatment and even greater at 12 hr (approximately a 1 on a $\log_{10}$ scale).[131] And Zhu et al found a significant increase at 12 hrs for pol ι (0.8 on a $\log_2$ scale), and a slightly less increase but still significant at 24 hr (approximately a .58 on a $\log_2$ scale).[132] When comparing this to our data, our NHF follow the same pattern that both Qi et al, and Zhu et al found, however our results are slightly less striking (NHF cells, pol η 24 hrs: 0.334 and pol ι at 24 hr was 0.288 on a $\log_{10}$ scale), probably due to the fact that our treatment was for a shorter duration of time. When we compare this to XP-V the pattern is not the same, in which we saw a decrease in pol ι and pol κ with a slight increase in Rev1 by 4 hr, which is likely due to the absence of the pol η protein. Although pol η may help bypass the O^6-MeG, it is normally repaired by mismatch repair (MMR). Mutation frequency has not been collected thus far for MNNG treatment, however this would be an interesting evaluation.

Next we evaluated for global significance by running a multivariant linear model in JMP. This statistical test allowed us to test for treatment, cell, time and gene effects. Overall, 40 mJ/cm^2 was significant compared to all other treatments. There were no significant cell based changes. The 1 hour time point was the most significant time point across all cells and treatments, and pol ι exhibited the most significant changes across treatments and cells. The reasoning behind the striking difference in the 40 mJ/cm^2 is likely due to its high dosage compared to the other treatments. The initial 1 hr suppression of TLS polymerase expression is fascinating and is likely due to cell cycle control by cell cycle checkpoints. This is novel information that links regulation of the polymerases to checkpoints, and will need to be further investigated to discover what causes of the rapid decrease in mRNA expression. It was a little surprising to not see a global difference between the cell types, however the linear model takes into account the variability that comes into account with a variable cell system, as well as so many time points and treatments, as well as it appears that the general response of down regulation followed by an increase in particular polymerases is a consistent pattern.

General

Overall, this investigation brings to light a lot of valuable information for the TLS field. We found that XP-V cells treated with 10 mJ/cm^2 initially had an overall suppression of their TLS polymerases followed by a delayed rise in pol ι, Rev1 and Rev3; whereas NHF also initially suppressed all their TLS polymerases but that was followed by a delayed raise of pol η at 8 hrs and an even further delay of pol ι at 24 hrs. When we evaluated these cells at 40 mJ/cm^2 we say an overall sustained suppression of the polymerases. Cisplatin initially

suppressed the polymerases in XP-V cells, then caused a small delayed increase in pol η, followed by a significant increase in pol ι and Rev3. This is compared to NHF cells which had a significant increase of pol η, followed by a significant decrease in pol ι mRNA. MNNG caused a delayed increase pol ι and η in NHF cells, whereas there was an increase in Rev1 in XP-V cells. Therefore there are many individual significant changes which are fascinating by themselves, but when evaluating everything together, learning that the one hour post treatment time point is so significantly different than the others is a fascinating jumping point for further research on the control and regulation of polymerases.

Figure 3.1 – Individual Gene Changes by Cell and Treatment. These genes cannot be cross compared. 0.0 is the line indicating where the untreated level of the gene is. Anything above 0.0 is an increase in expression, anything below 0.0 is a decrease in expression. Bar lines with * indicate differences between time points within a specific gene. * on their own on a bar indicate significant difference from that gene untreated. P values are represented by *, one star is significant at a p value < 0.05, ** < .001, *** < .0001, **** < .0001. Comparison of time points to untreated was performed by an Unpaired T-test with Welch's correction, comparison of time points to each other was performed by a one-way anova with a Tukey multiple comparison test, both were performed using GraphPad Prism version 6.00 for Windows, GraphPad Software, La Jolla California, USA, www.graphpad.com. (A) 10 mJ/cm^2 treatment on XP-V cells. (B) 10 mJ/cm^2 treatment on NHF cells. (C-D) Same order of cells as A-B but the dosage has been raised to 40 mJ/cm^2.

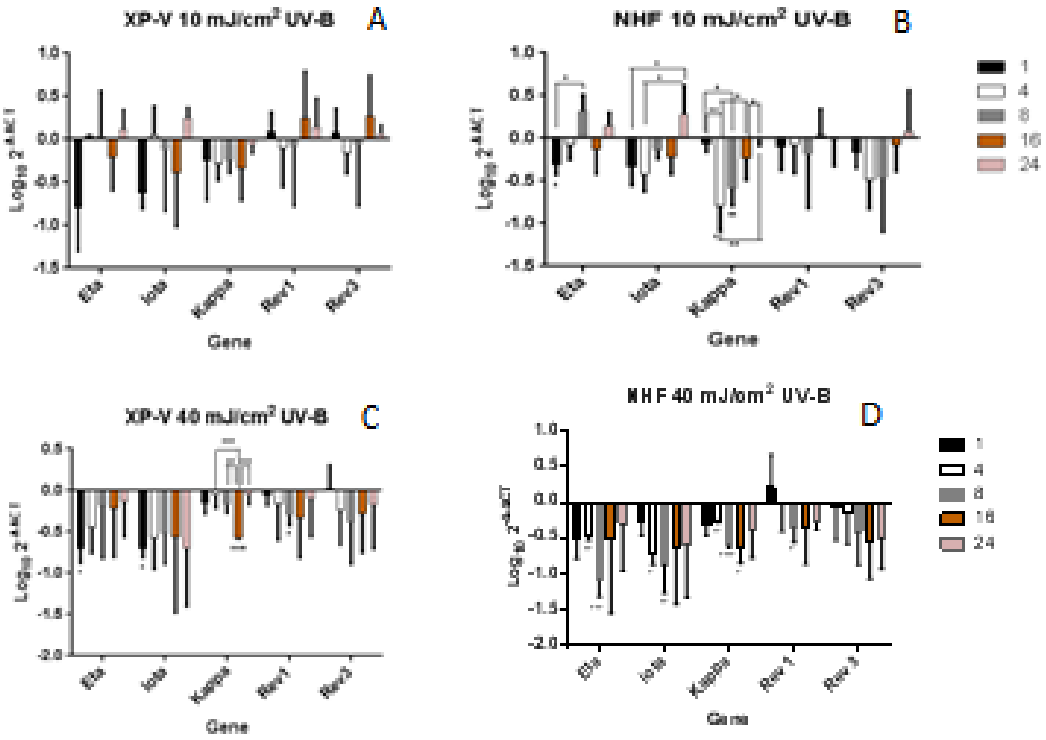
XP-V 10 mJ/cm² UV-B
A
NHF 10 mJ/cm² UV-B
B
XP-V 40 mJ/cm² UV-B
C
NHF 40 mJ/cm² UV-B
D
1
4
8
16
24
Eta
Iota
Kappa
Rev1
Rev3
Gene

Figure 3.2 – Additional Individual Gene Changes by Cell and Treatment. These genes cannot be cross compared. 0.0 is the line indicating where the untreated level of the gene is. Anything above 0.0 is an increase in expression, anything below 0.0 is a decrease in expression. Bar lines with * indicate differences between time points within a specific gene. * on their own on a bar indicate significant difference from that gene untreated. P values are represented by *, one star is significant at a p value < 0.05, ** < .001, *** < .0001, **** < .0001. Comparison of time points to untreated was performed by an Unpaired T-test with Welch's correction, comparison of time points to each other was performed by a one-way anova with a Tukey multiple comparison test, both were performed using GraphPad Prism version 6.00 for Windows, GraphPad Software, La Jolla California, USA, www.graphpad.com. (A) Cisplatin treatment on XP-V cells. (B) Cisplatin treatment on NHF cells. (C-D) Same order of cells as A-B but the cells are treated with MNNG.

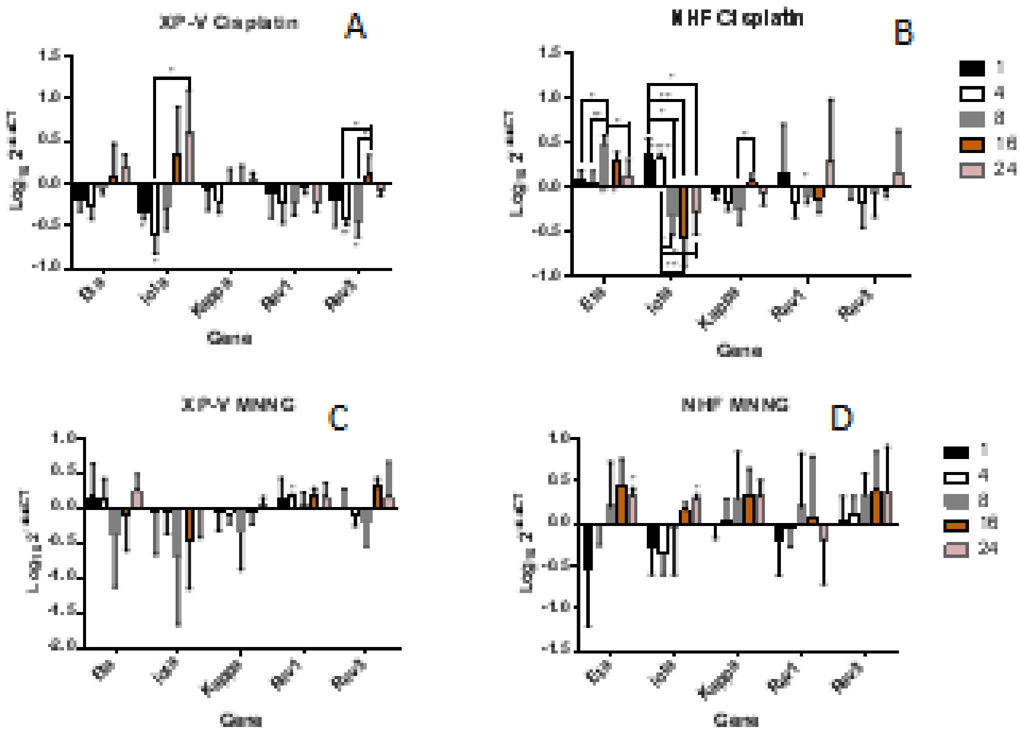
XP-V Cisplatin
A
NHF Cisplatin
B
XP-V MNNG
C
NHF MNNG
D
Eta
Iota
Kappa
Rev1
Rev3
Gene
1
4
8
16
24

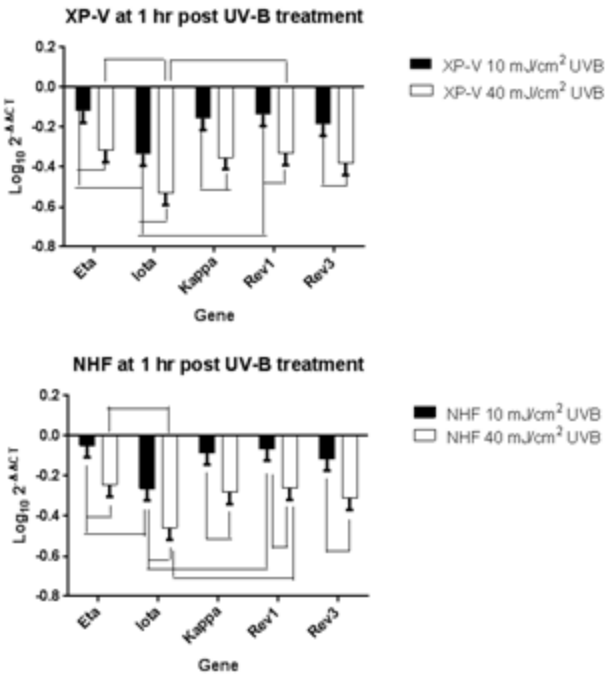

Figure 3.3 – Linear Model Analysis of UV-B treatments. Statistical analysis was performed using a fit linear model in JMP, Pro Version 11, SAS Institute Inc., Cary, NC, for least square means (LSM). The LSM were compared to Tukeys adjustment for multiple comparisons. On these graphs changes deemed significant to $p < 0.05$ were reported between genes within a specific treatment e.g. changes in eta compared to iota and kappa, however when comparing treatments, eg. between doses of UV-B, only a single gene is evaluated e.g. iota to iota, for simplicity sake in order to be able to understand the graph, and this is what we deemed most relevant to this study. (A) XP-V cells comparing UV-B doses across genes. (B) NHF cells comparing UV-B doses across genes.

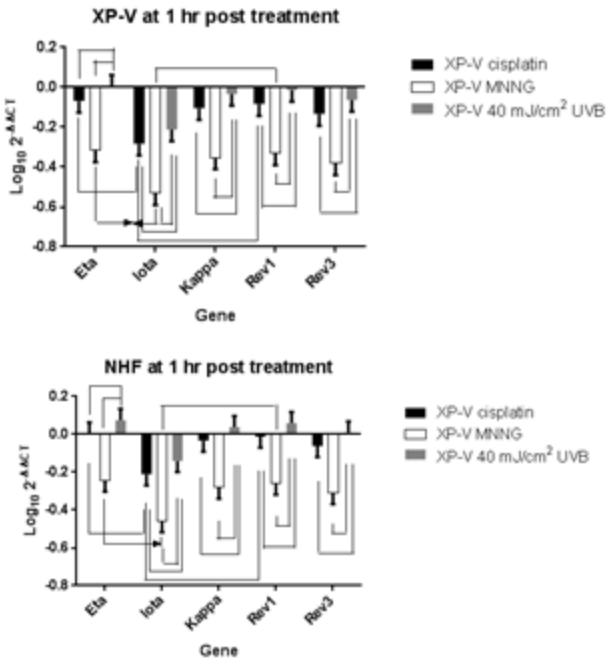

Figure 3.4 – Linear Model Cross-Treatment Analysis. Statistical analysis was performed using a fit linear model in JMP, Pro Version 11, SAS Institute Inc., Cary, NC, for least square means (LSM). The LSM were compared to Tukeys adjustment for multiple comparisons. On these graphs changes deemed significant to $p < 0.05$ were reported between genes within a specific treatment e.g. changes in eta compared to iota and kappa, however when comparing treatments, eg. between UV-B and MNNG, only a single gene is evaluated e.g. iota to iota, for simplicity sake in order to be able to understand the graph, and this is what we deemed most relevant to this study. (A) XP-V cells comparing UV-B, MNNG and cisplatin across genes. (B) NHF cells comparing UV-B, MNNG and cisplatin doses across genes.

Table 3.1 Primers for qPCR

Primer	Forward primer 5'→ 3'	Reverse primer 5'→ 3'	Source
B2M	TGCTGTCTCCATGTTTGATTGTATCT	TCTCTGCTCCCCACCTCTAAGT	RealTimePrimers.com Human Housekeeping Gene Primer Set
B-actin	AGCGAGCATCCCCCAAAGTT	GGGCACGAAGGCTCATCATT	Zhu et al[132]
Pol η	ACCCAGGCAACTACCCAAACC	GGGCTCAGTTCCTGTACTTTG	Choi et al[133]
Pol ι	AAAAATAAGATTGAAGAACTACTTGC	GAATATCTACTGGAAGCTGCTTGA	Generated in our lab
Pol κ	CCCAATGAAGAGGACAGGAA	TTGTTTATTCACGGCTTCACA	Generated in our lab
Rev1	GATGGAGGAAGCGAGCTGAAA	CCTTCTGCATAGCAGCATCTG	http://pga.mgh.harvard.edu/primerbank/
Rev3	CTCAGTCTGGTGCTGAGGTT	AATTCCAGTGGGTAGGGAAG	Realtimeprimers.com

GENERAL DISCUSSION

The replication of DNA within cells is a vital component to cell survival. This process must be completed in a fast and accurate manner in order to prevent errors from occurring. Additionally DNA can be damaged during replication, and this damage needs to be efficiently repaired to prevent downstream effects such as cell death, cancer or aging. DNA damage occurs from multiple sources, including intrinsically; such as replication errors and base deamination, or extrinsically; such as exposure to UV light, and chemicals in our food, water and atmosphere.[15-16, 18] There are multiple mechanisms to try and repair or tolerate DNA damage. One of these DNA damage tolerance pathways is TLS. TLS allows cells to bypass replication fork blockages by using specialized polymerases with wide open active sites to accommodate bulky lesions. These polymerases are able to insert a base across from the lesion, and extend past the lesion before allowing normal replication to continue. The TLS polymerases include Y-family polymerases pol η, ι, κ and Rev1 as well as B-family polymerase pol ζ. While these polymerases can insert the correct base across from a lesion, they can also insert the wrong base, which can fuel mutagenesis; however in the absence of specific TLS polymerases it can be even worse. Knocking out pol ζ is embryonically lethal in mice, and the absence of functional pol η leads to a disease phenotype of increased sun sensitivity and skin cancer known as XP-V.

Based on this information, we decided to evaluate the effects of the presence and absence of pol η on UV-B induced mutagenesis. We hypothesized that UV-B will cause DNA damage mainly in the form of CPDs and the presence of pol η will suppress

mutagenesis across from these lesions. We developed this hypothesis based on the previously published literature which showed UV-C created CPDs and that the lack of pol η caused increased mutagenesis across from UV-C based CPDs. Here we extended that work and looked at cell viability, mutation frequencies and mutation spectra at an environmentally relevant level of UV-B. What we found was that mutagenesis occurred in both normal cells and XP-V cells. This is important to note, as that means a few minutes out in the sun generates enough UV-B damage to generate mutations even in those who are "healthy", and this mutagenesis was even greater in XP-V cells, showing that the presence of pol η helps to suppress UV-B induced mutagenesis. Our study also showed that UV-B, while mutagenic, is less mutagenic than UV-C, which was expected due to the difference in wavelengths of UV-B and UV-C. UV-C is more potent and its wavelength is right at the peak absorption of DNA.[56, 92, 98] We also evaluated the mutation spectra in both normal and XP-V cells and found very different spectra between the two. In normal cells, in the presence of pol η, 50% of the mutations were deletions, 17% were insertions where only 33% were base substitutions. In XP-V cells, 74% of the changes were base substitutions and 26% were deletions. This shows that pol η helps prevent base substitution mutations. The actual base substitution changes were also different between the two cell lines. In normal cells, 50% of the photoproduct errors were T to A mutations, 17% were C to A and 33% were C to T mutations. In XP-V cells 45% were C to A, 27% were T to C, 9% were C to T, and 18% were T to A. The most likely reason for the difference is the presence of functional pol η in the normal cells which can more easily bypass CPD dimers than the other TLS polymerases that work as a backup when pol η is not around, likely pol ι is attempting to bypass CPDs in

pol ηs absence. The normal cells do have mutations at CPDs as well, and this is likely due to the fact that TLS by pol η is not error free.[46, 56] Therefore our hypothesis was proven correct by this study, in that most of the mutations found were across from CPD sites, and the mutation frequency was less in the normal cells than in the XP-V cells.

Next we decided to look at pol ηs role in oxidative stress induced mutagenesis. We believed that oxidative stress, particularly the oxidative lesions, 8-oxoG would cause mutagenesis, and that the presence of pol η would reduce this mutagenesis. We generated this hypothesis based on the biochemical data showing that pol η can bypass 8-oxoG in lesion bypass and plasmid based studies.[42, 91, 109-110, 113, 127] In this study we wanted evaluate mutagenesis within a cell based system, and therefore we used chemicals known to cause oxidative stress, including a general oxidative stress agent menadione MD, and an agent known to cause preferentially 8-oxoG, methylene blue plus light (MBL). In this study we evaluated by flow cytometry to make sure that oxidative stress was occurring, by measuring free radicals within the cell. Despite using levels and agents known to cause oxidative stress, we found very low levels, close to the detection limit of the assay of free radicals, except with MBL which was slightly increased of the baseline untreated. We also looked at downstream effects of oxidative stress by looking at protein oxidation in the form of carbonylated protein. What we found was slight increase in protein oxidation for most treatments, with the greatest effect being from the MBL treatment. Next we wanted to determine whether we were creating the 8-oxoG lesion that we desired; we first tested this by an alkaline gel which confirmed that MBL was generating 8-oxoG lesions. We went further to quantify the amount of 8-oxoG produced by using 2D mass spectrometry, and found

approximately a 10-11 fold increase in 8-oxoG lesions after MBL treatment compared to untreated controls, however, it appears that most of our 8-oxoG is located in the mitochondrial DNA and not in the nuclear DNA. Lastly we looked at mutagenesis as an endpoint using the HPRT assay that we previously used in our UV-B study, and found surprisingly low levels of mutations. We went one step further and looked in a yeast cell model which is more easily adapt to knockouts than cells, and did a multiple knockout of pol η and a 8-oxoG repair enzyme known as OGG1, and what we found was a slight increase in mutagenesis in the absence of OGG1, and an even greater increase in the double knockout of OGG1 and pol η. What this summarizes to is a single low dose oxidative stress agent is not sufficient to cause high levels of mutations, and that perhaps multiple exposures to varying agents, more like real world exposures are needed. Additionally, perhaps a pol η deficiency on its own is insufficient for oxidative stress mutagenesis due to the redundancies in the cell to repair the abundance of oxidative stress that cells are exposed to, and that multiple mechanisms would need to fail in order to see mutagenesis, as suggested by our double knockout of OGG1 and pol η. As such we learned that our hypothesis that pol η is used to suppress oxidative stress mutagenesis is not quite accurate and that multiple mechanisms in addition to pol η are likely responsible to suppress this mutagenesis.[32]

Lastly, we decided to explore a wide open field of mRNA expression in TLS polymerases and we hypothesized that pol η expression will increase after DNA damaging agents that cause CPDs, or platinum based cross-links, and that in the absence of pol η we will see an increase in a backup polymerase expression, most likely by pol ι. In order to test this hypothesis we evaluated NHF, our normal cells, to XP-V, our pol η deficient cells, on a

time course after treatment with either UV-B, cisplatin or MNNG. We then collected RNA and generated cDNA to run qPCR analysis with. We ran multiple statistical analyses to evaluate the significance of our findings. What we found was after 10 mJ/cm^2 UV-B treatment, that NHF cells had an initial suppression of all 5 TLS polymerases tested, with a significant suppression of pol κ mRNA, followed by a delayed rise at 8 hrs post treatment in pol η message and a further delayed increase in pol ι that occurred at 24 hr post treatment. XP-V cells were different, with an initial decrease in the polymerases followed by a delayed rise in pol ι, Rev1 and Rev3, however these rises were not significant. These results are very interesting as it suggests that a checkpoint response could be causing the one hour decrease in polymerases after treatment. The prolonged suppression of pol κ message is likely due to the fact that pol κ is not known to be involved in TT dimer bypass by TLS. We also used a 40 mJ/cm^2 UV-B treatment and found that this was likely a very damaging treatment based on the face that it caused prolonged decreases in all polymerases mRNA levels in both cell lines. Cisplatin results were as expected, since we know pol η can bypass platinum lesions *in vitro*. XP-V cells had an initial suppression in polymerase message followed by a small increase in pol η message, and a delayed increase in the presence of pol ι and Rev3 message, likely once the cells feedback mechanisms realized that no pol η protein was being generated. This is very different than NHF which had a significant increase in pol η message, and although there was a short-term increase in pol ι message, it was then decreased.[94] We also used MNNG due to some previously published data on pol η and ι message in response to MNNG. What we found, was that our NHF, normal cells, followed the pattern of the other cell line previously published in that, there was an increase in pol η followed by a later increase in pol

ι message.[131-132] When we ran a multivariant linear model, we found that the 40 mJ/cm^2 UV-B treatment was significantly different than all the other treatments that we ran, but that there we no cell based difference. We also found that the 1 hour time point was significant in all cells and treatments. These results are likely due to the high dose that 40 mJ/cm^2 is, compared to the other more mild treatments. And the 1 hr suppression of TLS polymerase expression is fascinating and will need to be investigated further in terms of the roles and controls of the cell cycle on the polymerase regulation. Overall, we proved our hypothesis as well as found a lot of other very interesting information that will be great to follow-up with in future studies.

What these studies have taught us so far is that pol η is intricately involved in the response to UV-B and UV-C, especially in the terms of suppressing mutagenesis from UV-B and UV-C. As well as that pol η on its own is insufficient to affect the mutagenic response to oxidative stress, however it is likely a small part of a larger intricate repair process to prevent oxidative stress mutagenesis including OGG1, and MutY. Because there is so much damaging insult to DNA cells have multiple mechanisms of repair and tolerance with TLS being one part of that. We also have shown that there is likely a very tightly controlled regulatory mechanism for TLS polymerases as seen by the decrease in mRNA expression levels of TLS polymerases following DNA damaging treatments followed by up regulation of mRNA of certain polymerases which could be involved in their bypass.

This research has answered many interesting questions and leads to many more. This research could be extended by looking into UV-A and simulated sunlight, evaluating for

mutagenesis and mutation spectra which would give clues as to what lesions are created by UV-A as well as the distribution of lesions and therefore mutations under simulated sunlight conditions which would be fascinating to determine the actual exposures to humans from sunlight. We could also extend the oxidative stress work into a double knockout cell system looking at effects of oxidative stress on cells in the absence of pol η and OGG1. And the polymerase expression work could be extended by looking at protein levels by SILAC protein quantification or by the using a pull down assay followed by mass spectrometry to ensure that we can definitively say which polymerase is found, as well as looking at what is regulating the mRNA levels, whether mRNA and protein are being stabilized, or upregulated, as well as investigate what parts of the cell cycle response are responsible for this regulation.

REFERENCES

1. Weaver, R. F., A Brief History. In *Molecular Biology*, McGraw-Hill Companies: New York City, 2008; pp 1-11.

2. Watson, J. D.; Crick, F. H., Genetical implications of the structure of deoxyribonucleic acid. *Nature* **1953,** *171* (4361), 964-7.

3. Watson, J. D.; Crick, F. H., The structure of DNA. *Cold Spring Harb Symp Quant Biol* **1953,** *18*, 123-31.

4. Campbell Neil A, R. J. B., *Biology*. Benjamin Cummings: 2002.

5. GM., C., *The Cell: A Molecular Approach*. Sinauer Associates: Sunderland, MA, 2000.

6. Lodish H, B. A., Zipursky SL, Matsudaira P, Baltimore D, Darnell J., *Molecular Cell Biology*. 4th ed.; W.H. Freeman: New York, 2000.

7. Dutta, A.; Bell, S. P., Initiation of DNA replication in eukaryotic cells. *Annu Rev Cell Dev Biol* **1997,** *13*, 293-332.

8. McCulloch, S. D.; Kunkel, T. A., The fidelity of DNA synthesis by eukaryotic replicative and translesion synthesis polymerases. *Cell Res* **2008,** *18* (1), 148-61.

9. Onesti, S.; MacNeill, S. A., Structure and evolutionary origins of the CMG complex. *Chromosoma* **2013,** *122* (1-2), 47-53.

10. MacNeill, S., The Eukaryotic Replisome: a Guide to Protein Structure and Function: A Guide to Protein Structure and Function. Springer Science & Business Media: 2012.

11. Makarova, K. S.; Koonin, E. V.; Kelman, Z., The CMG (CDC45/RecJ, MCM, GINS) complex is a conserved component of the DNA replication system in all archaea and eukaryotes. *Biol Direct* **2012,** *7*, 7.

12. Bambara, R. A.; Murante, R. S.; Henricksen, L. A., Enzymes and reactions at the eukaryotic DNA replication fork. *J Biol Chem* **1997,** *272* (8), 4647-50.

13. Horton H. Robert, M. L. A., Scrimgeour K. Gray, Perry Marc D., Rawn J. David, *Principles of Biochemistry*. Fourth ed.; Pearson Prentice Hall: Upper Saddle River, NJ, 2006.

14. Miyabe, I.; Kunkel, T. A.; Carr, A. M., The major roles of DNA polymerases epsilon and delta at the eukaryotic replication fork are evolutionarily conserved. *PLoS Genet* **2011,** *7* (12), e1002407.

15. Smart, R. C. H., E., *Molecular and Biochemical Toxicology*. 4 ed.; John Wiley & Sons: 2008.

16. Friedberg, E. W., G; Siede, W.; Wood, R.; Schultz, R.; Ellenberger, T., *DNA Repair and Mutagenesis*. 2nd ed.; ASM Press: 2006.

17. Loeb, L. A.; Cheng, K. C., Errors in DNA synthesis: a source of spontaneous mutations. *Mutat Res* **1990,** *238* (3), 297-304.

18. Loeb, L. A., Mutator phenotype may be required for multistage carcinogenesis. *Cancer Res* **1991,** *51* (12), 3075-9.

19. Loeb, L. A.; Monnat, R. J., Jr., DNA polymerases and human disease. *Nat Rev Genet* **2008,** *9* (8), 594-604.

20. Kunkel, T. A.; Bebenek, K., DNA replication fidelity. *Annu Rev Biochem* **2000,** *69*, 497-529.

21. Balakrishnan, L.; Bambara, R. A., Eukaryotic lagging strand DNA replication employs a multi-pathway mechanism that protects genome integrity. *J Biol Chem* **2011,** *286* (9), 6865-70.

22. Clark, D. P. P., Nanette Jean., Molecular Biology. Elsevier: 2012.

23. Fachinetti, D.; Bermejo, R.; Cocito, A.; Minardi, S.; Katou, Y.; Kanoh, Y.; Shirahige, K.; Azvolinsky, A.; Zakian, V. A.; Foiani, M., Replication termination at eukaryotic chromosomes is mediated by Top2 and occurs at genomic loci containing pausing elements. *Mol Cell* **2010,** *39* (4), 595-605.

24. Burgess, R. J.; Zhang, Z., Histones, histone chaperones and nucleosome assembly. *Protein Cell* **2010,** *1* (7), 607-12.

25. Boiteux, S.; Guillet, M., Abasic sites in DNA: repair and biological consequences in Saccharomyces cerevisiae. *DNA Repair (Amst)* **2004,** *3* (1), 1-12.

26. Ray, P. D.; Huang, B. W.; Tsuji, Y., Reactive oxygen species (ROS) homeostasis and redox regulation in cellular signaling. *Cell Signal* **2012,** *24* (5), 981-90.

27. Mates, J. M.; Segura, J. A.; Alonso, F. J.; Marquez, J., Oxidative stress in apoptosis and cancer: an update. *Arch Toxicol* **2012,** *86* (11), 1649-65.

28. May, J. M.; Qu, Z. C.; Whitesell, R. R., Generation of oxidant stress in cultured endothelial cells by methylene blue: protective effects of glucose and ascorbic acid. *Biochem Pharmacol* **2003,** *66* (5), 777-84.

29. McBride, T. J.; Schneider, J. E.; Floyd, R. A.; Loeb, L. A., Mutations induced by methylene blue plus light in single-stranded M13mp2. *Proc Natl Acad Sci U S A* **1992,** *89* (15), 6866-70.

30. Baran, I.; Ganea, C.; Scordino, A.; Musumeci, F.; Barresi, V.; Tudisco, S.; Privitera, S.; Grasso, R.; Condorelli, D. F.; Ursu, I.; Baran, V.; Katona, E.; Mocanu, M. M.; Gulino, M.; Ungureanu, R.; Surcel, M.; Ursaciuc, C., Effects of menadione, hydrogen peroxide, and quercetin on apoptosis and delayed luminescence of human leukemia Jurkat T-cells. *Cell Biochem Biophys* **2010,** *58* (3), 169-79.

31. Delwar, Z. M.; Avramidis, D.; Follin, E.; Hua, Y.; Siden, A.; Cruz, M.; Paulsson, K. M.; Yakisich, J. S., Cytotoxic effect of menadione and sodium orthovanadate in combination on human glioma cells. *Invest New Drugs* **2012,** *30* (4), 1302-10.

32. Herman, K. N.; Toffton, S.; McCulloch, S. D., Minimal Detection of Nuclear Mutations in XP-V and Normal Cells Treated with Oxidative Stress Inducing Agents. *J Biochem Mol Toxicol* **2014,** *28* (12), 568-77.

33. Haracska, L.; Yu, S. L.; Johnson, R. E.; Prakash, L.; Prakash, S., Efficient and accurate replication in the presence of 7,8-dihydro-8-oxoguanine by DNA polymerase eta. *Nat Genet* **2000,** *25* (4), 458-61.

34. Ahmad SI, H. F., *Molecular Mechanisms of Xeroderma Pigmentosum*. Springer Science + Business Media, LLC: 2008.

35. Bebenek, K.; Kunkel, T. A., Analyzing fidelity of DNA polymerases. *Methods Enzymol* **1995,** *262*, 217-32.

36. Biertumpfel, C.; Zhao, Y.; Kondo, Y.; Ramon-Maiques, S.; Gregory, M.; Lee, J. Y.; Masutani, C.; Lehmann, A. R.; Hanaoka, F.; Yang, W., Structure and mechanism of human DNA polymerase eta. *Nature* **2010,** *465* (7301), 1044-8.

37. Chang, D. J.; Cimprich, K. A., DNA damage tolerance: when it's OK to make mistakes. *Nat Chem Biol* **2009,** *5* (2), 82-90.

38. Cruet-Hennequart, S.; Gallagher, K.; Sokol, A. M.; Villalan, S.; Prendergast, A. M.; Carty, M. P., DNA polymerase eta, a key protein in translesion synthesis in human cells. *Subcell Biochem* **2010,** *50*, 189-209.

39. Goodman, M. F., Error-prone repair DNA polymerases in prokaryotes and eukaryotes. *Annu Rev Biochem* **2002,** *71*, 17-50.

40. McCulloch, S. D.; Kokoska, R. J.; Kunkel, T. A., Efficiency, fidelity and enzymatic switching during translesion DNA synthesis. *Cell Cycle* **2004,** *3* (5), 580-3.

41. McCulloch, S. D.; Kunkel, T. A., Measuring the fidelity of translesion DNA synthesis. *Methods Enzymol* **2006,** *408*, 341-55.

42. Suarez, S. C.; Beardslee, R. A.; Toffton, S. M.; McCulloch, S. D., Biochemical analysis of active site mutations of human polymerase eta. *Mutat Res* **2013,** *745-746*, 46-54.

43. Zhang, Y.; Yuan, F.; Wu, X.; Rechkoblit, O.; Taylor, J. S.; Geacintov, N. E.; Wang, Z., Error-prone lesion bypass by human DNA polymerase eta. *Nucleic Acids Res* **2000,** *28* (23), 4717-24.

44. Bebenek, K.; Kunkel, T. A., Functions of DNA polymerases. *Adv Protein Chem* **2004,** *69*, 137-65.

45. Yang, W.; Woodgate, R., What a difference a decade makes: insights into translesion DNA synthesis. *Proc Natl Acad Sci U S A* **2007,** *104* (40), 15591-8.

46. McCulloch, S. D.; Kokoska, R. J.; Masutani, C.; Iwai, S.; Hanaoka, F.; Kunkel, T. A., Preferential cis-syn thymine dimer bypass by DNA polymerase eta occurs with biased fidelity. *Nature* **2004,** *428* (6978), 97-100.

47. Yuan, F.; Zhang, Y.; Rajpal, D. K.; Wu, X.; Guo, D.; Wang, M.; Taylor, J. S.; Wang, Z., Specificity of DNA lesion bypass by the yeast DNA polymerase eta. *J Biol Chem* **2000,** *275* (11), 8233-9.

48. Goodman, M. F.; Tippin, B., The expanding polymerase universe. *Nat Rev Mol Cell Biol* **2000,** *1* (2), 101-9.

49. Yang, K.; Gong, P.; Gokhale, P.; Zhuang, Z., Chemical protein polyubiquitination reveals the role of a noncanonical polyubiquitin chain in DNA damage tolerance. *ACS Chem Biol* **2014,** *9* (8), 1685-91.

50. Frampton, J.; Irmisch, A.; Green, C. M.; Neiss, A.; Trickey, M.; Ulrich, H. D.; Furuya, K.; Watts, F. Z.; Carr, A. M.; Lehmann, A. R., Postreplication repair and PCNA modification in Schizosaccharomyces pombe. *Mol Biol Cell* **2006,** *17* (7), 2976-85.

51. Bienko, M.; Green, C. M.; Sabbioneda, S.; Crosetto, N.; Matic, I.; Hibbert, R. G.; Begovic, T.; Niimi, A.; Mann, M.; Lehmann, A. R.; Dikic, I., Regulation of translesion synthesis DNA polymerase eta by monoubiquitination. *Mol Cell* **2010,** *37* (3), 396-407.

52. Acharya, N.; Yoon, J. H.; Hurwitz, J.; Prakash, L.; Prakash, S., DNA polymerase eta lacking the ubiquitin-binding domain promotes replicative lesion bypass in humans cells. *Proc Natl Acad Sci U S A* **2010,** *107* (23), 10401-5.

53. Kannouche, P.; Fernandez de Henestrosa, A. R.; Coull, B.; Vidal, A. E.; Gray, C.; Zicha, D.; Woodgate, R.; Lehmann, A. R., Localization of DNA polymerases eta and iota to

the replication machinery is tightly co-ordinated in human cells. *Embo J* **2003,** *22* (5), 1223-33.

54. Kannouche, P.; Broughton, B. C.; Volker, M.; Hanaoka, F.; Mullenders, L. H.; Lehmann, A. R., Domain structure, localization, and function of DNA polymerase eta, defective in xeroderma pigmentosum variant cells. *Genes Dev* **2001,** *15* (2), 158-72.

55. Wang, Y.; Woodgate, R.; McManus, T. P.; Mead, S.; McCormick, J. J.; Maher, V. M., Evidence that in xeroderma pigmentosum variant cells, which lack DNA polymerase eta, DNA polymerase iota causes the very high frequency and unique spectrum of UV-induced mutations. *Cancer Res* **2007,** *67* (7), 3018-3026.

56. Herman, K. N.; Toffton, S.; McCulloch, S. D., Detrimental effects of UV-B radiation in a xeroderma pigmentosum-variant cell line. *Environ Mol Mutagen* **2014**.

57. Gueranger, Q.; Stary, A.; Aoufouchi, S.; Faili, A.; Sarasin, A.; Reynaud, C. A.; Weill, J. C., Role of DNA polymerases eta, iota and zeta in UV resistance and UV-induced mutagenesis in a human cell line. *DNA Repair (Amst)* **2008,** *7* (9), 1551-62.

58. Haracska, L.; Johnson, R. E.; Unk, I.; Phillips, B. B.; Hurwitz, J.; Prakash, L.; Prakash, S., Targeting of human DNA polymerase iota to the replication machinery via interaction with PCNA. *Proc Natl Acad Sci U S A* **2001,** *98* (25), 14256-61.

59. Haracska, L.; Johnson, R. E.; Unk, I.; Phillips, B.; Hurwitz, J.; Prakash, L.; Prakash, S., Physical and functional interactions of human DNA polymerase eta with PCNA. *Mol Cell Biol* **2001,** *21* (21), 7199-206.

60. Suarez, S. C.; Toffton, S. M.; McCulloch, S. D., Biochemical analysis of DNA polymerase eta fidelity in the presence of replication protein A. *PLoS One* **2014,** *9* (5), e97382.

61. Bavoux, C.; Hoffmann, J. S.; Cazaux, C., Adaptation to DNA damage and stimulation of genetic instability: the double-edged sword mammalian DNA polymerase kappa. *Biochimie* **2005,** *87* (7), 637-46.

62. Zhou, W.; Chen, Y. W.; Liu, X.; Chu, P.; Loria, S.; Wang, Y.; Yen, Y.; Chou, K. M., Expression of DNA translesion synthesis polymerase eta in head and neck squamous cell cancer predicts resistance to gemcitabine and cisplatin-based chemotherapy. *PLoS One* **2013,** *8* (12), e83978.

63. Albertella, M. R.; Lau, A.; O'Connor, M. J., The overexpression of specialized DNA polymerases in cancer. *DNA Repair (Amst)* **2005,** *4* (5), 583-93.

64. Ummat, A.; Rechkoblit, O.; Jain, R.; Roy Choudhury, J.; Johnson, R. E.; Silverstein, T. D.; Buku, A.; Lone, S.; Prakash, L.; Prakash, S.; Aggarwal, A. K., Structural basis for

cisplatin DNA damage tolerance by human polymerase eta during cancer chemotherapy. *Nat Struct Mol Biol* **2012,** *19* (6), 628-32.

65. Ceppi, P.; Novello, S.; Cambieri, A.; Longo, M.; Monica, V.; Lo Iacono, M.; Giaj-Levra, M.; Saviozzi, S.; Volante, M.; Papotti, M.; Scagliotti, G., Polymerase eta mRNA expression predicts survival of non-small cell lung cancer patients treated with platinum-based chemotherapy. *Clin Cancer Res* **2009,** *15* (3), 1039-45.

66. Marteijn, J. A.; Lans, H.; Vermeulen, W.; Hoeijmakers, J. H., Understanding nucleotide excision repair and its roles in cancer and ageing. *Nat Rev Mol Cell Biol* **2014,** *15* (7), 465-81.

67. Kim, Y. J.; Wilson, D. M., 3rd, Overview of base excision repair biochemistry. *Curr Mol Pharmacol* **2012,** *5* (1), 3-13.

68. Klaassen, C., *Toxicology: The Basic Science of Poisons*. 7 ed.; The McGraw-Hill Companies, Inc.: 2008.

69. Hodgson, E., *A Textbook of Modern Toxicology*. 4 ed.; John Wiley & Sons, Inc.: Hoboken, NJ, 2010.

70. Felsenfeld, G.; Groudine, M., Controlling the double helix. *Nature* **2003,** *421* (6921), 448-53.

71. Liu, Y.; Wilson, S. H., DNA base excision repair: a mechanism of trinucleotide repeat expansion. *Trends Biochem Sci* **2012,** *37* (4), 162-72.

72. Friedberg, E. C.; Wagner, R.; Radman, M., Specialized DNA polymerases, cellular survival, and the genesis of mutations. *Science* **2002,** *296* (5573), 1627-30.

73. Rigel, D. S., Cutaneous ultraviolet exposure and its relationship to the development of skin cancer. *J Am Acad Dermatol* **2008,** *58* (5 Suppl 2), S129-32.

74. Autier, P.; Dore, J. F.; Negrier, S.; Lienard, D.; Panizzon, R.; Lejeune, F. J.; Guggisberg, D.; Eggermont, A. M., Sunscreen use and duration of sun exposure: a double-blind, randomized trial. *J Natl Cancer Inst* **1999,** *91* (15), 1304-9.

75. Perdiz, D.; Grof, P.; Mezzina, M.; Nikaido, O.; Moustacchi, E.; Sage, E., Distribution and repair of bipyrimidine photoproducts in solar UV-irradiated mammalian cells. Possible role of Dewar photoproducts in solar mutagenesis. *J Biol Chem* **2000,** *275* (35), 26732-42.

76. de Lima-Bessa, K. M.; Armelini, M. G.; Chigancas, V.; Jacysyn, J. F.; Amarante-Mendes, G. P.; Sarasin, A.; Menck, C. F., CPDs and 6-4PPs play different roles in UV-induced cell death in normal and NER-deficient human cells. *DNA Repair (Amst)* **2008,** *7* (2), 303-12.

77. Sage, E., DNA damage and mutations induced by solar UV radiation. In *Fundamentals for the Assessment of Risks from Environmental Radiation.*, Baumstark-Khan C, K. S., Horneck G., Ed. Kluwer Academic Publismers: The Netherlands, 1999; pp 115-126.

78. Brown, D. B.; Peritz, A. E.; Mitchell, D. L.; Chiarello, S.; Uitto, J.; Gasparro, F. P., Common fluorescent sunlamps are an inappropriate substitute for sunlight. *Photochem Photobiol* **2000,** *72* (3), 340-4.

79. Kielbassa, C.; Roza, L.; Epe, B., Wavelength dependence of oxidative DNA damage induced by UV and visible light. *Carcinogenesis* **1997,** *18* (4), 811-6.

80. Ravanat, J. L.; Douki, T.; Cadet, J., Direct and indirect effects of UV radiation on DNA and its components. *J Photochem Photobiol B* **2001,** *63* (1-3), 88-102.

81. Lo, H. L.; Nakajima, S.; Ma, L.; Walter, B.; Yasui, A.; Ethell, D. W.; Owen, L. B., Differential biologic effects of CPD and 6-4PP UV-induced DNA damage on the induction of apoptosis and cell-cycle arrest. *BMC Cancer* **2005,** *5*, 135.

82. You, Y. H.; Lee, D. H.; Yoon, J. H.; Nakajima, S.; Yasui, A.; Pfeifer, G. P., Cyclobutane pyrimidine dimers are responsible for the vast majority of mutations induced by UVB irradiation in mammalian cells. *J Biol Chem* **2001,** *276* (48), 44688-94.

83. McCulloch, S. D.; Kokoska, R. J.; Chilkova, O.; Welch, C. M.; Johansson, E.; Burgers, P. M.; Kunkel, T. A., Enzymatic switching for efficient and accurate translesion DNA replication. *Nucleic Acids Res* **2004,** *32* (15), 4665-75.

84. Takasawa, K.; Masutani, C.; Hanaoka, F.; Iwai, S., Chemical synthesis and translesion replication of a cis-syn cyclobutane thymine-uracil dimer. *Nucleic Acids Res* **2004,** *32* (5), 1738-45.

85. Vaisman, A.; Takasawa, K.; Iwai, S.; Woodgate, R., DNA polymerase iota-dependent translesion replication of uracil containing cyclobutane pyrimidine dimers. *DNA Repair (Amst)* **2006,** *5* (2), 210-8.

86. Yu, S. L.; Johnson, R. E.; Prakash, S.; Prakash, L., Requirement of DNA polymerase eta for error-free bypass of UV-induced CC and TC photoproducts. *Mol Cell Biol* **2001,** *21* (1), 185-8.

87. Cadet, J.; Sage, E.; Douki, T., Ultraviolet radiation-mediated damage to cellular DNA. *Mutat Res* **2005,** *571* (1-2), 3-17.

88. Douki, T.; Perdiz, D.; Grof, P.; Kuluncsics, Z.; Moustacchi, E.; Cadet, J.; Sage, E., Oxidation of guanine in cellular DNA by solar UV radiation: biological role. *Photochem Photobiol* **1999,** *70* (2), 184-90.

89. Wang, D.; Kreutzer, D. A.; Essigmann, J. M., Mutagenicity and repair of oxidative DNA damage: insights from studies using defined lesions. *Mutat Res* **1998,** *400* (1-2), 99-115.

90. Neeley, W. L.; Essigmann, J. M., Mechanisms of formation, genotoxicity, and mutation of guanine oxidation products. *Chem Res Toxicol* **2006,** *19* (4), 491-505.

91. McCulloch, S. D.; Kokoska, R. J.; Garg, P.; Burgers, P. M.; Kunkel, T. A., The efficiency and fidelity of 8-oxo-guanine bypass by DNA polymerases delta and eta. *Nucleic Acids Res* **2009,** *37* (9), 2830-40.

92. Cordeiro-Stone, M.; Frank, A.; Bryant, M.; Oguejiofor, I.; Hatch, S. B.; McDaniel, L. D.; Kaufmann, W. K., DNA damage responses protect xeroderma pigmentosum variant from UVC-induced clastogenesis. *Carcinogenesis* **2002,** *23* (6), 959-65.

93. King, N. M.; Nikolaishvili-Feinberg, N.; Bryant, M. F.; Luche, D. D.; Heffernan, T. P.; Simpson, D. A.; Hanaoka, F.; Kaufmann, W. K.; Cordeiro-Stone, M., Overproduction of DNA polymerase eta does not raise the spontaneous mutation rate in diploid human fibroblasts. *DNA Repair (Amst)* **2005,** *4* (6), 714-24.

94. Bassett, E.; King, N. M.; Bryant, M. F.; Hector, S.; Pendyala, L.; Chaney, S. G.; Cordeiro-Stone, M., The role of DNA polymerase eta in translesion synthesis past platinum-DNA adducts in human fibroblasts. *Cancer Res* **2004,** *64* (18), 6469-75.

95. Yoon, K.; Smart, R. C., C/EBPalpha is a DNA damage-inducible p53-regulated mediator of the G1 checkpoint in keratinocytes. *Mol Cell Biol* **2004,** *24* (24), 10650-60.

96. Yang, J. L.; Maher, V. M.; McCormick, J. J., Amplification and direct nucleotide sequencing of cDNA from the lysate of low numbers of diploid human cells. *Gene* **1989,** *83* (2), 347-54.

97. Freshney, R. I., *Culture of Animal Cells: A Manual of Basic Techniques and Specialized Applications*. 6 ed.; Wiley-Blackwell: 2010; p 796.

98. Maher, V. M.; Ouellette, L. M.; Curren, R. D.; McCormick, J. J., Frequency of ultraviolet light-induced mutations is higher in xeroderma pigmentosum variant cells than in normal human cells. *Nature* **1976,** *261* (5561), 593-5.

99. Stary, A.; Kannouche, P.; Lehmann, A. R.; Sarasin, A., Role of DNA polymerase eta in the UV mutation spectrum in human cells. *J Biol Chem* **2003,** *278* (21), 18767-75.

100. Kaufmann, W. K.; Heffernan, T. P.; Beaulieu, L. M.; Doherty, S.; Frank, A. R.; Zhou, Y.; Bryant, M. F.; Zhou, T.; Luche, D. D.; Nikolaishvili-Feinberg, N.; Simpson, D. A.; Cordeiro-Stone, M., Caffeine and human DNA metabolism: the magic and the mystery. *Mutat Res* **2003,** *532* (1-2), 85-102.

101. Lin, Q.; Clark, A. B.; McCulloch, S. D.; Yuan, T.; Bronson, R. T.; Kunkel, T. A.; Kucherlapati, R., Increased susceptibility to UV-induced skin carcinogenesis in polymerase eta-deficient mice. *Cancer Res* **2006,** *66* (1), 87-94.

102. Pfeifer, G. P.; Besaratinia, A., UV wavelength-dependent DNA damage and human non-melanoma and melanoma skin cancer. *Photochem Photobiol Sci* **2012,** *11* (1), 90-7.

103. Kozmin, S. G.; Pavlov, Y. I.; Kunkel, T. A.; Sage, E., Roles of Saccharomyces cerevisiae DNA polymerases Poleta and Polzeta in response to irradiation by simulated sunlight. *Nucleic Acids Res* **2003,** *31* (15), 4541-52.

104. Maher, V. M.; Ouellette, L. M.; Curren, R. D.; McCormick, J. J., Caffeine enhancement of the cytotoxic and mutagenic effect of ultraviolet irradiation in a xeroderma pigmentosum variant strain of human cells. *Biochem Biophys Res Commun* **1976,** *71* (1), 228-34.

105. Mitchell, D. L.; Jen, J.; Cleaver, J. E., Sequence specificity of cyclobutane pyrimidine dimers in DNA treated with solar (ultraviolet B) radiation. *Nucleic Acids Res* **1992,** *20* (2), 225-9.

106. Cooke, M. S.; Olinski, R.; Evans, M. D., Does measurement of oxidative damage to DNA have clinical significance? *Clin Chim Acta* **2006,** *365* (1-2), 30-49.

107. De Bont, R.; van Larebeke, N., Endogenous DNA damage in humans: a review of quantitative data. *Mutagenesis* **2004,** *19* (3), 169-85.

108. Beard, W. A.; Batra, V. K.; Wilson, S. H., DNA polymerase structure-based insight on the mutagenic properties of 8-oxoguanine. *Mutat Res* **2010,** *703* (1), 18-23.

109. Brieba, L. G.; Eichman, B. F.; Kokoska, R. J.; Doublie, S.; Kunkel, T. A.; Ellenberger, T., Structural basis for the dual coding potential of 8-oxoguanosine by a high-fidelity DNA polymerase. *Embo J* **2004,** *23* (17), 3452-61.

110. Tolentino, J. H.; Burke, T. J.; Mukhopadhyay, S.; McGregor, W. G.; Basu, A. K., Inhibition of DNA replication fork progression and mutagenic potential of 1, N6-ethenoadenine and 8-oxoguanine in human cell extracts. *Nucleic Acids Res* **2008,** *36* (4), 1300-8.

111. Vaisman, A.; Woodgate, R., Unique misinsertion specificity of poliota may decrease the mutagenic potential of deaminated cytosines. *Embo J* **2001,** *20* (22), 6520-9.

112. Irimia, A.; Eoff, R. L.; Guengerich, F. P.; Egli, M., Structural and functional elucidation of the mechanism promoting error-prone synthesis by human DNA polymerase kappa opposite the 7,8-dihydro-8-oxo-2'-deoxyguanosine adduct. *J Biol Chem* **2009,** *284* (33), 22467-80.

113. Lee, D. H.; Pfeifer, G. P., Translesion synthesis of 7,8-dihydro-8-oxo-2'-deoxyguanosine by DNA polymerase eta in vivo. *Mutat Res* **2008,** *641* (1-2), 19-26.

114. Kawamura, F.; Nakanishi, M.; Hirashima, N., Effects of menadione, a reactive oxygen generator, on leukotriene secretion from RBL-2H3 cells. *Biol Pharm Bull* **2010,** *33* (5), 881-5.

115. Floyd, R. A.; West, M. S.; Eneff, K. L.; Schneider, J. E., Methylene blue plus light mediates 8-hydroxyguanine formation in DNA. *Arch Biochem Biophys* **1989,** *273* (1), 106-11.

116. Jena, S.; Chainy, G. B., Effect of methylene blue on oxidative stress and antioxidant defence parameters of rat hepatic and renal tissues. *Indian J Physiol Pharmacol* **2008,** *52* (3), 293-6.

117. Petta, T. B.; Nakajima, S.; Zlatanou, A.; Despras, E.; Couve-Privat, S.; Ishchenko, A.; Sarasin, A.; Yasui, A.; Kannouche, P., Human DNA polymerase iota protects cells against oxidative stress. *Embo J* **2008,** *27* (21), 2883-95.

118. Ishii, T.; Yasuda, K.; Akatsuka, A.; Hino, O.; Hartman, P. S.; Ishii, N., A mutation in the SDHC gene of complex II increases oxidative stress, resulting in apoptosis and tumorigenesis. *Cancer Res* **2005,** *65* (1), 203-9.

119. Matthijssens, F.; Back, P.; Braeckman, B. P.; Vanfleteren, J. R., Prooxidant activity of the superoxide dismutase (SOD)-mimetic EUK-8 in proliferating and growth-arrested Escherichia coli cells. *Free Radic Biol Med* **2008,** *45* (5), 708-15.

120. Nakamura, A.; Goto, S., Analysis of protein carbonyls with 2,4-dinitrophenyl hydrazine and its antibodies by immunoblot in two-dimensional gel electrophoresis. *J Biochem* **1996,** *119* (4), 768-74.

121. Yasuda, K.; Ishii, T.; Suda, H.; Akatsuka, A.; Hartman, P. S.; Goto, S.; Miyazawa, M.; Ishii, N., Age-related changes of mitochondrial structure and function in Caenorhabditis elegans. *Mech Ageing Dev* **2006,** *127* (10), 763-70.

122. Miyazawa, M.; Tsuji, Y., Evidence for a Novel Antioxidant Function and Isoform-specific Regulation of the Human p66Shc Gene. *Mol Biol Cell* **2014**.

123. Sambrook, J.; Russell, D. W., Alkaline agarose gel electrophoresis. *CSH Protoc* **2006,** *2006* (1).

124. Boysen, G.; Collins, L. B.; Liao, S.; Luke, A. M.; Pachkowski, B. F.; Watters, J. L.; Swenberg, J. A., Analysis of 8-oxo-7,8-dihydro-2'-deoxyguanosine by ultra high pressure liquid chromatography-heat assisted electrospray ionization-tandem mass spectrometry. *J Chromatogr B Analyt Technol Biomed Life Sci* **2010,** *878* (3-4), 375-80.

125. Pavlov, Y. I.; Mian, I. M.; Kunkel, T. A., Evidence for preferential mismatch repair of lagging strand DNA replication errors in yeast. *Curr Biol* **2003,** *13* (9), 744-8.

126. Pavlov, Y. I.; Nguyen, D.; Kunkel, T. A., Mutator effects of overproducing DNA polymerase eta (Rad30) and its catalytically inactive variant in yeast. *Mutat Res* **2001,** *478* (1-2), 129-39.

127. Beardslee, R. A.; Suarez, S. C.; Toffton, S. M.; McCulloch, S. D., Mutation of the little finger domain in human DNA polymerase eta alters fidelity when copying undamaged DNA. *Environ Mol Mutagen* **2013,** *54* (8), 638-51.

128. Patra, A.; Nagy, L. D.; Zhang, Q.; Su, Y.; Muller, L.; Guengerich, F. P.; Egli, M., Kinetics, Structure, and Mechanism of 8-Oxo-7,8-dihydro-2'-deoxyguanosine Bypass by Human DNA Polymerase eta. *J Biol Chem* **2014,** *289* (24), 16867-16882.

129. Silverstein, T. D.; Jain, R.; Johnson, R. E.; Prakash, L.; Prakash, S.; Aggarwal, A. K., Structural basis for error-free replication of oxidatively damaged DNA by yeast DNA polymerase eta. *Structure* **2010,** *18* (11), 1463-70.

130. Schmitt, M. W.; Kennedy, S. R.; Salk, J. J.; Fox, E. J.; Hiatt, J. B.; Loeb, L. A., Detection of ultra-rare mutations by next-generation sequencing. *Proc Natl Acad Sci U S A* **2012,** *109* (36), 14508-13.

131. Qi, H.; Zhu, H.; Lou, M.; Fan, Y.; Liu, H.; Shen, J.; Li, Z.; Lv, X.; Shan, J.; Zhu, L.; Chin, Y. E.; Shao, J., Interferon regulatory factor 1 transactivates expression of human DNA polymerase eta in response to carcinogen N-methyl-N'-nitro-N-nitrosoguanidine. *J Biol Chem* **2012,** *287* (16), 12622-33.

132. Zhu, H.; Fan, Y.; Jiang, H.; Shen, J.; Qi, H.; Mei, R.; Shao, J., Response of human DNA polymerase iota promoter to N-methyl-N'-nitro-N-nitrosoguanidine. *Environ Toxicol Pharmacol* **2010,** *29* (1), 79-86.

133. Choi, J. H.; Pfeifer, G. P., The role of DNA polymerase eta in UV mutational spectra. *DNA Repair (Amst)* **2005,** *4* (2), 211-20.